Multifaceted regulation of V(D)J recombination

Guannan Wang

A Dissertation Presented in Partial Fulfillment
of the Requirements for the Degree
Doctor of Philosophy

Approved April 2012 by the
Graduate Supervisory Committee:

Yung Chang, Chair
Marcia Levitus
Karen Anderson
Rajeev Misra

ARIZONA STATE UNIVERSITY

May 2012

ABSTRACT

V(D)J recombination is responsible for generating an enormous repertoire of immunoglobulins and T cell receptors, therefore it is a centerpiece to the formation of the adaptive immune system. The V(D)J recombination process proceeds through two steps, site-specific cleavage at RSS (Recombination Signal Sequence) site mediated by the RAG recombinase (RAG1/2) and the subsequent imprecise resolution of the DNA ends, which is carried out by the ubiquitous non-homologous end joining pathway (NHEJ). The V(D)J recombination reaction is obliged to be tightly controlled under all circumstances, as it involves generations of DNA double strand breaks, which are considered the most dangerous lesion to a cell. Multifaceted regulatory mechanisms have been evolved to create great diversity of the antigen receptor repertoire while ensuring genome stability. The RAG-mediated cleavage reaction is stringently regulated at both the pre-cleavage stage and the post-cleavage stage. Specifically, RAG1/2 first forms a pre-cleavage complex assembled at the boarder of RSS and coding flank, which ensures the appropriate DNA targeting. Subsequently, this complex initiates site-specific cleavage, generating two types of double stranded DNA breaks, hairpin-ended coding ends (HP-CEs) and blunt signal ends (SEs). After the cleavage, RAG1/2 proteins bind and retain the recombination ends to form post-cleavage complexes (PCC), which collaborates with the NHEJ machinery for appropriate transfer of recombination ends to NHEJ for proper end resolution.

However, little is known about the molecular basis of this collaboration, partly attributed to the lack of sensitive assays to reveal the interaction of PCC with HP-CEs. Here, for the first time, by using two complementary fluorescence-based techniques, fluorescence anisotropy and fluorescence resonance energy transfer (FRET), I managed to monitor the RAG1/2-catalyzed cleavage reaction in real time, from the pre-cleavage to the post-cleavage stages. By examining the dynamic fluorescence changes during the RAG-mediated cleavage reactions, and by manipulating the reaction conditions, I was able to characterize some fundamental properties of RAG-DNA interactions before and after cleavage. Firstly, Mg^{2+}, known as a physiological cofactor at the excision step, also promotes the HP-CEs retention in the RAG complex after cleavage. Secondly, the structure of pre-cleavage complex may affect the subsequent collaborations with NHEJ for end resolution. Thirdly, the non-core region of RAG2 may have differential influences on the PCC retention of HP-CEs and SEs. Furthermore, I also provide the first evidence of RAG1-mediated regulation of RAG2. Our study provides important insights into the multilayered regulatory mechanisms, in modulating recombination events in developing lymphocytes and paves the way for possible development of detection and diagnotic markers for defective recombination events that are often associated immunodeficiency and/or lymphoid malignancy.

DEDICATION

I dedicate my dissertation to my parents, Runshun Wang (王润顺) and Xianying He (何宪英), for their constant love and support. Without them, it is impossible to finish my dissertation.

ACKNOWLEDGMENTS

I thank my advisor, Dr. Yung Chang, for her endless guidance and support. With her help, I have grown so much both personally and professionally over the last few years. Dr. Marcia Levitus is like my second advisor, and I greatly appreciate her insights and advices and her dedication to my projects.

My husband, Ming Wu, have been so supportive for my PhD study and everything else in my life, I will be forever indebted for his love and support.

TABLE OF CONTENTS

CHAPTER Page

LIST OF TABLES

LIST OF FIGURES

CHAPTER 1

INTRODUCTION

Overview Of V(D)J Recombination

Despite the constant exposure to a wide range of pathogenic microorganisms and environmental hazards, it is remarkable that we are healthy in general, owing to both the innate and the adaptive immune systems, which provide an excellent defense against these microbes and harmful agents. The adaptive immune system renders high specificity and great diversity against virtually any invaders (1). These two unique features, specificity and diversity, of the adaptive immune response are achieved by the production of an enormous repertoire of antigen receptor molecules, including immunoglobulins and T-cell receptors, where each individual receptor molecule bares a unique antigen-binding specificity conferred by the distinctive structure at the antigen binding site (known as variable or V region) (2). However, the diverse repertoire of antigen receptors contrasts with our limited genome size, which would not accommodate such a vast number of individual genes that encode these antigen receptor proteins. Instead, a sophisticated and elegant mechanism, known as V(D)J recombination, has evolved to fulfill the mission of generating the immense repertoire of antigen receptors (3–5). V(D)J recombination is a somatic recombination mechanism that assembles separate pieces of gene segments that include the variable (V), diversity (D) and joining (J) region into one complete gene encoding

the variable region of *Ig* genes (2, 3, 6, 7). Much of the diversity seen in the adaptive immune system is generated through combinations of V, D and J gene segments located at *Ig* or *Tcr* loci, and random assortment of H and L chains, as well as additional junctional variations introduced during the process of V(D)J recombination (8, 9). Thus, the V(D)J recombination process is pivotal to the formation of the adaptive immune system.

For successful assembly of antigen receptor genes, the loci corresponding to variable gene segments (i.e., V, D, and J) is first cleaved to generate double stranded breaks (DSBs), then the appropriate "excised" V, D or J segments are brought together into close juxtaposition (10, 11). The initial cleavage phase is mediated by lymphocyte specific recombinase complex, encoded by *recombination activating gene* 1 and 2 (*rag1* and *rag2*, respectively), while the subsequent joining is mediated primarily by the ubiquitous non-homologous end joining (NHEJ) pathway. RAG1 protein contains both a DNA-binding and an endonuclease catalytic domain while RAG2 protein functions to regulate RAG1, together, both RAG1 and RAG2 proteins are essential for initiating site-specific DNA recognition and the excision step (12, 13). Specifically, the RAG1 and RAG2 complex (RAG1/2) recognizes and binds to unique sequences flanking the rearranging gene segments. These sequences, known as recombination signal sequence (RSS), are composed of a conserved heptamer with the consensus sequence "CACAGTG" and a conserved

nonamer with the preferable sequence “ACAAAAACC”, The heptamer and nonamer is separated by a spacer region composed of either 12 or 23 base pairs. The length of spacer defines two types of RSS: 12RSS and 23RSS. The 12RSS and 23RSS play a major role in regulating the correct order of joining, known as the “12/23” rule, i.e. gene segment containing 12RSS can only be recombined with the one that contains 23RSS (14–16) ,see Figure 1. After recognizing the RSS, the RAG1/2 recombinase introduces a site-specific nicking at the coding-signal junction, thereby leaving a free 3’-OH group at the end of coding segment. Then two coding gene segments containing different RSSs (obeying the “12/23” rule) are brought together to form a synaptic complex, followed by a direct transesterification using the free 3’OH to attack the opposing strand, yielding two hairpin coding ends (CEs) and two blunt signal ends (SEs) (11, 17, 18), as illustrated in Figure 2.

The cleavage reaction has been recapitulated in a cell-free system, which allows extensive biochemical characterization of this reaction (14). In addition to the RAG recombinase and RSSs, several other components are also required for the cleavage phase of V(D)J recombination, such as a high mobility group (HMG) and divalent metal ions. The HMG stimulates synaptic complex formation and coupled cleavage by facilitating DNA conformational changes such that the DNA substrates are more accommodative to RAG-mediated binding and subsequent cleavage (19, 20). In addition, divalent metal ions are essential cofactors for the catalytic

activity of the RAG recombinase, where Mg^{2+} is believed to be a physiological cofactor in cells (14, 21).

In the second phase of V(D)J recombination, the non homologous end joining pathway (NHEJ) is primarily utilized to repair the RAG recombinase mediated double strand breaks (DSB) (22–24). In comparison to homologous recombination (HR), another major pathway for DSB repair, NHEJ is intrinsically error-prone, because it introduces deletions and insertions at the junction of rearranged products (25, 26). The imprecision of NHEJ-mediated end resolution further diversifies the antigen receptor gene pool (27, 28).

NHEJ machinery consists of a series of proteins, including Ku70/Ku80, DNA-PKcs, Artemis, poly mu, poly lambda, TdT, XRCC4: DNA ligase IV: XLF. Ku70/Ku80 heterodimer serves as the sensors of DSB, detecting and binding to DNA ends (29, 30). DNA-PKcs (DNA-dependent protein kinase catalytic subunit) is then recruited to the ends in a Ku-dependent manner and the interaction with the DNA ends of DNA-PKcs stimulates its serine/threonine kinase activity (31, 32). The potential substrate of DNA-PKcs is thought to be DNA-PKcs itself or Artemis, and the phosphorylation of which activates the endonuclease activity of Artemis (9, 33–35). Thus, by collaborating with DNA-PKcs, Artemis serves as an endonuclease to nick and open the hairpin coding ends (36). The opened ends are then processed to be compatible for ligation by Pol mu, pol lambda, and TdT (Terminal deoxynucleotidyl transferase). TdT

mediates non-template nucleotide addition at the junction, introducing further variations to the repertoire of immunoglobulins and T-cell receptors (28, 37). The actual end joining is carried out by XRCC4: DNA ligase IV, with XLF (also known as Cernunnos) stimulating incompatible DNA end ligation (38).

Together, the combinatorial diversity generated during the first phase of V(D)J recombination achieved by randomly selecting from a large repertoire of V, D and J gene segments and the junctional diversity created during the joining phase, accounts for an exceedingly diverse repertoire of immunoglobulins and TCRs.

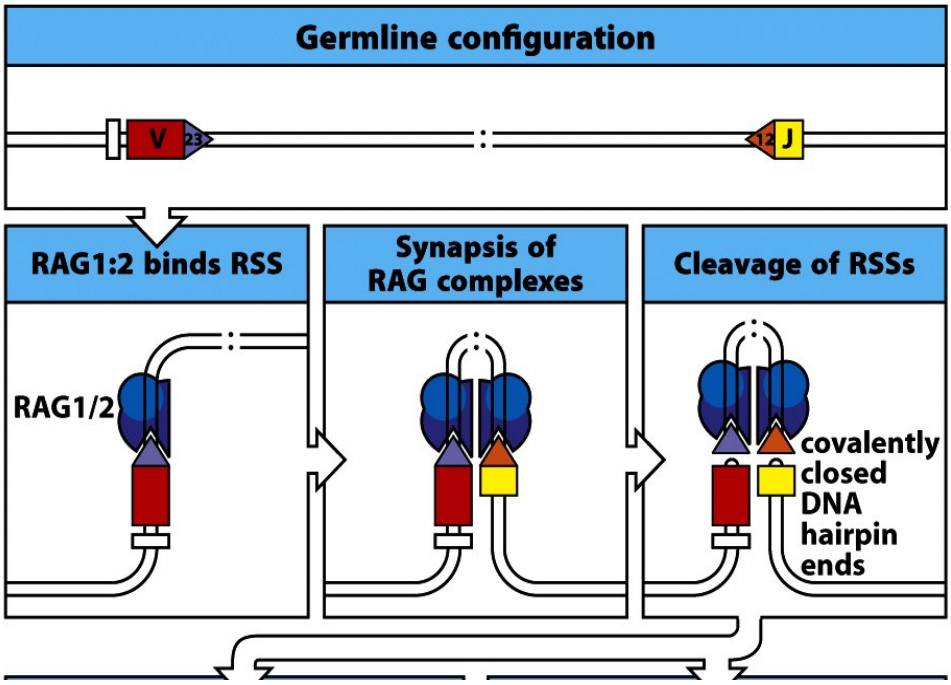

Figure 1. The first phase of V(D)J recombination.

The RAG recombinase-mediated lymphocyte specific cleavage on the antigen-receptor loci.

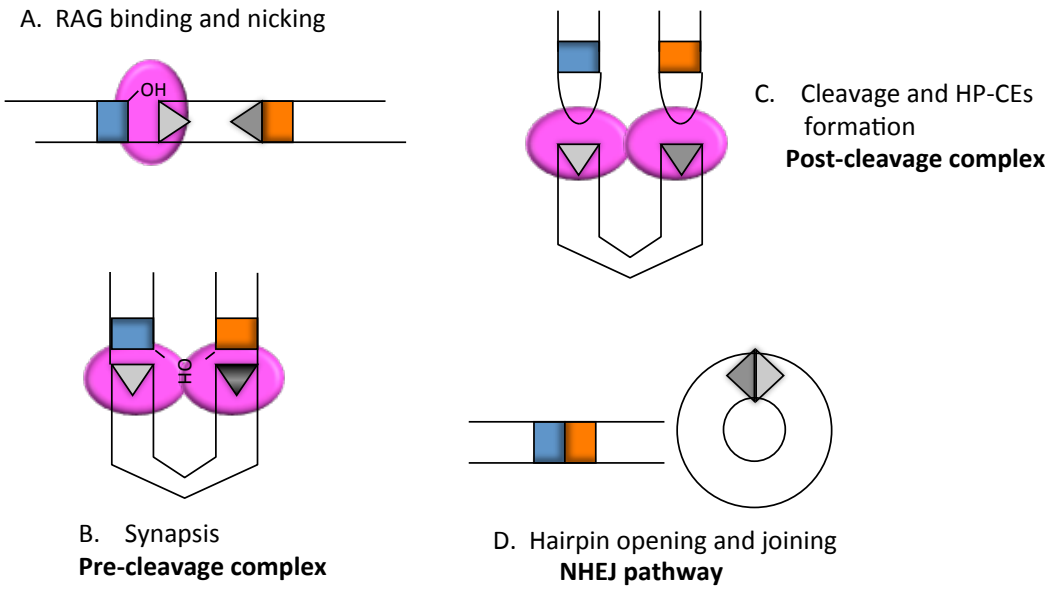

Figure 2. Biochemical procedures of *in vivo* V(D)J recombination

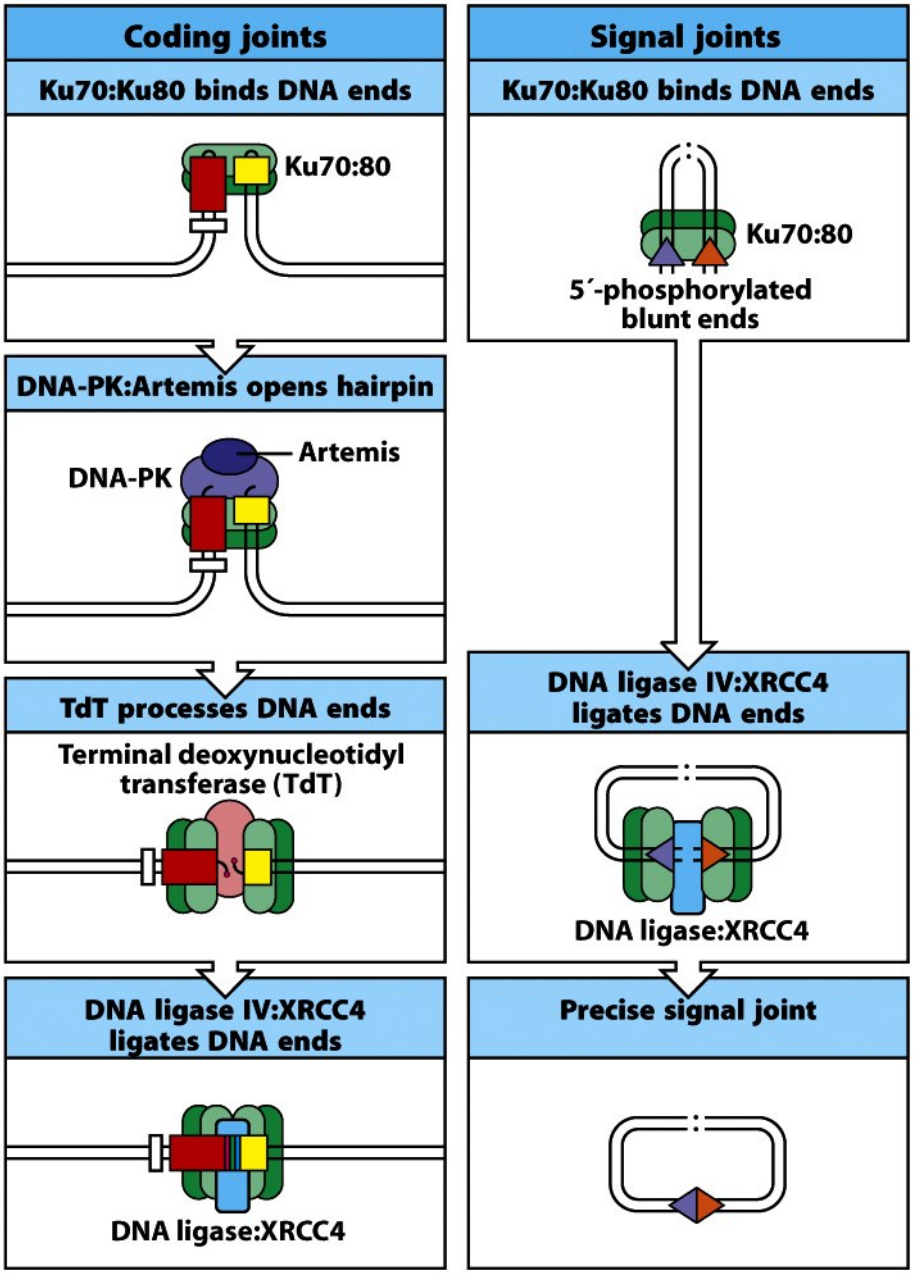

Figure 4-7 part 2 of 2 Immunobiology, 7ed. (© Garland Science 2008)

Figure 3. Second phase of V(D)J recombination.

Ubiquitous NHEJ pathway mediated joining of HP-CEs and SEs generated by the RAG recombinase.

The machinery of V(D)J recombination

Historical perspective of RAG recombinase and its origin and evolution

Like all other scientific studies, the mechanism underlying V(D)J recombination was revealed through a series of breakthroughs, among which was the discovery of RAG1 and RAG2 proteins as lymphoid-specific recombinase (12, 13). The development of extra-chromosomal recombination assays and subsequent demonstration of a cell-free recombination system made it possible to determine the structural and functional properties of the RAG recombinase and to delineate the biochemical steps of the recombination cleavage, and the subsequent end resolution (14, 17).

It is now clear that RAG1/2 play a major role in the first phase of V(D)J recombination, by generating DSBs at different gene segments for rearrangement to occur. In addition, the RAG recombinase is also believed to be critical in the subsequent joining phase as RAG mutations were found to lead to abnormal rearranged products (39–41). Further more, RAG proteins have been shown to catalyze transposition by inserting the signals ends fragment into a non-specific DNA tarets, or forming other non-standard joints made between signal ends and coding ends, including hybrid joints and open-shut junctions (42–46). Together, the “cut and paste” nature of the RAG recombinase resembles bona fide transposes and retroviral integrases, suggesting that the RAG

recombinase might have been originated from a mobile DNA element (47, 48). The origination of RAG from an DNA transposon was further supported by the following findings: 1) the compact structure of RAG gene locus, such that RAG1 and RAG2 lie adjacent to each other without introns that are often present in most eukaryotic genes (12); 2) the structural feature of RAG1 protein, including a specific DNA binding domain that recognizes targeted DNA (49) and a catalytic center composed of a triad of acidic amino acids “DDE” that chelates divalent metal ions for DNA excision (50–52); 3) RSS, which the RAG recombinase recognizes, is analogous to the terminal inverted repeats (TIR), residing at the end of a mobile DNA elements (49, 53); 4) the similar biochemical reaction for cleavage, which proceeds through hydrolysis and transesterification (20, 54). Together, the similarity between the RAG recombinase and the transposase support the model that RAG may have originated from a transposase. Furthermore, RAG was thought to be a driving force for the evolution of the adaptive immune system in jawed vertebrate, presumably by horizontal transfer (55, 56). However, the high conservation of RAG1 to some trasib-like transposases present in several invertebrates suggests that the RAG1 acquisition appears much earlier than the stage of jawed vertebrates. Furthermore, the recent evidence for the existence of the adaptive system in the absence of V(D)J recombination implies that the origin of adaptive immunity might not be simply due to the emergence of the RAG-mediated recombination (47).

Clearly, more evidence will be required to further elucidate the origin and evolution of the RAG recombinase (2, 48, 57).

Biochemistry and domain structure of RAG recombinase

Despite the essential role of the RAG recombinase in V(D)J recombination as well as in lymphocyte development, most biochemical studies of the RAG 1/2 proteins have relied on the core RAG1 and core RAG2 proteins (cRAG1 and cRAG2, see table for nomenclature) because they have higher expression level and better solubility than full-length RAG, which makes it possible to isolate and purify a large quantity of RAG proteins for their biochemical characterization. cRAG1 and cRAG2 are the smallest functional truncation mutants that are sufficient for enzymatic activity in the reconstituted cell free system (58–61). However, it is important to note that, although very active in the *in vitro* cell-free recombination system, core RAG displays much less efficiency on V(D)J recombination taking place in cells (through rearrangement of extra-chromosomal recombination substrates) (62) or in core RAG knock-in mice (rearrangement made at the endogenous gene loci). In addition, core RAG mediated V(D)J recombination is frequently associated with the elevated aberrant recombination. Therefore, replacement of full length RAG with core RAG in cRAG2 knock-in mice can severely impairs T and B cell development, and increases genome instability and lymphomagenesis (63–66). These studies imply that non-core regions are indispensible to retain the efficiency and fidelity of physiological V(D)J

recombination. Although extensive mutagenesis and foot-printing assays help delineates structural domains and residues important for the cleavage reaction, (10, 45), see Figure 4 for details, the role of non-core regions of RAG1 and RAG2 have not completely defined.

Core region of RAG1

The RAG1 core region (residues 384-1008) includes three separate domains: 1) A nonamer binding domain (NBD, residues 389-442), which primarily recognize and interacts with the RSS nonamer region. 2) A central domain (residues 528-760), which interacts with RAG2 and mediates heptamer contact after initial nicking. 3) A C-terminal domain (residues 761-979) which binds to the RSS-flanking coding sequence non-specifically (10). In addition to the aforementioned distinct regions, a feature structure that is essential for the enzymatic activity of RAG1, the catalytic center, also resides in core region. The catalytic center is comprised of three discretely distributed acidic amino acids, D600, D708, E962 (51, 52, 67, 68). The “DDE” triad is highly conserved in the transpose family and functions to chelates divalent metal ions through non-covalent bonds (50, 69). The definitive role of the divalent metal ions in RAG-mediated reactions remains elusive. However, a two-metal ion principle for phosphor-transfer was proposed in the study of 3’-5’ exonuclease activity of DNA polymerase and further extended in the study of Tn5 and Tn10 transposases (70, 71), and these proteins share similar phenotypes and mechanisms with the RAG recombinase. Specifically, two

metal ions are recruited to the catalytic center through non-covalent bonds, both of which lie within bonding distance with the non-bridging oxygen of the scissile phosphate. One metal ion activates an oxygen of water molecule and promotes the formation of hydroxide ion that then executes a nucleophilic attack of the non-esterified oxygen of the scissile phosphate at the cleavage site of DNA. The other metal ion serves to stabilize the intermediate covalent species and activate the nucleophilic 3' OH to attack the 5' phosphate on the opposite strand of DNA at the cleavage site (70, 71). The active site acidic amino acids "DDE" serve to orient and coordinate the metal ions and the hydroxyl ion through salt bridges, and are the key for appropriate and sequential generation of various intermediate species that lead to the ultimate DSB formation (70–72).

Mg^{2+} is believed to be a physiological metal ion important for RAG-catalyzed cleavage, although other divalent cations can also function as a cofactor in the *in vitro* cell-free recombination system, such as Mn^{2+} or Ca^{2+} (14, 58). The detailed influence of metal ions on RAG-mediated reaction will be discussed and studied in the later chapter.

Non-core region of RAG1

Although dispensable for the *in vitro* catalysis reaction, N-terminal RAG1 is evolutionarily conserved and critical to the efficiency and fidelity of physiological V(D)J recombination (62, 63, 73–75). Even though several distinct domain structures have been identified, their function remains

poorly defined, such as cysteine-containing elements (residues 1-250), central non-core domain (CND, interacting with two zinc ions, residues 87-217), Lysine/Arginine-rich basic motifs (residues 218-264), zinc dimerization domain (ZDD, residues 265-380, dimerization of RAG) and a RINE domain located within the classic C_2H_2 zinc finger domain (within ZDD, residues 287-351). These structures have been implicated to be involved in the regulation of catalysis activity, nucleus localization, interaction with other proteins, protein stability, and ultimately the efficiency of V(D)J recombination (62, 73, 75–78). Among all N-terminal domains, the C_3HC_4 RING domain, which possesses some characteristics of a family of E3 ubiquitin ligase, has become an area of interest because of the implication of RAG1 as a self-regulator of the recombinase, besides its direct action as a recombinase (79, 80). This notion was supported in several reconstituted cell-free ubiquitination systems, where the tentative targets of RAG1 E3 ligase included KPNA1, RAG1 itself, histone H3, and RAG2, etc. (76, 81–83). However, it still remains elusive as to whether RAG1 functions *in vivo* as a single subunit E3 ligase or by collaborating with other partners to form a multi-component E3 ligase. A recent study by Swanson's group demonstrated that full-length RAG1 interact with a cullin RINE E3 ligase complex, VprBP/DDB1/Cul4A/Roc1 *in vivo*, possibly through the interaction between VprBP and the N-terminus of RAG1. Together, this complex assembled *in vitro* supports cell-free ubiquitination activity and may be accountable for the RAG1 E3 ligase activity previously

ascribed to the RAG1 (76, 82). More importantly, VprBP is required for both the high fidelity of physiological V(D)J recombination events and the normal development of B cells, since disruption of VprBP results in impairment of V_H-DJ_H and V_K-J_K rearrangement and arrest of B cell development at the pro- to pre- transition (84). This study was a big step forward towards the elucidation of RAG1 or its interaction with others to mediate ubiquitination reaction *in vivo*.

Core region of RAG2

Murine RAG2 contains an N-terminal six bladed β-propeller-like structure (residues 1-350), a middle acidic hinge region (residues360-408) and a C-terminal plant homeodomain (PHD, residues 414-487), among which the N terminal has proved to be essential for assisting the catalytic activity of RAG1, and thus is termed the core RAG2 region (62, 64–66, 85). Although there is scarce evidence for the direct binding of RAG2 to RSS, the presence of RAG2 greatly increases the binding affinity and the specificity of RAG1–RSS interactions, possibly by changing the conformation of RAG1 for better and extensive binding to the RSS, as a result of direct association between RAG1 and RAG2 (78, 86, 87).

Non-core region of RAG2

Similar to the non-core region of RAG1, the non-core region of RAG2 is also indispensable for physiological V(D)J recombination (62, 64–66). The non-core RAG2 is composed of a portion of flexible “hinge” region (residues 360-408) and a non-canonical C-terminal PHD domain

(residues 414-487) (88). The presence of an intact PHD domain is required for normal V(D)J recombination and development of the functional adaptive immune system (89). Mutations at this region are found in patients with various types of immunodeficiency, e.g. Severe combined immunodeficiency (SCID), Omenn Syndrome (OS) (78). The PHD domain interacts robustly and specifically with the modified chromatin histone H3 tri-methylated on Lys4 (H3K4me3) (89, 90), which is known associated with transcriptionally active or open chromatin regions. Disruption of the interaction between the PHD domain and H3K4me3, such as mutation of a critical residue, W453A, in the PHD domain, or reduced tri-methylation level on H3K4, can lead to severe impairment of V(D)J recombination *in vivo* (90). Therefore, the interaction between the RAG PHD domain and H3K4me3 renders chromosomal accessibility to the recombinase, which is a key regulatory mechanism to ensure lineage specificity and allelic exclusion of V(D)J recombination in developing lymphocytes (see detailed discussion in section 3). In addition, H3K4me3 can also alleviate the RAG1/2 C-terminus mediated intrinsic inhibitory effect on hairpin formation, and therefore enhance the enzymatic activity of the RAG recombinase (91). Based on the crystal structure of RAG2-PHD domain alone or the structure composed of PHD domain and H3 peptide, it was found that RAG2 PHD can recognize both tri-methylated lysine 4 and di-methylated Arginine 2, a feature that is different from the traditional PHD domain. The double recognition mechanism probably

accounts for the enhanced binding affinity of the RAG2-chromatin interactions at the transcriptional active gene loci (85). Another activity of the PHD domain is phosphatidylinositol phosphate (PIP) binding (92), although the exact function of this interaction remains unknown. Together, the interaction between RAG2 PHD domain and H3K4me3 of the chromatin can modulate the V(D)J recombination reaction in a cell. On the other hand, the flexible hinge region that contains several acidic amino acids (residues 360-408, which flanks the C-terminal core region and N-terminal non-core region) can bind to either modified or non-modified core histone. The interaction of this hinge region to core histone is of particular importance during V to DJ rearrangement on the IgH locus, although the underlying mechanism is not yet clear (93).

The non-core region is also responsible for the cell-cycle dependent degradation of RAG2 at the G1/S boundary, which is mediated through the T490 residue at the far end of the C-terminus (94). T490 is phosphorylated by the cyclin-dependent kinase Cdk2 (95). The phosphorylated RAG2 is then ubiquitination by Skp2-SCF complexes, which leads to its ultimate degradation by the 26S proteasome (96). The temporal degradation of RAG2 restricts V(D)J recombination at the G0/G1 phase of the cell cycle, thus greatly minimizes uncontrolled cleavage during the S phase and reduces genome instability (97).

V(D)J recombination is a great genetic mechanism for generating and sustaining the enormous diversity that is highly advantageous for our

adaptive immune response. However, the great diversity created by V(D)J recombination events is at the expense of genomic instability, and propensity for lymphoid malignancy. To reduce the risk of genome abnormalities, the V(D)J recombination process is tightly regulated at multiple levels, which is discussed in detail in the subsequent sections.

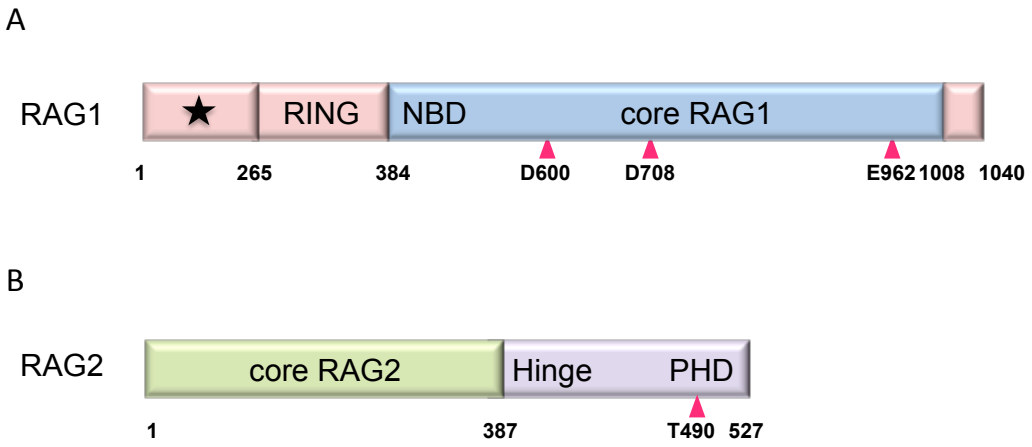

Figure 4. Schematic illustration of RAG1 and RAG2 structure.

(A) RAG1 structure, ★represent the far N-terminus region that is rich in cysteines and basic amino acids. Pink boxes represent non core region of RAG1, blue box represent core RAG1.

(B) RAG2 structure, which contains N-terminal core region (green) ,middle Hinge domain and C-terminal PHD domain (purple).

V(D)J recombination is tightly regulated at multiple levels

RAG expression is controlled at both transcriptional and post-translational level

RAG-generated DSBs are essential intermediates in the course of creating an enormous antigen receptor gene pool. Given the lethality of DSBs to a cell in the absence of appropriate and prompt repair (98), the activity of the RAG recombinase has to be stringently controlled in developing lymphocytes, which is mainly mediated *via* regulation of RAG expression, including both transcriptional and post-translational regulation (99). The RAG proteins are primarily found in B and T cells, known as lineage specificity. The expression of RAG mRNA displays two distinct waves during lymphocyte development, showing a peak at the pro-B/pro-T cell stage, followed by a decline during the expansion of pre-B/pre-T cells and then a resurge after the expansion of pre-B/pre-T cells. The first wave results in the rearrangement of immunoglobulin heavy chain (IgH) and TCRβ gene, and the second wave activates the assembly of immunoglobulin light chain (IgL) and TCRα gene (100). The transcription of RAG 1 and RAG2 is regulated by a network of transcriptional factors, such as E2A, PAX5, Foxo1 and FoxP1 (101–106). These factors act on some cis-elements to exert lineage-dependent expression, such as Erag and Ep in B cells and ASE in T cells, where these cis-elements cooperate with the promoter region to enhance transcription (107). Most studies so far have been focusing on how RAG transcription is activated by

transcriptional factors and cis-elements while the mechanisms of RAG down-regulation at the transcriptional level during the expansion of pre-B/-pre-T stages remain elusive. A recent study by Schlissel's group identified a new transcriptional repressor Gfi1b that functions as a negative regulator of RAG expression (108), opening a new avenue in the study of RAG expression regulation. In addition, signals transduced from cytokine receptors or pre-B/pre-T cell receptors can also influence the RAG expression. It has been shown that IL-7, an essential cytokine for the survival and proliferation of developing lymphocytes, plays an important role in repressing the RAG expression during the proliferating stages of pre- B or pre-T cells before IgL or TCRα locus rearrangement (103, 109, 110). Together, these factors establish a developmental specific and lineage-specific pattern of RAG expression. Recently, the PI3K/AKT signaling pathway has been implicated in relaying the signals received from B cell receptor (BCR) or IL7R in B cells, and the corresponding pathway in T cells is Abl/Erk pathway (111). For example, the B cell receptor (BCR) in immature B cells represses RAG expression through PI3K and AKT pathway. Loss of BCR signal, upon BCR internalization, causes an inhibition of the PI3K and AKT pathways and thereby results in a reduction of phosphorylation at Foxo1 and Foxo3A, which ultimately leads to elevated RAG expression, as non- or low phosphorylated Foxo1 and Foxo3A function as positive regulators of the RAG gene (107). On the other hand, the cell cycle progression promoted by IL-7 exerts another

level of controls on RAG expression. Oscillation of RAG2 expression level in dividing lymphoid cells was first observed by Desiderio's group and the corresponding change was not observed in its steady-state transcript level, implying a post-transcriptional regulation (94). Subsequent studies further defined the underlying mechanism of this cell-cycle dependent RAG2 regulation at the post-translational level, i.e., RAG2 protein degradation targeted at S/G2/M phases. Mutagenesis revealed that the major determinant of RAG2 instability is Threonine 490, which is a phosphorylation site by the cyclin-dependent kinase 2, cdk2. The phosphorylated T490 residue serves as a signal for RAG2 degradation. Indeed, cyclin/cdk2 has been proved to be a positive regulator of RAG2 degradation through both genetic approaches and biochemical approaches (95). On the other hand, an inhibitor of cyclin-dependent kinase, p21, was considered a negative regulator of RAG2 degradation, because of its ability to induce cdk2 down-regulation. (95) Mutation of Thr490 disrupts the cdk2-mediated phosphorylation, thus completely abolishing cell cycle dependent RAG2 degradation (94). Furthermore, cell extracts isolated at different cell cycle stages recapitulated the *in vivo* feature of cell-cycle dependent appearance of RAG2. The biochemical characterization in these cell-free systems demonstrated that the RAG2 degradation is induced by the ubiquitin-mediated proteasomal degradation pathway. In particular, an E3 ligase SCF-Skp2, that is well known to promote cell cycle progression through the ubiquitination-mediated

disruption of p27, was found to also ubiquitinate T490-phosphorylated RAG2 proteins, leading to their degradation (96). Thus, cell cycle dependent RAG2 degradation couples the V(D)J recombination reaction to the cell cycle control, restricting V(D)J recombination to G0/G1 phase. This restriction not only minimizes the potential genomic instability caused by DSB in the cycling cell but also limits the repair of RAG-mediated DSB solely to NHEJ, which is a DNA repair pathway prevalent in the G1 phase (97). In addition to the cell cycle dependent post-translational regulation, as well as the transcriptional regulation, other mechanisms may also exist to account for the delicate control of RAG protein level, which will be discussed in more detail in chapter 5.

Target specificity determined by RSS

The recombination signal sequence (RSS) is an essential component for RAG-mediated site-specific recombination and it determines the specific recognition, binding, and cleavage of RAG at the variable region gene segments of Ig and TCR loci (58). This notion has been further substantiated by an *in vivo* ChIP-seq (chromatin immunoprecipitation-sequence) study, proving that RSS is the main determinant for RAG1 binding (112). The RSS is composed of a heptamer and a nonamer, separated by a spacer region of either 12 or 23 base pairs, based on which 12 RSS and 23RSs are defined. The RSS nonamer is the main binding surface for the RAG1 NBD domain, which mediates the initial binding of RAG to RSS. Heptamer region mediates the initial

recognition of RAG-RSS and provides the binding surface for RAG after the cleavage step (113, 114). The heptamer region is the most conserved component of the RSS, with the first three nucleotides “CAC” having more than 99% conservation among all RSSs. A mutation of any one of these nucleotides will completely abolish the RAG-mediated reaction. The last four nucleotides of the heptamer (77-91% conservation) and the nonamer (some positions less than 75% conservation) are less conserved. The spacer region is conserved in length, with either 12±1 or 23±1 base pairs, and bears a relatively variable sequence when compared to the heptamer and nonamer regions (115). However, some positions of the spacer are not completely subjected to random exchanges because they show a certain level of conservation among all the available RSS (40-60%) (115). Moreover, using experimental approaches, another group showed that the spacer sequence plays a determinant role in the frequency of recombination in the reconstitute cell free system and the *in vitro* effect correlates very nicely with the efficiency of rearrangement *in vivo* (116). Notably, despite a certain level of variation, RSSs adjoining V, D, J gene segments are still readily recognized and bound by RAG recombinase, indicating that RAG bares a wide-range of tolerance to recognize variable RSSs, which is advantageous in generating the diversified repertoire of antibodies and TCRs that is essential for the adaptive immune system (117). However, the intrinsic flexibility of the recognition between RAG and RSS increases the risk of potential mis-targeting of non-RSSs at the sites

other than legitimate *Ig* or TCR loci, invoking genome instability. Indeed, RAG was found to recognize and cleave cryptic RSS sites, causing aberrant DSB and aberrant repair, and at times, oncogenic chromosome translocationss, which have been a major cause of lymphoid neoplasm (118). Taken together, the relative conservation of the RSS, especially the heptamer and the nonamer, allows the direct recognition and specific interaction between RAG and the target gene segments, thereby establishing the site specificity of V(D)J recombination. On the other hand, the variation of RSS sequence, especially at the spacer region, seems to modulate the efficiency of RAG mediated reaction which in turn might account for the unequally usage of different gene segments during V(D)J recombination (119, 120). Therefore, an appropriate balance between conservation and variation of the RSS seem to play an important role in retaining the diversity and fidelity of V(D)J recombination as well as genome stability.

In addition to regulating the fidelity and efficiency of V(D)J recombination, the RSS also enforces an appropriate order of rearrangement that involves different V, D and J segments, the “12/23” rule, i.e. only gene segments that are flanked with different RSS can be joined together (14, 15, 121). One significant example of “12/23”rule is that it prevents the direct joining of V_H to J_H segment during the generation of the variable region of the heavy chain because they are both flanked with the 23RSS. Rather, 12/23 rule ensures that D_H is placed in between V_H

and J_H, since D_H has 12RSS on both sides and thus is eligible to be linked with both V_H and J_H. The detailed mechanism of how the 12RSS and the 23RSS are brought together to form a synaptic complex remains unclear. Previously, it was hypothesized that the synaptic complex was formed through the capture of a 23RSS gene segment by a pre-formed 12RSS-RAG complex (15, 16, 122). However, a recent *in vivo* study by CHIP-Seq (Chromatin immunoprecipitation-sequence) demonstrates that the initial RSS engagement is not restricted to the 12RSS, rather it occurs with whichever RSS is found within the recombination centers followed by recruiting the partner RSS, which argues against the sequential capture of the 12RSS and the 23RSS (112). Nevertheless, 12/23 rule ensures the correct order of rearrangement and thus the fidelity of V(D)J recombination.

Despite the importance of “12/23 rule”, the RSS seems to impose additional constraints on variable region gene assembly beyond the scope of the “12/23” rule. For example, during rearrangement of β chain of the TCR, V_β does not directly link to J_β although they are flanked with different RSS and thus is compatible with “12/23” rule. This phenomenon is referred as “beyond 12/23”, the detailed mechanism has not been clearly defined, but it has been suggested that the restriction may be imposed during the DNA cleavage step of TCR beta rearrangement. Specifically, a low level and slow nicking made at the J_β region and inefficient V_β-J_β synapses have been speculated to hinder the V_β to J_β rearranging process

(123). Subsequent analyses suggest that the poor V_β-to-J_β recombination activity is attributed to the coding flank and RSS sequence at the J_β locus, further substantiating the importance of the RSS in regulating V(D)J recombination at various levels (124).

Control of V(D)J recombination at chromosomal level

Although the highly controlled RAG expression and the composition of the RSS sequence dictates the site-specific V(D)J recombination in cell-cycle dependent and developmental stage-ordered fashion, some aspects of the regulation of V(D)J recombination are incompletely defined. For example, V(D)J recombination is restricted to the *Ig* locus or the *TCR* locus in developing B or T cells, respectively, despite the availability of RAG recombinase in both cell types (125, 126). Meanwhile, it was consistently found that rearrangement is preceded by the transcription activation and changes of chromatin modifications, such as the appearance of RNA transcripts that define the boundary of rearrangement domain, nucleosome remodeling, and activating histone modifications such as acetylation (127, 128).The tight link between transcription and rearrangement suggests the possibility that chromosomal accessibility underlines the distinct pattern of V(D)J recombination observed in different cell types. Previously, it was thought that an open (enriched with activating histone modifications, such as acetylation) or a closed state (primaryly with repressing histone modifications, such as H3K9me3) of chromatin alone determined the accessibility (129). Recent finding that the RAG2

PHD domain interacting specifically with H3K4me3 (histone 3 tri-methylated at Lysine 4, reviewed in previous section) suggested that the RAG recombinase not only passively obeys the chromatin code (i.e., RSS in the context of chromosome), but also actively participates in recognizing the chromosomal modification that reflects the accessibility of the locus. The chromatin accessibility is likely created through interactions between local cis-elements, e.g. enhancers or promoters, and trans-acting factors, e.g. transcriptional factors that can recruit nucleosome remodeling machinery and chromatin modifying enzymes and RNA polymerase II, increasing transcription activity through the region. In addition to histone modification, other epigenetic modulations, such as *de novo* demethylation of DNA at the *Ig* or *TCR* loci, have also been shown to occur prior to the rearrangement. Together, chromatin modifications at both histone and DNA contribute to the chromatin accessibility (130, 131). Furthermore, the important role of chromatin accessibility in regulating V(D)J recombination was further substantiated by Schatz's group in a whole genome-wide ChIP analysis (112). They demonstrated that RAG1 and RAG2 each have distinct *in vivo* binding patterns to the genome that are independent of each other, with RAG1 binding more tightly to the RSS regions whereas RAG2 binding more broadly at sites with substantial levels of H3K4me3. Each of these small RAG-bound regions that contain both RAG1 and RAG2 is referred to a "recombination center" and the formation of these "recombination centers" is highly dynamic, displaying a

developmental stage-specificity and lineage specificity. The more restricted RAG1 binding contrasts with the loose binding of RAG2, which prevents the RAG-1 mediated non-specific targeting and cleavage , thereby minimizing genome instability. However, the broad RAG2 binding to the whole genome may introduce an additional regulatory function of V(D)J recombination, e.g., by increasing recombination activity at the accessible gene loci (112). Together, these studies show that chromosomal accessibility play an important role in regulating and maintaining the specificity and fidelity of V(D)J recombination.

Regulation of V(D)J recombination at the cleavage reaction step

The RAG-mediated cleavage reaction is the first phase of V(D)J recombination, which involves a collaboration of multiple factors, such as the RAG recombinase, RSS, HMG and a metal ion cofactor, as well as epigenetic modifications on the chromatin as discussed above.. The importance of the RAG recombinase and the RSS has been summarized in the previous sections. Briefly, RAG is the major machinery of V(D)J recombination and mutations of RAG can cause loss of recombination activity and block of lymphocyte development in varying degrees of seriousness (12–14). The RSS is the major target site of RAG and depending on how closely it resembles the consensus RSS, it can determine cleavage efficiency and the usage frequency of the adjoining coding gene segment. Illegitimate RAG activity has been implicated in chromosomal translocations, through recognition and cleavage made by

RAG at cryptic RSS or distorted DNA structure, consequence of which is devastating and is a major cause for lymphoid malignancy (132).

Although not as essential as RAG, the HMG protein also plays a role in regulating the efficiency and fidelity of V(D)J recombination by promoting synaptic complex formation and stimulating coupled cleavage involving both 12RSS and 23RSS. The probable function of HMG is to facilitate DNA bending, which become more accommodative to the RAG binding and DNA excision (19, 133). On the other hand, HMG by itself can recognize and stabilize distorted DNA structures and damaged DNA. This activity may also induce the mis-targeting and cleavage of RAG at a region that does not have an authentic RSS, thereby increasing the chances of illegitimate RAG-mediated cleavage and potential genome instability (132). Last but not least, a metal ion cofactor is essential for the RAG-mediated cleavage reaction (14, 21). A detailed mechanism of how the metal ion modulates physiological V(D)J recombination remains elusive, which is primarily due to the complexity of *in vivo* metal ion condition in terms of their composition and concentration. The complicated background of metal ion makes it impossible to definitively determine the metal ion condition prerequisite for V(D)J recombination *in vivo*. Hence most knowledge of metal ion participation in V(D)J recombination has been obtained from *in* vitro reconstituted cell free systems. The essential role of divalent metal ions in V(D)J recombination was first suggested based on the finding that addition of EDTA to the nuclear extracts resulted

in complete abolishment of the RAG-mediated cleavage activity (14). Mg^{2+} was later found to be the physiological metal ion cofactor because the RAG-mediated cleavage reaction in Mg^{2+} requires two RSSs bearing different spacer lengths for efficient cleavage and hairpin formation, which was consistent with the physiological "12/23"rule, while a single RSS is only nicked by RAG at the coding-signal junction in the presence of Mg^{2+} (14, 134). Besides Mg^{2+}, other metal ions have also been tested in the *in vitro* recombination system although their roles in physiological V(D)J recombination remain unclear. Mn^{2+} uncouples the requirement of the "12/23" rule and promotes the nicking and hairpin formation on single RSS, thus Mn^{2+} is considered a permissive cation (15). On the contrary, Ca^{2+}only allows the specific interaction between RAG and RSS but does not support RAG enzymatic activities (15). The various outcomes in the presence of different cations (as shown in Figure 5) have been attributed to the ability of the cations to induce different RAG conformations that allow different RAG-RSS interactions (135). For example, Mn^{2+} confers RAG to form a structure that is more amiable to cleavage on RSS substrates and has a very loose requirement in terms of temperature, pH, HMG intactness and RSS fidelity, in stark contrast to the more demanding requirement when Mg^{2+} is present, which induces a less poised RAG architecture and thus is forced to coordinate multiple factors to achieve the catalysis stage (21, 72, 136). However, the stringent requirement and relative inert nature of RAG-mediated cleavage in the presence of Mg^{2+}

ensures the rigorous and elegant multi-layered regulations during physiological V(D)J recombination, which helps to minimize the genome instability caused by aberrant activity of RAG. In conclusion, metal ion cofactors seem to participate not only in the catalysis step, but also in determining RAG conformation, RAG-RSS recognition and binding, and the structure of the pre-cleavage complex. Along this line, it is intriguing to think that metal ions may also affect the post-cleavage complex, which will be discussed in more detail in chapter 2.

End joining process mediated by Classic-NHEJ pathway

The RAG-cleaved DSB is primarily resolved by the non-homologous end joining (NHEJ) pathway, which is considered the second phase of V(D)J recombination (137). Selection of NHEJ in V(D)J recombination is very significant, because it not only mediates the joining of broken ends, the error-prone nature of NHEJ also promotes the introduction of additional variation at the junction (junctional diversity) during the joining process (138) which is one of the major sources accounting for the diversity of V(D)J recombination (2). Four recombination ends are generated during the first phase of V(D)J recombination, two hairpin coding ends (HP-CEs) and two blunt signal ends (SEs). HP-CEs need to be opened before joining, which can occur asymmetrically (35, 38). The opening of HP-CEs made away from the apex site, which is catalyzed by the concerted action of Artemis and DNA-PKcs, can give rise to palindromic nucleotide addition, known as P

nucleotides (27). In addition, opened coding ends can also be subjected to nucleotide deletion by exonuclease, and non-templated nucleotide addition mediated by terminal deoxynucleotidyl Transferase (TdT) (28). The deletion and addition of nucleotides during this process is somewhat random in terms of the sequence and number (usually less than 10), therefore introduces an additional level of variations at the coding joints.

Furthermore, NHEJ occurs throughout the cell cycle and is the major DSB repair pathway in the cells at the G1 stage, unlike the homologous recombination (HR), which is restricted to the late S and G2 phases (25). Thus, NHEJ is the most suitable pathway in repairing the RAG-generated DSB, as it coincides with the RAG activity that is also limited to the G1 phase (94, 139). The timely resolving of RAG-generated DSB in the G1 phase is essential to efficiently avoid the deleterious effect of unresolved DSBs to a cycling cell.

Although the V(D)J recombination reaction relies on the NHEJ machinery for the generation of a functional repertoire of antigen receptors, alterations of this machinery does not completely abolish repair of RAG-generated DSBs, suggesting the existence of other DSB repair pathways for resolving the recombination ends (140–142). One possible candidate of the substitute repair is alternative-NHEJ, known as a-NHEJ, which is characterized by frequent usage of micro-homology that relies on excessive deletions (142). The process of a-NHEJ results in aberrant joining products with extensive nucleotide deletions and even

chromosomal translocations, which are rarely observed in the junction made by the classic NHEJ (c-NHEJ). Alternative-NHEJ occurs at an extremely low level in wild type cells but shows significantly elevated activity in cells defective in c-NHEJ and thereby provides a back-up repair system to the c-NHEJ-deficient cells. However, due to its error-prone nature in DSB repair, a-NHEJ is frequently implicated in the tumorigenesis, presumably by distablizing genome stability, e.g., in human bladder tumors (118, 143). Therefore, increased repair by this pathway in V(D)J recombination may cause chromosome translocations, and oncogenic transformation, leading to development of lymphoid malignancy. Thus, in the absence of functional c-NHEJ, RAG recombinase has to collaborate with the a-NHEJ machinery for end joining. In addition, the defective recombinase, due to mutations in RAG1 and RAG2, has also been speculated to be “forced” into this error-prone a-NHEJ for rejoining the ends. Indeed, a recent study showed that the core form of RAG2 (cRAG2) lacking C-terminus tends to channel DNA ends to the alternative-NHEJ pathway for DNA ends resolution, As a result, severely disruptive genome stability and robust thymic lymphoma was observed in the cRAG2-knock in-mice that were also p53 deficient (64). Fortunately, in wild-type cells, a-NHEJ is greatly suppressed by classic-NHEJ, which is mainly mediated by the core classic-NHEJ components, such as Ku, DNA-PK, and XRCC4-LigIV (144–146). In summary, NHEJ-mediated RAG DSB repair plays an essential role in regulating V(D)J

recombination, 1) It introduces further variations to the antigen receptor gene repertoire, which is pivotal to the adaptive immune system. 2) It retains genome stability by inhibiting the detrimental effects caused by unattended RAG DSB. 3) It suppresses other undesired DNA repair pathways, thereby minimizing the chances of genomic instability.

Regulation of the transition between phase I and phase II during V(D)J recombination

Although V(D)J recombination has two seemingly distinctive phases, i.e., RAG-catalyzed cleavage and NHEJ-mediated joining, more and more evidence shows that RAG machinery and NHEJ machinery collaborate closely in order for the proper function of V(D)J recombination. Most evidences have been derived from *in vitro* recombination studies, such as: (1) the presence of Ku and DNA-PKcs proteins in the RAG-mediated reactions seemed to modulate the cleavage activity and to increase the fidelity of 12/23 rule by inhibiting 12/12 and 23/23 DNA cleavage (147); (2) Ku was found to directly interact with the non-core region of full length RAG1 (148); (3) Intentionally linking the non-RAG-mediated-DSB to the RAG recombinase complexes directed the DSB to the NHEJ pathway, suggesting the active role of RAG in selecting an appropriate DNA repair pathway (149). However, the most convincing evidence for the tight interactions between phase I and phase II is the revelation of several RAG2 mutants that have normal cleavage activity but display a severe defects in joining, either by impairing the recruitment of

the NHEJ component or by blocking the hairpin opening process (41). More importantly, RAG was believed to continuously retain the newly cleaved DSBs in a stable post-cleavage complex (PCC), and shepherd them to the NHEJ machinery. The failure to maintain PCC stability as observed in certain RAG mutations has been implicated in causing an increased tendency of aberrant DNA repair pathways, such as HR or alternative-NHEJ (39, 150, 151). These findings significantly substantiate the importance of RAG throughout V(D)J recombination, both cleavage and resolution phases, and further prove the tight collaboration between the two. By far, the importance of RAG in the joining step has been mostly attributed to the stability of the post-cleavage complex (PCC, see nomenclature), which seems vital for appropriate and efficient repair during V(D)J recombination and a major causal factor for aberrant joining of RAG DSB and potential genomic instability if the PCC stability is compromised in any way (64, 151, 152). Therefore, it is of great importance to identify and characterize the factors that influence the PCC stability. In addition to RAG mutations, the sequence alteration of the heptamer in a RSS and mutations in a checkpoint protein, ATM, has also been found to reduce PCC stability. These genetic alterations result in higher levels of recombination ends being directed to the HR and alternative-NHEJ, leading to genome instability like chromosomal translocations, and a high frequency of lymphoid malignancies (118, 153).

It has been noted that, after cleavage, RAG retains all four DNA ends in the PCC, including two signal ends and two hairpin coding ends (40, 154), which differ in the strength of retention, the end processing steps, the requirement of NHEJ factors, as well as the rate and precision of resolution (9, 23). Thus, depending on the compositttion of the DNA ends, the PCC has evolved into two sub-complexes, the signal end complex (SEC) and the coding end complex (CEC). As a matter of fact, all of the aforementioned studies on PCC stability were focused on the SEC stability because it is intrinsically stable, thus any changes in signal ends retention can be readily detected. HP-CEs, on the other hand, were believed to be only transiently associated with the RAG complex. And the weak binding makes it relatively difficult to characterize these complexes, except for some indirect evidences (38, 58). Since the fate of coding ends are more significantly important than signale ends in generating antigen receptor diversity as well as preserving genome integrity, it is important to study the interaction and retention of coding ends within the CEC and the factors that might influence CEC stability. However, the effort to address these issues has yielded little progress, because of technical difficulties in revealing very weak interactions. Here I explore two complementary fluorescence-based techniques, steady-state fluorescence anisotropy and fluorescence resonance energy transfer (FRET), to 1) monitor the RAG-mediated recombination reaction in real time and measure the stability of PCC in terms of HP-CEs retention, 2) assess many parameters that might

affect the HP-CEs retention, such as metal ion cofactors, non-core regions of the RAG recombinase, and various forms of RAG mutations, 3) compare the retention of HP-CEs and SEs in the same monitoring system under various conditions, allowing for examination in depth the mechanism of retaining HP-CEs and SEs. Our study introduces a powerful tool to study the biochemistry of the RAG recombination and may shed some light on the mechanism of physiological V(D)J recombination. Furthermore, the PCC could also be regulated by targeted destruction, i.e., RAG1-mediated degradation of RAG complex. By comparing expression of core and full-length RAG1 and RAG2 in transient transfection assays, I provided evidence for a rapid regulatory mechanism, which could promptly eliminate the RAG-mediated pre-cleavage and post-cleavage complexes.

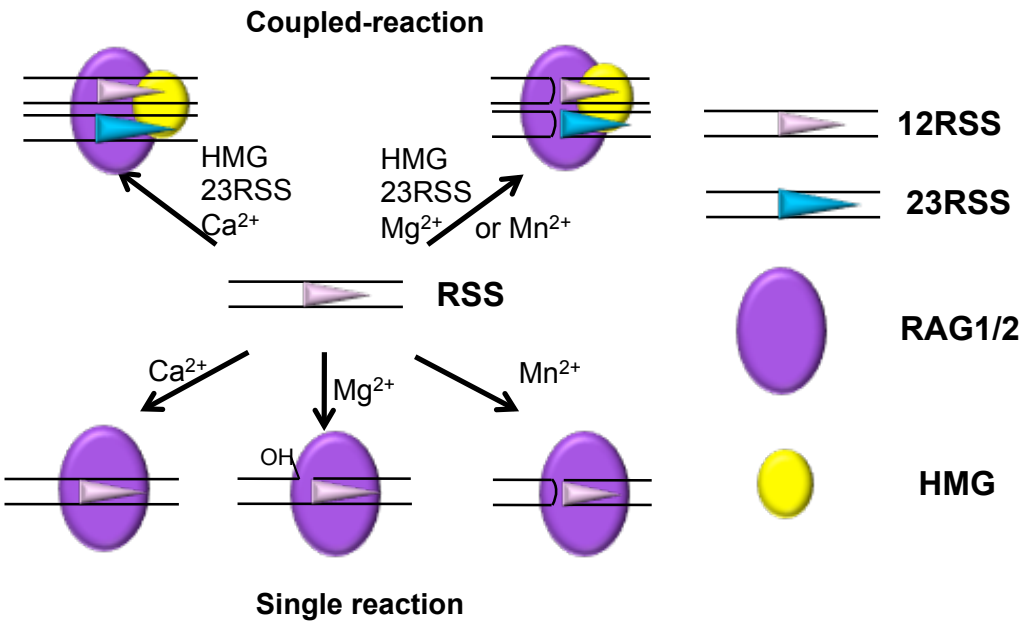

Figure 5. *In vitro* RAG-mediated cleavage reaction under three cations.

Mg^{2+} requires the formation of synaptic complex that is composed of both 12RSS and 23RSS in order to generate double strand breaks. Mg^{2+} only allows nicking with a single RSS.

Mn^{2+} induces cleavage on a single RSS without synapsis.

Ca^{2+} supports specific binding but is inhibitory of cleavage.

Reference

1. Cooper MD, Alder MN (2006) The Evolution of Adaptive Immune Systems. *Cell* 124:815–822.

2. Murphy KM, Travers P, Walport M (2007) *Janeway's Immunobiology (Immunobiology: The Immune System* (Garland Science). 7th Ed.

3. Hozumi N, Tonegawa S (1976) Evidence for somatic rearrangement of immunoglobulin genes coding for variable and constant regions. *Proc. Natl. Acad. Sci. U.S.A.* 73:3628–3632.

4. Alt FW, Baltimore D (1982) Joining of Immunoglobulin Heavy Chain Gene Segments: Implications from a Chromosome with Evidence of Three D-JH Fusions. *PNAS* 79:4118–4122.

5. Lewis S, Gellert M (1989) The mechanism of antigen receptor gene assembly. *Cell* 59:585–588.

6. Brack C, Hirama M, Lenhard-Schuller R, Tonegawa S (1978) A complete immunoglobulin gene is created by somatic recombination. *Cell* 15:1–14.

7. Early P, Huang H, Davis M, Calame K, Hood L (1980) An immunoglobulin heavy chain variable region gene is generated from three segments of DNA: VH, D and JH. *Cell* 19:981–992.

8. Lieber MR (2010) The Mechanism of Double-Strand DNA Break Repair by the Nonhomologous DNA End-Joining Pathway. *Annual Review of Biochemistry* 79:181–211.

9. Rooney S, Chaudhuri J, Alt FW (2004) The role of the non-homologous end-joining pathway in lymphocyte development. *Immunol. Rev.* 200:115–131.

10. Schatz DG, Swanson PC (2011) V(D)J recombination: mechanisms of initiation. *Annu. Rev. Genet.* 45:167–202.

11. Gellert M (2002) V(D)J RECOMBINATION: RAG PROTEINS, REPAIR FACTORS, AND REGULATION*. *Annual Review of Biochemistry* 71:101–132.

12. Oettinger MA, Schatz DG, Gorka C, Baltimore D (1990) RAG-1 and RAG-2, Adjacent Genes That Synergistically Activate V(D)J Recombination. *Science* 248:1517–1523.

13. Schatz DG, Oettinger MA, Baltimore D (1989) The V(D)J recombination activating gene, RAG-1. *Cell* 59:1035–1048.

14. van Gent DC et al. (1995) Initiation of V(D)J recombination in a cell-free system. *Cell* 81:925–934.

15. Hiom K, Gellert M (1997) A stable RAG1-RAG2-DNA complex that is active in V(D)J cleavage. *Cell* 88:65–72.

16. Mundy CL, Patenge N, Matthews AGW, Oettinger MA (2002) Assembly of the RAG1/RAG2 Synaptic Complex. *Mol Cell Biol* 22:69–77.

17. McBlane JF et al. (1995) Cleavage at a V(D)J recombination signal requires only RAG1 and RAG2 proteins and occurs in two steps. *Cell* 83:387–395.

18. van Gent DC, Mizuuchi K, Gellert M (1996) Similarities between initiation of V(D)J recombination and retroviral integration. *Science* 271:1592–1594.

19. van Gent DC, Hiom K, Paull TT, Gellert M (1997) Stimulation of V(D)J cleavage by high mobility group proteins. *EMBO J* 16:2665–2670.

20. Sawchuk DJ et al. (1997) V(D)J Recombination: Modulation of RAG1 and RAG2 Cleavage Activity on 12/23 Substrates by Whole Cell Extract and DNA-bending Proteins. *The Journal of Experimental Medicine* 185:2025 –2032.

21. Santagata S, Aidinis V, Spanopoulou E (1998) The effect of Me2+ cofactors at the initial stages of V(D)J recombination. *J. Biol. Chem* 273:16325–16331.

22. Bassing CH, Swat W, Alt FW (2002) The mechanism and regulation of chromosomal V(D)J recombination. *Cell* 109 Suppl:S45–55.

23. Lieber MR (2010) The Mechanism of Double-Strand DNA Break Repair by the Nonhomologous DNA End-Joining Pathway. *Annu. Rev. Biochem.* 79:181–211.

24. Helmink BA, Sleckman BP (2011) The Response to and Repair of RAG-Mediated DNA Double-Strand Breaks. *Annual Review of Immunology*. Available at: http://www.ncbi.nlm.nih.gov/pubmed/22224778 [Accessed March 24, 2012].

25. Mao Z, Bozzella M, Seluanov A, Gorbunova V (2008) Comparison of nonhomologous end joining and homologous recombination in human cells. *DNA Repair (Amst.)* 7:1765–1771.

26. Mao Z, Bozzella M, Seluanov A, Gorbunova V (2008) DNA repair by nonhomologous end joining and homologous recombination during cell cycle in human cells. *Cell Cycle* 7:2902–2906.

27. Lewis SM (1994) P nucleotides, hairpin DNA and V(D)J joining: making the connection. *Semin. Immunol.* 6:131–141.

28. Gilfillan S, Dierich A, Lemeur M, Benoist C, Mathis D (1993) Mice lacking TdT: mature animals with an immature lymphocyte repertoire. *Science* 261:1175–1178.

29. Downs JA, Jackson SP (2004) A means to a DNA end: the many roles of Ku. *Nat Rev Mol Cell Biol* 5:367–378.

30. Mari P-O et al. (2006) Dynamic assembly of end-joining complexes requires interaction between Ku70/80 and XRCC4. *Proceedings of the National Academy of Sciences* 103:18597 –18602.

31. Gottlieb TM, Jackson SP (1993) The DNA-dependent protein kinase: requirement for DNA ends and association with Ku antigen. *Cell* 72:131–142.

32. Yaneva M (1997) Interaction of DNA-dependent protein kinase with DNA and with Ku: biochemical and atomic-force microscopy studies. *The EMBO Journal* 16:5098–5112.

33. Meek K, Douglas P, Cui X, Ding Q, Lees-Miller SP (2007) trans Autophosphorylation at DNA-dependent protein kinase's two major autophosphorylation site clusters facilitates end processing but not end joining. *Mol. Cell. Biol* 27:3881–3890.

34. Mahaney BL, Meek K, Lees-Miller SP (2009) Repair of ionizing radiation-induced DNA double strand breaks by non-homologous end-joining. *Biochem J* 417:639–650.

35. Moshous D et al. (2001) Artemis, a Novel DNA Double-Strand Break Repair/V(D)J Recombination Protein, Is Mutated in Human Severe Combined Immune Deficiency. *Cell* 105:177–186.

36. Ma Y, Pannicke U, Schwarz K, Lieber MR (2002) Hairpin opening and overhang processing by an Artemis/DNA-dependent protein kinase complex in nonhomologous end joining and V(D)J recombination. *Cell* 108:781–794.

37. Lieber MR (2008) The mechanism of human nonhomologous DNA end joining. *J. Biol. Chem* 283:1–5.

38. Lu H et al. (2008) A Biochemically Defined System for Coding Joint Formation in V(D)J Recombination. *Mol Cell* 31:485–497.

39. Tsai C-L, Drejer AH, Schatz DG (2002) Evidence of a critical architectural function for the RAG proteins in end processing, protection, and joining in V(D)J recombination. *Genes & Development* 16:1934 – 1949.

40. Agrawal A, Schatz DG (1997) RAG1 and RAG2 Form a Stable Postcleavage Synaptic Complex with DNA Containing Signal Ends in V(D)J Recombination. *Cell* 89:43–53.

41. Qiu JX, Kale SB, Yarnell Schultz H, Roth DB (2001) Separation-of-function mutants reveal critical roles for RAG2 in both the cleavage and joining steps of V(D)J recombination. *Mol. Cell* 7:77–87.

42. Sekiguchi J, Whitlow S, Alt FW (2001) Increased Accumulation of Hybrid V(D)J Joins in Cells Expressing Truncated versus Full-Length RAGs. *Molecular Cell* 8:1383–1390.

43. Elkin SK, Matthews AG, Oettinger MA (2003) The C-terminal portion of RAG2 protects against transposition in vitro. *EMBO J* 22:1931–1938.

44. Neiditch MB, Lee GS, Landree MA, Roth DB (2001) RAG Transposase Can Capture and Commit to Target DNA before or after Donor Cleavage. *Mol Cell Biol* 21:4302–4310.

45. Swanson PC (2004) The bounty of RAGs: recombination signal complexes and reaction outcomes. *Immunol. Rev.* 200:90–114.

46. Posey JE, Pytlos MJ, Sinden RR, Roth DB (2006) Target DNA Structure Plays a Critical Role in RAG Transposition. *PLoS Biol* 4:e350.

47. Fugmann SD, Messier C, Novack LA, Cameron RA, Rast JP (2006) An ancient evolutionary origin of the Rag1/2 gene locus. *Proc. Natl. Acad. Sci. U.S.A.* 103:3728–3733.

48. Sebastian D. F (2010) The origins of the Rag genes—From transposition to V(D)J recombination. *Seminars in Immunology* 22:10–16.

49. Sakano H, H|[uuml]|ppi K, Heinrich G, Tonegawa S (1979) Sequences at the somatic recombination sites of immunoglobulin light-chain genes. *, Published online: 26 July 1979; | doi:10.1038/280288a0* 280:288–294.

50. Dreyfus DH, Jones JF, Gelfand EW (1999) Asymmetric DDE (D35E)-like sequences in the RAG proteins: implications for V(D)J recombination and retroviral pathogenesis. *Med. Hypotheses* 52:545–549.

51. Landree MA, Wibbenmeyer JA, Roth DB (1999) Mutational analysis of RAG1 and RAG2 identifies three catalytic amino acids in RAG1 critical for both cleavage steps of V(D)J recombination. *Genes Dev* 13:3059–3069.

52. Kim DR, Dai Y, Mundy CL, Yang W, Oettinger MA (1999) Mutations of acidic residues in RAG1 define the active site of the V(D)J recombinase. *Genes Dev* 13:3070–3080.

53. Max EE, Seidman JG, Leder P (1979) Sequences of Five Potential Recombination Sites Encoded Close to an Immunoglobulin Kappa Constant Region Gene. *PNAS* 76:3450–3454.

54. Ferrier P ed. *V(D)J Recombination* Available at: http://www.springerlink.com/content/978-1-4419-0296-2#section=641426&page=1 [Accessed March 23, 2012].

55. Schatz DG (2004) Antigen receptor genes and the evolution of a recombinase. *Semin. Immunol.* 16:245–256.

56. Jones JM, Gellert M (2004) The taming of a transposon: V(D)J recombination and the immune system. *Immunol. Rev.* 200:233–248.

57. Litman GW, Rast JP, Fugmann SD (2010) The origins of vertebrate adaptive immunity. *Nat. Rev. Immunol.* 10:543–553.

58. Fugmann SD, Lee AI, Shockett PE, Villey IJ, Schatz DG (2000) The RAG proteins and V(D)J recombination: complexes, ends, and transposition. *Annu. Rev. Immunol* 18:495–527.

59. Cuomo CA, Oettinger MA (1994) Analysis of regions of RAG-2 important for V(D)J recombination. *Nucleic Acids Res.* 22:1810–1814.

60. Silver DP, Spanopoulou E, Mulligan RC, Baltimore D (1993) Dispensable sequence motifs in the RAG-1 and RAG-2 genes for plasmid V(D)J recombination. *Proc. Natl. Acad. Sci. U.S.A.* 90:6100–6104.

61. Kirch SA, Sudarsanam P, Oettinger MA (1996) Regions of RAG1 protein critical for V(D)J recombination. *European Journal of Immunology* 26:886–891.

62. Steen SB, Han J-O, Mundy C, Oettinger MA, Roth DB (1999) Roles of the "Dispensable" Portions of RAG-1 and RAG-2 in V(D)J Recombination. *Molecular and Cellular Biology* 19:3010 –3017.

63. Dudley DD et al. (2003) Impaired V(D)J Recombination and Lymphocyte Development in Core RAG1-Expressing Mice. *J Exp Med* 198:1439–1450.

64. Deriano L et al. (2011) The RAG2 C terminus suppresses genomic instability and lymphomagenesis. *Nature* 471:119–123.

65. Akamatsu Y et al. (2003) Deletion of the RAG2 C Terminus Leads to Impaired Lymphoid Development in Mice. *PNAS* 100:1209–1214.

66. Liang H-E et al. (2002) The "dispensable" portion of RAG2 is necessary for efficient V-to-DJ rearrangement during B and T cell development. *Immunity* 17:639–651.

67. Huye LE, Purugganan MM, Jiang M-M, Roth DB (2002) Mutational analysis of all conserved basic amino acids in RAG-1 reveals catalytic,

step arrest, and joining-deficient mutants in the V(D)J recombinase. *Mol. Cell. Biol* 22:3460–3473.

68. Fugmann SD, Villey IJ, Ptaszek LM, Schatz DG (2000) Identification of two catalytic residues in RAG1 that define a single active site within the RAG1/RAG2 protein complex. *Mol. Cell* 5:97–107.

69. Dreyfus DH (2006) The DDE recombinases: diverse roles in acquired and innate immunity. *Ann. Allergy Asthma Immunol* 97:567–576; quiz 576–578, 602.

70. Beese LS, Steitz TA (1991) Structural basis for the 3'-5' exonuclease activity of Escherichia coli DNA polymerase I: a two metal ion mechanism. *EMBO J.* 10:25–33.

71. Lovell S, Goryshin IY, Reznikoff WR, Rayment I (2002) Two-metal active site binding of a Tn5 transposase synaptic complex. *Nat Struct Mol Biol* 9:278–281.

72. Allingham JS, Pribil PA, Haniford DB (1999) All three residues of the Tn10 transposase DDE catalytic triad function in divalent metal ion binding. *Journal of Molecular Biology* 289:1195–1206.

73. McMahan CJ, Difilippantonio MJ, Rao N, Spanopoulou E, Schatz DG (1997) A basic motif in the N-terminal region of RAG1 enhances V(D)J recombination activity. *Mol Cell Biol* 17:4544–4552.

74. Noordzij JG et al. (2000) N-Terminal Truncated Human RAG1 Proteins Can Direct T-Cell Receptor but Not Immunoglobulin Gene Rearrangements. *Blood* 96:203–209.

75. Santagata S et al. (2000) N-Terminal RAG1 Frameshift Mutations in Omenn's Syndrome: Internal Methionine Usage Leads to Partial V(D)J Recombination Activity and Reveals a Fundamental Role in Vivo for the N-Terminal Domains. *PNAS* 97:14572–14577.

76. Simkus C, Makiya M, Jones JM (2009) Karyopherin alpha 1 is a putative substrate of the RAG1 ubiquitin ligase. *Molecular Immunology* 46:1319–1325.

77. Arbuckle JL, Rahman NS, Zhao S, Rodgers W, Rodgers KK (2011) Elucidating the domain architecture and functions of non-core RAG1: The

capacity of a non-core zinc-binding domain to function in nuclear import and nucleic acid binding. *BMC Biochem* 12:23.

78. Schatz DG, Swanson PC (2011) V(D)J recombination: mechanisms of initiation. *Annu. Rev. Genet.* 45:167–202.

79. Jackson PK et al. (2000) The lore of the RINGs: substrate recognition and catalysis by ubiquitin ligases. *Trends Cell Biol.* 10:429–439.

80. Yurchenko V, Xue Z, Sadofsky M (2003) The RAG1 N-Terminal Domain Is an E3 Ubiquitin Ligase. *Genes Dev.* 17:581–585.

81. Grazini U et al. (2010) The RING Domain of RAG1 Ubiquitylates Histone H3: A Novel Activity in Chromatin-Mediated Regulation of V(D)J Joining. *Molecular Cell* 37:282–293.

82. Jones JM, Gellert M (2003) Autoubiquitylation of the V(D)J Recombinase Protein RAG1. *PNAS* 100:15446–15451.

83. Jones JM, Simkus C (2009) The roles of the RAG1 and RAG2 "non-core" regions in V(D)J recombination and lymphocyte development. *Arch. Immunol. Ther. Exp. (Warsz.)* 57:105–116.

84. Kassmeier MD et al. (2011) VprBP binds full-length RAG1 and is required for B-cell development and V(D)J recombination fidelity. *EMBO J* advance online publication. Available at: http://dx.doi.org/10.1038/emboj.2011.455 [Accessed January 29, 2012].

85. Ramón-Maiques S et al. (2007) The plant homeodomain finger of RAG2 recognizes histone H3 methylated at both lysine-4 and arginine-2. *Proceedings of the National Academy of Sciences* 104:18993 –18998.

86. Zhao S, Gwyn LM, De P, Rodgers KK (2009) A non-sequence specific DNA binding mode of RAG1 is inhibited by RAG2. *J Mol Biol* 387:744–758.

87. Akamatsu Y, Oettinger MA (1998) Distinct roles of RAG1 and RAG2 in binding the V(D)J recombination signal sequences. *Mol. Cell. Biol* 18:4670–4678.

88. Callebaut I, Mornon J-P (1998) The V(D)J recombination activating protein RAG2 consists of a six-bladed propeller and a PHD fingerlike

domain, as revealed by sequence analysis. *Cellular and Molecular Life Sciences* 54:880–891.

89. Liu Y, Subrahmanyam R, Chakraborty T, Sen R, Desiderio S (2007) A plant homeodomain in RAG-2 that binds Hypermethylated lysine 4 of histone H3 is necessary for efficient antigen-receptor-gene rearrangement. *Immunity* 27:561–571.

90. Matthews AGW et al. (2007) RAG2 PHD finger couples histone H3 lysine 4 trimethylation with V(D)J recombination. *Nature* 450:1106–1110.

91. Grundy GJ, Yang W, Gellert M (2010) Autoinhibition of DNA cleavage mediated by RAG1 and RAG2 is overcome by an epigenetic signal in V(D)J recombination. *Proceedings of the National Academy of Sciences* 107:22487 –22492.

92. Elkin SK et al. (2005) A PHD Finger Motif in the C Terminus of RAG2 Modulates Recombination Activity. *J. Biol. Chem.* 280:28701–28710.

93. West KL et al. (2005) A Direct Interaction between the RAG2 C Terminus and the Core Histones Is Required for Efficient V(D)J Recombination. *Immunity* 23:203–212.

94. Li Z, Dordai DI, Lee J, Desiderio S (1996) A conserved degradation signal regulates RAG-2 accumulation during cell division and links V(D)J recombination to the cell cycle. *Immunity* 5:575–589.

95. Lee J, Desiderio S (1999) Cyclin A/CDK2 regulates V(D)J recombination by coordinating RAG-2 accumulation and DNA repair. *Immunity* 11:771–781.

96. Jiang H et al. (2005) Ubiquitylation of RAG-2 by Skp2-SCF links destruction of the V(D)J recombinase to the cell cycle. *Mol. Cell* 18:699–709.

97. Zhang L, Reynolds TL, Shan X, Desiderio S (2011) Coupling of V(D)J recombination to the cell cycle suppresses genomic instability and lymphoid tumorigenesis. *Immunity* 34:163–174.

98. Jackson SP (2002) Sensing and Repairing DNA Double-Strand Breaks. *Carcinogenesis* 23:687–696.

99. Grawunder U et al. (1995) Down-regulation of RAG1 and RAG2 gene expression in PreB cells after functional immunoglobulin heavy chain rearrangement. *Immunity* 3:601–608.

100. Wilson A, Held W, MacDonald HR (1994) Two Waves of Recombinase Gene Expression in Developing Thymocytes. *J Exp Med* 179:1355–1360.

101. Chen Z et al. (2011) Transcription factors E2A, FOXO1 and FOXP1 regulate recombination activating gene expression in cancer cells. *PLoS ONE* 6:e20475.

102. Amin RH, Schlissel MS (2008) Foxo1 directly regulates the transcription of recombination-activating genes during B cell development. *Nat. Immunol.* 9:613–622.

103. Lazorchak AS et al. (2010) Sin1-mTORC2 suppresses rag and il7r gene expression through Akt2 in B cells. *Mol. Cell* 39:433–443.

104. Hsu L-Y, Liang H-E, Johnson K, Kang C, Schlissel MS (2004) Pax5 activates immunoglobulin heavy chain V to DJ rearrangement in transgenic thymocytes. *J. Exp. Med.* 199:825–830.

105. Zhang Z et al. (2006) Transcription factor Pax5 (BSAP) transactivates the RAG-mediated V(H)-to-DJ(H) rearrangement of immunoglobulin genes. *Nat. Immunol.* 7:616–624.

106. Hu H et al. (2006) Foxp1 is an essential transcriptional regulator of B cell development. *Nature Immunology* 7:819–826.

107. Kuo TC, Schlissel MS (2009) Mechanisms controlling expression of the RAG locus during lymphocyte development. *Curr. Opin. Immunol.* 21:173–178.

108. Schulz D et al. (2012) Gfi1b negatively regulates Rag expression directly and via the repression of FoxO1. *The Journal of Experimental Medicine* 209:187 –199.

109. Bednarski JJ et al. (2012) RAG-induced DNA double-strand breaks signal through Pim2 to promote pre–B cell survival and limit proliferation. *The Journal of Experimental Medicine* 209:11 –17.

110. Hikida M et al. (1998) Expression of Recombination Activating Genes in Germinal Center B Cells: Involvement of Interleukin 7 (IL-7) and the IL-7 Receptor. *J Exp Med* 188:365–372.

111. Liu Y, Zhang L, Desiderio S (2009) Temporal and spatial regulation of V(D)J recombination: interactions of extrinsic factors with the RAG complex. *Adv. Exp. Med. Biol.* 650:157–165.

112. Ji Y et al. (2010) The In Vivo Pattern of Binding of RAG1 and RAG2 to Antigen Receptor Loci. *Cell* 141:419–431.

113. Ramsden DA, McBlane JF, van Gent DC, Gellert M (1996) Distinct DNA sequence and structure requirements for the two steps of V(D)J recombination signal cleavage. *EMBO J* 15:3197–3206.

114. Akamatsu Y et al. (1994) Essential Residues in V(D)J Recombination Signals. *J Immunol* 153:4520–4529.

115. Ramsden DA, Baetz K, Wu GE (1994) Conservation of sequence in recombination signal sequence spacers. *Nucleic Acids Res* 22:1785–1796.

116. Nadel B, Tang A, Escuro G, Lugo G, Feeney AJ (1998) Sequence of the Spacer in the Recombination Signal Sequence Affects V(D)J Rearrangement Frequency and Correlates with Nonrandom Vκ Usage In Vivo. *The Journal of Experimental Medicine* 187:1495–1503.

117. Cuomo CA, Mundy CL, Oettinger MA (1996) DNA sequence and structure requirements for cleavage of V(D)J recombination signal sequences. *Mol Cell Biol* 16:5683–5690.

118. Arnal SM, Holub AJ, Salus SS, Roth DB (2010) Non-consensus heptamer sequences destabilize the RAG post-cleavage complex, making ends available to alternative DNA repair pathways. *Nucleic Acids Res* 38:2944–2954.

119. Montalbano A et al. (2003) V(D)J recombination frequencies can be profoundly affected by changes in the spacer sequence. *J. Immunol.* 171:5296–5304.

120. Feeney AJ, Tang A, Ogwaro KM (2000) B-cell repertoire formation: role of the recombination signal sequence in non-random V segment utilization. *Immunol. Rev.* 175:59–69.

121. Eastman QM, Leu TMJ, Schatz DG (1996) Initiation of V(D)J recombination in vitro obeying the 12/23 rule. *, Published online: 07 March 1996; | doi:10.1038/380085a0* 380:85–88.

122. Jones JM, Gellert M (2002) Ordered assembly of the V(D)J synaptic complex ensures accurate recombination. *The EMBO Journal* 21:4162–4171.

123. Jung D et al. (2003) Extrachromosomal recombination substrates recapitulate beyond 12/23 restricted VDJ recombination in nonlymphoid cells. *Immunity* 18:65–74.

124. Drejer-Teel AH, Fugmann SD, Schatz DG (2007) The beyond 12/23 restriction is imposed at the nicking and pairing steps of DNA cleavage during V(D)J recombination. *Mol. Cell. Biol.* 27:6288–6299.

125. Cobb RM, Oestreich KJ, Osipovich OA, Oltz EM (2006) in *Advances in Immunology* (Academic Press), pp 45–109. Available at: http://www.sciencedirect.com/science/article/pii/S0065277606910025 [Accessed March 25, 2012].

126. Schatz DG, Oettinger MA, Schlissel MS (1992) V(D)J Recombination: Molecular Biology and Regulation. *Annual Review of Immunology* 10:359–383.

127. Feeney A (2010) Epigenetic regulation of V(D)J recombination. *Seminars in Immunology* 22:311–312.

128. Bergman Y, Cedar H (2010) Epigenetic control of recombination in the immune system. *Seminars in Immunology* 22:323–329.

129. del Blanco B, García V, García-Mariscal A, Hernández-Munain C (2011) Control of V(D)J Recombination through Transcriptional Elongation and Changes in Locus Chromatin Structure and Nuclear Organization. *Genetics Research International* 2011:1–10.

130. Cherry SR, Baltimore D (1999) Chromatin remodeling directly activates V(D)J recombination. *Proc. Natl. Acad. Sci. U.S.A.* 96:10788–10793.

131. Bergman Y, Cedar H (2010) Epigenetic control of recombination in the immune system. *Seminars in Immunology* 22:323–329.

132. Zhang M, Swanson PC (2009) HMGB1/2 can target DNA for illegitimate cleavage by the RAG1/2 complex. *BMC Molecular Biology* 10:24.

133. Rodgers KK et al. (1999) A dimer of the lymphoid protein RAG1 recognizes the recombination signal sequence and the complex stably incorporates the high mobility group protein HMG2. *Nucleic Acids Res* 27:2938–2946.

134. van Gent DC, Ramsden DA, Gellert M (1996) The RAG1 and RAG2 proteins establish the 12/23 rule in V(D)J recombination. *Cell* 85:107–113.

135. Shlyakhtenko LS et al. (2009) Molecular mechanism underlying RAG1/RAG2 synaptic complex formation. *J. Biol. Chem* 284:20956–20965.

136. Kriatchko AN, Bergeron S, Swanson PC (2008) HMG-box domain stimulation of RAG1/2 cleavage activity is metal ion dependent. *BMC Mol. Biol* 9:32.

137. Taccioli GE et al. (1993) Impairment of V(D)J Recombination in Double-Strand Break Repair Mutants. *Science* 260:207–210.

138. Gong C et al. (2005) Mechanism of nonhomologous end-joining in mycobacteria: a low-fidelity repair system driven by Ku, ligase D and ligase C. *Nature Structural & Molecular Biology* 12:304–312.

139. Lin WC, Desiderio S (1994) Cell Cycle Regulation of V(D)J Recombination-Activating Protein RAG-2. *PNAS* 91:2733–2737.

140. Weinstock DM, Jasin M (2006) Alternative pathways for the repair of RAG-induced DNA breaks. *Mol. Cell. Biol* 26:131–139.

141. Bennardo N, Cheng A, Huang N, Stark JM (2008) Alternative-NHEJ is a mechanistically distinct pathway of mammalian chromosome break repair. *PLoS Genet* 4:e1000110.

142. Iliakis G (2009) Backup pathways of NHEJ in cells of higher eukaryotes: Cell cycle dependence. *Radiotherapy and Oncology* 92:310–315.

143. Bentley J, Diggle CP, Harnden P, Knowles MA, Kiltie AE (2004) DNA Double Strand Break Repair in Human Bladder Cancer Is Error Prone and Involves Microhomology-Associated End-Joining. *Nucl. Acids Res.* 32:5249–5259.

144. Bennardo N, Cheng A, Huang N, Stark JM (2008) Alternative-NHEJ Is a Mechanistically Distinct Pathway of Mammalian Chromosome Break Repair. *PLoS Genet* 4.

145. Perrault R, Wang H, Wang M, Rosidi B, Iliakis G (2004) Backup pathways of NHEJ are suppressed by DNA-PK. *J. Cell. Biochem* 92:781–794.

146. Simsek D, Jasin M (2010) Alternative end-joining is suppressed by the canonical NHEJ component Xrcc4-ligase IV during chromosomal translocation formation. *Nat. Struct. Mol. Biol* 17:410–416.

147. Sawchuk DJ et al. (2004) Ku70/Ku80 and DNA-dependent Protein Kinase Catalytic Subunit Modulate RAG-mediated Cleavage. *Journal of Biological Chemistry* 279:29821 –29831.

148. Raval P, Kriatchko AN, Kumar S, Swanson PC (2008) Evidence for Ku70/Ku80 association with full-length RAG1. *Nucleic Acids Research* 36:2060 –2072.

149. Cui X, Meek K (2007) Linking double-stranded DNA breaks to the recombination activating gene complex directs repair to the nonhomologous end-joining pathway. *Proc. Natl. Acad. Sci. U.S.A* 104:17046–17051.

150. Lee GS, Neiditch MB, Salus SS, Roth DB (2004) RAG proteins shepherd double-strand breaks to a specific pathway, suppressing error-prone repair, but RAG nicking initiates homologous recombination. *Cell* 117:171–184.

151. Corneo B et al. (2007) Rag mutations reveal robust alternative end joining. *Nature* 449:483–486.

152. Deriano L, Stracker TH, Baker A, Petrini JHJ, Roth DB (2009) Roles for NBS1 in alternative nonhomologous end-joining of V(D)J recombination intermediates. *Mol. Cell* 34:13–25.

153. Bredemeyer AL et al. (2006) ATM stabilizes DNA double-strand-break complexes during V(D)J recombination. *Nature* 442:466–470.

154. Jones JM, Gellert M (2001) Intermediates in V(D)J recombination: A stable RAG1/2 complex sequesters cleaved RSS ends. *Proceedings of the National Academy of Sciences* 98:12926 –12931.

CHAPTER 2

REGULATION OF RAG-MEDIATED REACTION BY METAL ION COFACTOR - REAL TIME MONITORING OF RAG-MEDIATED CLEAVAGE REACTION REVEALS THAT CEC IS MORE STABLE IN MAGNESUIM

Introduction

The principles and applications of fluorescence anisotropy and FRET

Fluorescence anisotropy is a frequently used fluorescence-based technique, which measures the rotational mobility of a fluorophore (1, 2). The relative comparison of a fluorophore between its tumbling time in solution and its intrinsic fluorescent lifetime (nano-seconds scale) determines its anisotropy value (ranging from 0 to 0.4), i.e. if a fluorophore rotates very slowly in solution, a large anisotropy value will be generated; if a fluorophore tumbles very rapidly in solution, anisotropy value will be smaller. The nature of fluorescence anisotropy measurement makes it applicable to reveal the interaction between two molecules, and it is more accurate if the fluorophore is labeled at a small molecule. Binding of the fluorophore-labeled small molecule to a larger molecule will significantly decrease the rotational mobility of the fluorophore, resulting in increased anisotropy. Thus, fluorescence anisotropy is very suitable to measure the protein-DNA interaction, where a relatively small DNA molecule is labeled with fluorophore and interaction with a protein can be readily revealed by increase in anisotropy (3). In addition, the degree of anisotropy changes

upon protein binding may reflect three aspects of protein-DNA interaction: 1) strength of the interaction between two molecules, from which the binding constant of the interaction can be derived; 2) size of DNA-protein complex; 3) property of the binding pocket if the fluorophore is labeled close to the binding site. Nevertheless, the most advantageous aspect of anisotropy measurement is that it can directly measure the protein-DNA interaction in solution without perturbations arising from the separating steps that are required in other assays, such as electrophoresis or filtration. To summarize, the solution-based fluorescence anisotropy measurement is adopted in this study because it can determine very weak binding, which is otherwise very difficult to reveal by conventional methods. In addition, it measures the protein-DNA interaction in the most natural environment, in terms of salt concentration, pH range, temperature, etc., rather than changing into a complete different condition that is required for the separation of the DNA-protein complexes. Last but not least, It allows continuous collection of data points without interruption, which makes possible the kinetics measurement over the course of a reaction (2, 3).

Another fluorescence-based technique, Fluorescence Resonance Energy Transfer (FRET), is the most widely used technique in many diverse disciplines such as physics, chemistry and biology. FRET reflects the energy transfer between the excited states of two fluorophores in the distance-dependent manner. The energy transfer is inversely proportional

to the six power of the distance between donor and acceptor, and thus is extremely sensitive to the distance changes (within 1-10nm range) (4). In addition to distance, several other parameters can also influence FRET efficiency, such as the relative orientation of the emission and absorption dipole moment, the refractive index of the medium, and the overlap between the donor emission spectrum and the acceptor excitation spectrum (4). Because of its well-established principle and relatively easy access, FRET is universally used in many fields and it is referred to as "spectroscopic ruler" to measure behaviors at the molecular level, such as interaction of two molecules, conformation change, folding and the dynamics of these behaviors. Similar to fluorescence anisotropy, FRET is also amenable to solution-based measurement, but has been extended to other types of measurements, such as FRET microscopy (5), which makes FRET technique even more powerful.

However, disadvantages of anisotropy and FRET measurements are also apparent, e.g. the sensitivity of fluorescence is much less than that of radioactivity and thus higher concentration of labeled molecule is required in order to obtain sufficient signal. Therefore, it is very important to combine these fluorescence-based techniques with other measurements to provide a comprehensive understanding on protein-DNA interaction, which will be discussed in detail in the result section.

Application of fluorescence techniques in RAG-mediated reactions

V(D)J recombination is essential to generate a diverse repertoire of antibodies and T cell receptors. Physiological V(D)J recombination is divided into two-phases, lymphocyte specific cleavage phase mediated by the RAG recombinase (RAG1/2) and the joining phase mediated by the ubiquitous non-homologous end joining (NHEJ) pathway (6, 7) The processes of physiological V(D)J recombination has been reviewed in detail in chapter 1. Briefly, the RAG1/2 mediated cleavage results in the generation of two hairpin-coding ends (HP-CEs) and blunt signal ends (SEs), which are then primarily resolved by NHEJ pathway to form coding joints and signal joints (8), (9). The RAG-mediated catalysis reaction has been recapitulated in the cell-free system, where recombinant RAG1 and RAG2 proteins are both necessary and sufficient to catalyze the site-specific cleavage on an extrochromosomal DNA substrate that contains RSS. The biochemistry of RAG-mediated reaction has been extensively investigated, including the RAG-RSS interaction, enzymatic details, stoichiometry of RAG proteins during cleavage or after cleavage (10–12). Even more so, the whole process of V(D)J recombination has been successfully reconstituted in the *in vitro* cell free system using thirteen highly purified proteins, such as RAG1, RAG2, HMGB1, DNA-PKcs, Artemis, DNA ligase IV:XRCC4, etc. (13). However, few studies can reveal th Note that the ratioe dynamic changes of the reaction in the time-dependent manner, instead, most of them have been relying on the detection of the end results, such as the production of CEs, SEs, or coding

joints (CJs) and signal joints (SJs), which precludes the revelation of many important aspects in the course of the reaction.

Here in this study, I took advantage of two complementary fluorescence-based techniques, fluorescent anisotropy and FRET, to monitor the RAG-mediated recombination cleavage reaction in real time. The real-time monitoring system, for the first time, enables us to record the kinetics of the interaction between RAG and RSS or between RAG and the reaction intermediates, i.e. HP-CEs and blunt-SEs, which will provide important insights on 1) the initial binding properties, including possible conformational changes and the binding affinity measurement, 2) the stability of post-cleavage complex, i.e. HP-CEs retention and SEs retention. These studies will allow us to characterize the role and function of each participating factor in the course of RAG-mediated reactions, and to identify parameters that could potentially affect any of the above-mentioned processes.

Materials and Methods

Protein purification

Maltose binding protein (MBP) tagged core RAG1 (residues 384-1008) and core RAG2 (residues 1-387) proteins were co-expressed in 293T cells using the Plus/Lipofectamine reagent (Invitrogen, Carlsbad, CA). Other MBP-fused RAG proteins were also prepared, including a catalytically inactive RAG1 mutant D600A (dRAG1, 384-1008) (14), a gain-of-function RAG1 mutant E649A (eRAG1, 384-1008) (15), Various combinations of wild type or mutant RAG1 and RAG2 were co-expressed in 293T cells, which are listed in Table 1, along with the nomenclatures of these proteins and various PCCs. The expressed proteins were purified following the procedure described by Bergeron *et al.* (16). The protein concentration was measured with the Nanodrop Spectrophotometer (Thermo SCIENTIFIC, Wilmington, DE) and verified by SDS-PAGE, in which no bands other than RAG1 and RAG2 were visible, as shown in Figure 1. The same amount of RAG proteins was used in the binding or cleavage reactions unless described otherwise.

DNA substrates

The sequence of the DNA substrate used in this study are shown below: 12RSS Top: 5'-TATCAGCTGATAGCTAACACAGTGCTACAGA-CTGGAACAAAAACCCTGCT-3'; 12RSS bottom: 5'-AGCAGGGTTTTTG-T-TC-CAGTCTGTAGCACTGTGTTAGCTATCAGCTGATC-3'; 23RSS top: 5'-ATCGAAGTACCAGTAGCACAGTGGTAGTACGCGTCTGTCTGGCTG-

TACAAAAACCATGGATCCT-3'; 23RSS bottom: 5'-AGGATCCATGGTT-TTTGTACAGCCAGACAGACGCGTACTACCACTGTGCTACTGGTACTT-CGAT-3'. The 12RSS top strand was labeled with TAMRA, either at 5'-end, or internally at the 3rd nucleotides (T) 5' to the heptamer. The 12RSS bottom strand was labeled with ATTO647N (hereafter referred to as ATTO) at the spacer region, 6th nucleotides (T) 3' to the nonamer. The fluorescence labeled-DNA nucleotides were obtained from IBA BioTAGnology (Göttingen, Germany) and the unlabeled ones from Integrated DNA Technologies Inc. (Coralville, IA). 12RSS top strand with the internal labeled TAMRA was annealed to the ATTO-labeled bottom strand and were purified by native polyacrylamide gel electrophoresis to remove any residual single-stranded DNA. The dually labeled 12RSS oligonucleotide substrates were examined in the FRET experiments while the 5' end-TAMRA-labeled 12RSS substrates were analyzed by the fluorescence anisotropy. As controls for analyzing fluorescence quenching effect, the singly labeled substrates were obtained by annealing the internal labeled TAMRA strand to the unlabeled bottom strand or the unlabeled top strand to the ATTO labeled bottom strand.

***In vitro* cleavage assay**

The cleavage reaction of the fluorescence-labeled 12RSS (20 nM) was catalyzed by RAG proteins (65 nM) in 10 ml reaction containing 10 mM Tris-HCl [pH 7.5], 50 mM NaCl and 100 μg/μl BSA in Mn^{2+} (0.2 mM) and Mg^{2+} (2.5 mM). The reaction inactive for cleavage was also included

as a control, i.e., the same probe incubated in the same reaction buffer, except with Ca^{2+} (2.5 mM) or using the catalysis-defective RAG1 mutant (dRAG1) paired with cRAG2. For the coupled cleavage reactions, HMGB1 protein (30 ng/μl, Sigma-Aldrich) and 23RSS (150 nM) were included. The reaction mixture was incubated at 37°C for various times as indicated in the figures, and stopped by adding 10 ml denaturing loading dye containing 90% formamide for denaturation at 95°C and quick chill on ice before being loaded onto a 16% Tris-Borate-EDTA-7 M urea-polyacrylamide gel. After electrophoresis, the gel was imaged on a Typhoon scanner (GE Healthcare) with laser excitation at 532 nm and emission filter of 580 nm to detect TAMRA fluorescence.

Electrophoretic Mobility Shift Assay (EMSA)

EMSA was performed to analyze the interactions between RAG proteins and RSS. Samples were prepared as described for the *in vitro* cleavage assay. The reaction was stopped by adding 5 μl 100% glycerol for every 10 μl reaction, and the sample was immediately loaded onto a discontinuous native polyacrylamide gel (top half 4% and bottom half 16%, with 19:1 acrylamide: bisacrylamide). Samples were subjected to electrophoresis at 200 V, 4°C for 2.5 hours. The resulting gel was imaged on the Typhoon scanner (GE Healthcare).

Fluorescence anisotropy.

A Photon Technology International QuantaMaster-4/2005SE Spectrofluorometer was used for all fluorescence experiments. A 3 mm ×

3 mm quartz micro-cuvette with a 50 µl-sample chamber was used in all measurements, and temperature was controlled by a circulating water bath and set at 37°C except where noted. The fluorophore-labeled sample is excited by a polarized beam light, which allows photo-selection of a fraction of fluorophores that are properly oriented relative to the incoming light. The anisotropy is defined as $\langle r \rangle = (I_{VV} - GI_{VH})/(I_{VV}+2GI_{VH})$, where I is the fluorescent intensity, V and H reflects the vertical and horizontal orientation by which the emission and excitation polarizer is mounted,. The factor G is defined as, I_{HV}/I_{HH}, the intensity ratio of the vertical emission to horizontal emission when the sample is excited with horizontal polarized light. G factor is dependent on the monochromator wavelength and slit width and is used to correct for polarization-dependent effects in detection sensitivity. The excitation and the emission wavelengths were set at 510 nm and 580 nm, and data was acquired every 10 seconds. Background correction was applied to all the measurements. The anisotropy of the 5'-TAMRA-labeled 12RSS in the appropriate buffer (with cations indicated in the figures) was measured before and after the addition of RAG proteins. The temperature was maintained at 37°C for the duration of the experiment (~3 hours). The final concentration of all the components was the same as used in the *in vitro* cleavage reactions. At the end of cleavage reactions, SDS and proteinase K was added to disrupt the protein-DNA complex, resulting a complete release of HP-CEs,

where the anisotropy of free HP-CEs is lower than the free probe or DNA with a nick.

Fluorescence Resonance Energy Transfer (FRET)

The same instrument and setting are used for FRET experiment as those in fluorescence anisotropy measurement. Samples were excited at 510 nm, except in the control experiments with ATTO-only RSS, where the excitation wavelength was set at 600 nm. Sample reactions were assembled as described for the *in vitro* cleavage assay, except that sample components were scaled up five-fold so that the final concentration of all the components was the same as used in the *in vitro* cleavage reaction. The FRET efficiency of the TAMRA-ATTO-labeled 12RSS probe was measured before and after adding the purified RAG proteins. Emission scans were recorded every 10 min during the first hour and then every 20 min for another 2 hours. The ratio $I_{acceptor}$ /I_{donor} was calculated from the peak intensities of the acceptor and donor, and used as a measure of the FRET efficiency. Note that the ratio, $I_{acceptor}$ /I_{donor}, does not represent the actual FRET efficiency. Because I do not attempt to obtain the distance information between donor-acceptor, rather I would like to have a relative comparison of the FRET efficiency changes, and thus the ratio $I_{acceptor}$ /I_{donor} was used instead for its simplicity.

For the experiment involving the step-wise addition of cations, the cleavage reaction was initiated by e/cRAG in Mg^{2+} for 2 hrs and then continued after the addition of different cations to the desired final

concentrations (Mn^{2+} = 0.2mM, Mg^{2+} = 2.5 mM and Ca^{2+} = 2.5 mM). A mock treatment without the cation addition was also included as a control. These reactions were monitored by FRET and analyzed by denaturing gel electrophroresis for the production of HP-CEs. The experiment involving a temperature ramp was conducted on the cleavage reaction initiated by e/cRAG or e/fsRAG in Mg^{2+} at 37°C for 1 hour followed by a temperature increase to 55°C over 15 min. The emission intensities of TAMRA and ATTO were monitored over the temperature-ramp every 2°C, and then every 20 min over the next 1 hour.

Data fitting.

Kinetic traces of FRET and fluorescence anisotropy experiment were fitted using the program embedded in OriginPro8, to either a mono-exponential decay ($I_{acceptor}$ /I_{donor} = A*exp*(-t/τ)+A_∞), or to a sum of two mono-exponential decays ($I_{acceptor}$ /I_{donor} = A_1 *exp*(-t/τ_1)+ A_2 *exp*(-t/τ_2)+ A_∞). The latter was used if the former failed to generate a satisfactory fit, which reflects the non-random residues during fitting. In these equations, *t* represents time, τ represents the dissociation lifetime, and A_∞ represents the $I_{acceptor}$ /I_{donor} ratio where all generated HP-CEs is liberated from the RAG complex. Because in some reactions, HP-CEs was not completely released by the end of 3 hours acquisition time, meaning the lifetime is longer than 3 hours, the parameter A_∞ was determined by either adding a denaturing agent (SDS/Proteinase K) at the end of the experiment, or by increasing the temperature to 55 °C to dissociate all hairpins. Both

methods yield the same value, which was used as a fixed parameter in the fitting procedures.

Result

Proof of concept demonstration in the RAG-mediated reaction system with Mn^{2+}

The probe for fluorescence anisotropy measurement is a 50 base pair 12RSS substrate that is labeled with TAMRA at the 5'end of coding flank, hereafter referred to TAMRA-12RSS. Fluorescence anisotropy can reflect RAG-RSS interaction in both the pre-cleavage complex and post-cleavage complex, the scenarios of which are illustrated in Figure 2A. Free probe displays a relatively low anisotropy $\langle r \rangle$. Upon RAG addition, the specific interaction between RAG and TAMRA-12RSS causes a slower rotational mobility of TAMRA, therefore increased $\langle r \rangle$. Excision of TAMRA-12RSS by RAG to generate TAMRA-labeled hairpin-coding ends (HP-CEs) and the subsequent release of the smaller-sized TAMRA-HP-CEs from CEC will cause a decrease in $\langle r \rangle$, On the other hand, $\langle r \rangle$ stays constant if the cleaved HP-CE is retained in CEC.

To test these scenarios, I first need to make sure fluorescence anisotropy is applicable and sensitive enough to reveal the changes of interaction between RAG and the RSS or the cleavage intermediate, e.g. HP-CEs. As a proof of concept demonstration, I compared the c/cRAG (RAG recombinase containing coreRAG1 and core RAG2, see Table 1 for nomenclature) mediated-cleavage reactions on single TAMRA-12RSS, in the presence of various cations, i.e. Mg^{2+}, Ca^{2+}, Mn^{2+}, which results in different cleavage outcomes and thus is suitable for testing different

scenarios. Among these cations, Mn^{2+} is of particular interest, because it supports uncoupled cleavage on a single RSS, and thus is considered a permissive cation, which was speculated to allow rapid HP-CEs dissociation from the CEC. Indeed, as shown in Figure 2B, Mn^{2+} induced an initial higher increase of $\langle r \rangle$ upon c/cRAG addition (which will be discussed in more detail in the later section), followed by a continuous $\langle r \rangle$ decrease during the incubation time, most likely due to the release of generated HP-CEs from CEC. On the other hand, RAG-mediated binding alone in Ca^{2+} and nicking alone in Mg^{2+} both displayed initial anisotropy increase over the free probe upon RAG addition and $\langle r \rangle$ remained rather constant afterwards, consistent with their lack of HP-CEs generation and release from CEC.

The demonstration of fluorescence anisotropy in revealing various recombination outcomes was very encouraging. However, we could not exclude the possibility that the $\langle r \rangle$ reduction observed only in Mn^{2+} was due to dissociation of intact TAMRA-12RSS from the RAG complex, instead of premature release of HP-CEs from the CEC. To delineate whether the $\langle r \rangle$ reduction is due to release of intact RSS or HP-CEs and to definitively measure HP-CEs release, we applied another fluorescence detection system, FRET, to monitor the same cleavage reaction. The 12RSS probe for the FRET study was labeled with TAMRA (donor) at the coding flank next to heptamer of the top strand and with ATTO 647N (acceptor, henceforth referred to as ATTO) at the spacer region of the bottom strand.

The distance between donor and acceptor fluorophore in intact 12RSS is 5.4nm (16 bp apart), such that an excitation of TAMRA is expected to result in the appearance of an additional fluorescence band corresponding to the ATTO emission spectrum and meanwhile a reduction in TAMRA emission, since within such short distance, a fraction of energy absorbed by TAMRA can be transferred to ATTO, as shown in Figure 3A. The possible scenarios of RAG-mediated cleavage reaction on TAMRA-ATTO 12RSS are illustrated in Figure 3B, RAG binding or nicking alone is not supposed to change FRET efficiency, as donor-acceptor distance remains the same. However, in some cases, if RAG-RSS interactions distort DNA so that the orientation (less likely distance) between donor-acceptor dipole is affected, FRET efficiency may fluctuate without an actual excision of the 12RSS. For example, due to DNA bending, a decreased distance between TAMRA-ATTO, possibly is likely to increase of ATTO and decrease of TAMRA. On the other hand, reduction in FRET has also been observed in the absence of recombination cleavage, which will be discussed in more detail in chapter 4. Nevertheless, the more apparent change in FRET efficiency is caused by physical change in distance, e.g. increased distance due to hairpin dissociation from CEC will lead to reduction of ATTO emission (I_{donor}) and corresponding increase of TAMRA emission (I_{donor}). Thus, the ratio $I_{acceptor}/I_{donor}$ is a direct measure of the relative distance between TAMRA and ATTO, and is used here to model changes of FRET efficiency corresponding to the interaction of 12RSS or the

cleaved HP-CEs with RAG in both single cleavage reactions or coupled cleavage reactions.

Indeed, RAG mediated reactions containing Mg^{2+} (only causes nicking) or Ca^{2+} (only induces specific binding) have very stable FRET efficiency over the incubation time, as shown in Figure 3C. While in the presence of Mn^{2+}, the ratio $I_{acceptor}/I_{donor}$ decays significantly, a result of reduced ATTO emission and enhanced TAMRA emission caused by distance increase between donor and acceptor molecule. Changes of FRET efficiency represented by $I_{acceptor}/I_{donor}$ is consistent with the anisotropy decrease, denoted as $\langle r \rangle$, under the same condition and is a definitive proof of HP-CEs release from CEC. Furthermore, changes of $I_{acceptor}/I_{donor}$ and $\langle r \rangle$ can be fitted into a single exponential decay, and both of them generate a lifetime around 120min, reflecting the dissociation kinetics of newly generated HP-CEs (TARMA) away from the CEC and cleaved signal ends (ATTO), as well. The excellent agreement of lifetime generated from anisotropy and FRET further indicates that both methods monitor the same kinetics of the cleavage process. Thus, the combination of fluorescence anisotropy and FRET techniques provide us with great tools to real time monitor kinetics of RAG-mediated reaction and most importantly, for the first time, enable us to measure the HP-CEs retention in CEC.

Reveal the distinct interaction between RAG and RSS in the presence of different cations

Noted that in the anisotropy measurements of c/cRAG mediated reaction under various cations, Mn^{2+} renders the highest $\langle r \rangle$ upon RAG addition, which either reflect c/cRAG binding to 12RSS with higher affinity or c/cRAG and 12RSS forms a larger complex in the presence of Mn^{2+}. This observation was very interesting, because among all the studies that compared Mg^{2+} and Mn^{2+} under various conditions (summarized in introduction), where Mn^{2+} in general relaxes the specificity of RAG-mediated reaction while Mg^{2+} ensures the specificity stringently, no direct biochemical evidence has been reported to distinguish the binding affinities of RAG and RSS under different metal ions. On the contrary, EMSA studies from several labs showed no obvious variations of c/cRAG binding to RSS under various cations (17–19). However, as indicated in the first section of this chapter, EMSA is relatively insensitive in determining the true binding affinity and especially too harsh to reveal the weak binding, thus the real effect of cation on RAG-RSS binding has not been thoroughly investigated. Here the sensitive and non-disruptive fluorescence anisotropy revealed a significant difference on the initial RAG interaction with 12RSS among different metal ions, allowing us to have more detailed comparison on their roles in RAG-RSS interactions. First, I applied fluorescence anisotropy in dose-dependent RAG-RSS interactions to measure affinities of initial binding at 37°C between c/cRAG and 12RSS in the presence of Ca^{2+}, Mn^{2+} and Mg^{2+}, from which the binding constants could be derived. As shown in Figure 4A, the binding constant is 13.5 ±

2.3 nM in Ca^{2+}, 3.9 ± 3 nM in Mn^{2+}, and 14.5 ± 2.4 nM in Mg^{2+}, respectively, which provides clear evidence that Mn^{2+} induce stronger binding of c/cRAG to the 12RSS substrates than the other cations. I then made a direct comparison on the c/cRAG-RSS complex formation at 37°C over a period of time in the presence of different cations based on EMSA experiment, which is different from the previous EMSA studies where the complexes were assembled at a much lower temperature to avoid actual cleavage, e.g. 4°C or 15°C. As shown in Figure 4B, the complexes formed at the beginning of the reaction in three cations are indistinguishable, however, the complex formed under Mn^{2+} is most stable despite the continuous generation of hairpin, as it is still retained after 3 h incubation. So the combination of fluorescence anisotropy and a modified EMSA measurement revealed the stronger binding of c/cRAG and RSS in the presence of Mn^{2+}, which may partly explain the excessive cleavage activity rendered by Mn^{2+} in RAG-mediated cleavage.

Mg^{2+} induces RAG to form more stable PCC in both single and coupled reactions in comparison to Mn^{2+}

Given that the assembly of pre-cleavage c/cRAG-RSS complex is significantly affected by the metal ion cofactor, it is conceivable that the metal ion might also affect the stability of post-cleavage complex. I investigated this possibility using both fluorescence anisotropy and FRET measurement. However, the direct comparison between Mg^{2+} and Mn^{2+} is impossible in the single cleavage reaction, since Mg^{2+} doesn't support the

generation of HP-CEs on single 12RSS but rather requires synaptic complex (12RSS and 23RSS, coupled reaction) formation in order for efficient cleavage, while Mn^{2+} allows cleavage on a single RSS in the absence of synapsis. Then, it is not clear whether the previous observation of rapid HP-CEs dissociation from CEC in the presence of Mn^{2+} is due to an uncoupled reaction or an intrinsic property of Mn^{2+} in destabilizing CEC. To address this issue, I took advantage of a gain-of function E649A core RAG1 (eRAG1) mutant, which has been reported to permit site-specific excision in the single cleavage reaction even in the presence of Mg^{2+} (15). This mutant was found to closely resemble its wild-type counterpart (cRAG1) in their DNA binding activity, transposition activity (catalysis of other DNA strand transfer), and most important, in end resolution of both SEs and CEs on a plasmids substrates containing 12/23RSS pair. The similarity in end resolution suggested that cRAG1 and eRAG1 exhibits a comparable level of post-cleavage complex stability, which allows us to determine the effect of Mg^{2+} or Mn^{2+} on HP-CEs retention from CEC.

First, I performed the time-course analysis of *in vitro* cleavage reaction under various conditions, e/cRAG (eRAG1 paired with cRAG2, see Table 1 for nomenclature) together with Mn^{2+}, c/cRAG with Mn^{2+} and e/cRAG with Mg^{2+}, as shown in the left panels of Figure 5A, B and C. Reaction containing e/cRAG and Mn^{2+} displayed a very fast kinetics of hairpin generation, with a calculated life time of 10 min ($\tau_{HP\text{-}P}$ = 10 min),

compared to 60 min ($\tau_{HP\text{-}P}$ = 60 min) for both c/cRAG in Mn^{2+} and e/cRAG in Mg^{2+}. However, besides the expected nicked and HP-CEs products, an unknown band at the position above the HP-CEs also appeared only in the reaction mediated by e/cRAG in Mn^{2+} (denoted with *). The nature of this band remains unidentified, but it was most likely related to the ATTO labeling at the spacer region, possibly reflecting an excision product made near the ATTO site, since no such band was observed when the 12RSS labeled only with TAMRA was tested under the same reaction condition. Nevertheless, once the above three reaction conditions were compared by FRET measurement, I found that despite the different kinetics of hairpin production, the reactions mediated by e/cRAG in Mn^{2+} and c/cRAG in Mn^{2+} displayed similar patterns of FRET changes, in which a rapid increase in the TAMRA intensity coincided with a decrease in the ATTO intensity, as shown in right panel of Figure 5A, indicating a significant FRET decrease, the $I_{acceptor}/I_{donor}$ ratio changes of which are summarized in Figure 5E. On the other hand, in the reaction containing e/cRAG and Mg^{2+}, the emission intensity of TAMRA and ATTO changed at a much slower rate compared to the reactions containing Mn^{2+}, as shown in the right panel of Figure 5C. Specifically, the $I_{acceptor}/I_{donor}$ ratio remained fairly constant during the first 50 min of the reaction, and showed a much slower decay afterwards, with a lifetime $\tau_{HP\text{-}R}$ of 400 ± 14 min (Figure 5E). Although the level and kinetics of HP-CEs generation is similar between the reactions mediated by e/cRAG in Mg^{2+} and c/cRAG in Mn^{2+}, their HP-

CEs release rate differs significantly, suggesting that hairpin-CEs are retained much better in CEC in the presence of Mg^{2+} than that in the presence of Mn^{2+}. As negative controls, in reactions that is lack of cleavage, such as the catalytic-inactive mutant d/cRAG (dRAG1 paired with cRAG2) with Mn^{2+} or e/cRAG with Ca^{2+}, FRET efficiency is not changed in both cases, as shown in Figure 5D.

The significant difference between Mn^{2+} and Mg^{2+} in HP-CEs retention was very intriguing, but I noticed that FRET decrease in e/cRAG with Mn^{2+} seemed to be a bi-phasic process, with an early faster phase (τ_1 = 12 min) and a later slower phase (τ_2 = 370 min), different from that of c/cRAG in Mn^{2+}. The slower phase at the later stage greatly bothered us because it suggested the possibility that e/cRAG also played a role in holding HP-CEs. On the other hand, I cannot rule out the possibility that the slower FRET decrease at the later stage might be attributed to the unknown band exist only under this condition, which was indeed generated in a delayed manner compared to HP-CEs product (left panel of Figure 5A) and may interfere with the rapid hairpin release. To delineate these two possibilities, I performed the cleavage reaction with step-wise addition of cations in both FRET experiment and *in vitro* cleavage experiment. The reactions were initiated with e/cRAG in the presence of Mg^{2+} for 2 hours, a time long enough for the reaction to occur and to generate a significant amount of hairpin, and then additional Mg^{2+}, Mn^{2+}, or Ca^{2+} was dispensed into the pre-incubated reaction. A mock treatment

of simply disturbing the incubation by repetitive pipetting was also included to control for the possible artifact arising from the pipetting procedure. It is important to note that the step-wise addition of any cation induced no further HP-CEs production, and it also prevented the generation of the unknown band associated with e/cRAG in Mn^{2+}, as revealed by the *in vitro* cleavage reaction in Figure 6B. However, in FRET measurement, addition of Mn^{2+} resulted in significant decrease in FRET efficiency, possibly due to the dissociation of HP-CEs that would otherwise be bound to CEC in the presence of Mg^{2+}, since no additional hairpin were generated. On the other hand, addition of Mg^{2+} and Ca^{2+} triggers no apparent HP-CEs release since they displayed similar FRET decrease with that of mock treatment, as shown in Figure 6A. Therefore, by sequentially adding cations to a pre-incubated reaction, I alleviate the complexity associated with the unknown band as well as the bi-phasic FRET decrease, and substantiate our previous finding that CEC formed in the presence of Mg^{2+} is more stable than the one in Mn^{2+}, and adding Mn^{2+} disrupts this complex and causes the premature release of that the PCC formed in Mg^{2+}.

I then extended my FRET analysis to assess the influence of metal ions on the stability of CEC formed during coupled reaction. Both c/cRAG and e/cRAG mediated coupled reaction were tested, with the addition of HMG and unlabeled 23RSS, in the presence of Mn^{2+} or Mg^{2+}, as shown in Figure 7. The initial increase in $I_{acceptor}/I_{donor}$ present in three conditions,

c/cRAG with Mn^{2+}, c/cRAG with Mg^{2+}, and e/cRAG with Mg^{2+}, may reflect the DNA bending effect caused by HMG and RAG together (20, 21), because DNA bending shortens the distance between donor-TAMRA and acceptor-ATTO and therefore causes increase in FRET efficiency. On the other hand, the lack of the initial $I_{acceptor}/I_{donor}$ increase observed in e/c RAG with Mn^{2+} could be because that DNA bending-induced FRET increase was overcome by the rapid FRET reduction due to hairpin release under this condition. Nevertheless, the initial increase was also observed in e/cRAG mediated reaction in the presence of Ca^{2+} Figure 8A and B, suggesting that it is not associated with actual cleavage but rather reflect a structural change of DNA. However, the change of $I_{acceptor}/I_{donor}$ ratio could also be due to differential quenching of TAMRA or ATTO by RAG/HMG in the coupled reaction. To test this scenario, I performed the same reactions using single labeled probe, i.e. TAMRA-top strand paired with unlabeled bottom strand and unlabeled top strand paired with ATTO-bottom strand, and monitor the fluorescence intensity changes in e/cRAG mediated coupled reaction. As shown in Figure 8C and D, the fluorescence intensity of the single probe stays rather constant over the course of incubation, which proves that the changes seen using doubly-labeled probe is indeed due to FRET change.

Regardless of the initial FRET increase, the dissociation of hairpin is much slower in the presence of Mg^{2+} than that with Mn^{2+}, which is consistent with the finding in single reactions. Specifically, in coupled

reaction containing e/cRAG and Mn^{2+}, HP-CEs dissociated at a rate of $\tau_{HP\text{-}R}$ = 12 min, which is identical to the rate observed in the single reaction (Compare Figure 5E to Figure 7B). The faster HP-CEs release rate was again observed in coupled reactions catalyzed by c/cRAG together with Mn^{2+}, $\tau_{HP\text{-}R}$ = 186 min, which is within the same range of that in single reaction, where $\tau_{HP\text{-}R}$ = 120 min (summarized in Table 2). These data indicated that, in the presence of Mn^{2+}, CEC fails to effectively retain HP-CEs to its close proximity, regardless of whether they are in the context of synaptic complex produced during a coupled reaction or single complex formed in a single reaction. On the other hand, in coupled reaction catalyzed by c/cRAG or e/cRAG in Mg^{2+}, except for the initial increase, FRET efficiency stayed fairly constant, indicating the strong retention of HP-CEs in CEC formed with a pair of RSS. Furthermore, $I_{acceptor}/I_{donor}$ signal remains higher at all time points in coupled reactions than those observed in the single reactions over the course of incubation, indicating that HP-CEs are retained better in paired-CEC than in single-CEC, which is consistent with the previous notion on this matter (comparing Figure 7A and Figure 5E). Overall, for the first time, I demonstrated the importance of Mg^{2+} in modulating the stability of post-cleavage complex in HP-CEs retention. Our study reinforces the irreplaceable role of Mg^{2+} serving as a physiological cofactor for V(D)J recombination, because of its ability to exerts stringent regulations at various stages during recombination, from

pre-cleavage assembly to cleavage reaction, now even extended to the control of CEC stability.

Discussion

As reviewed in chapter1, PCC stability is a very important aspect that can potentially interfere with the ability of RAG recombinase to choose the appropriate repair pathway for resolving the RAG mediated DSB. Between the two types of PCC, SEC is relatively easy to study due to its intrinsic high stability, and abnormalities associated with a less stable SEC has been reported by several groups (22, 23). CEC, on the other hand, has long been recognized to only transiently retain the HP-CEs, so the effect of CEC stability on V(D)J recombination and genome stability remains elusive, largely due to the technique difficulties to reveal very weak binding. By combining fluorescence anisotropy and FRET techniques, I build a very elegant system that allows real-time monitoring of the RAG-mediated cleavage reaction. For the first time, I can directly assess the interaction between HP-CEs and CEC after cleavage. My quantitative and real time monitoring system empowers us to evaluate various factors that might influence the RAG mediated cleavage and most importantly, the HP-CEs retention in CEC. Indeed, I found that the metal ion cofactor, which was previously thought to only affect pre-cleavage complex formation as well as the catalysis step, also exert significant influence on HP-CEs retention in CEC.

Real-time monitoring of the RAG-catalyzed cleavage reaction and the kinetics of HP-CE release.

Fluorescence anisotropy and FRET techniques provide us great tools to real time monitor the HP-CEs release dissociation from the CEC, but noted that the dissociation kinetic derived from these two methods are actually influenced by the rate of two events, HP-CEs generation ($\tau_{HP\text{-}p}$) and HP-CEs release ($\tau_{HP\text{-}R}$).

To interpret the kinetic data of these two events, I considered the following simplified mechanism, in which the first step represents the production of HP-CE and the second step represents its release from the CEC, leaving SEC.

$$12\ RSS + RAG \xrightarrow{k_1} HP\text{-}CE/CEC \xrightarrow{k_2} HP\text{-}CE + SEC$$

The rate of the first step (k_1) can be easily calculated based on a time-course *in vitro* cleavage reaction revealed by a denaturing gel electrophoresis (Figure 5A, B, C right pannel). The rate of the second step (k_2) is primarily determined by FRET measurement. Specifically, FRET efficiency is only changed proportionally to the released HP-CEs, however, in the reaction mixture at certain moment, a fraction of HP-CEs may still be retained in CEC which does not change FRET efficiency, so the rate determined in this experiment is in principle a combination of k_1 and k_2. Based on the relative values of k_1 and k_2, three situations can be distinguished, reflecting different dissociation kinetics. (1) If $k_2 >> k_1$, i.e. the rate limiting step is hairpin production, the rates measured by FRET and denaturing electrophoresis will be the same, as the hairpin is released

as soon as it is formed ($\tau_{HP\text{-}p} = \tau_{HP\text{-}R}$). This seems to be the situation observed in DNA cleavage reactions catalyzed by several restriction endonucleases, where the cleaved products quickly dissociate from the enzyme (56). The rapid FRET reduction in the initial phase of the cleavage reaction catalyzed by e/cRAG in Mn^{2+} seems to fit into this category, where $\tau_{HP\text{-}R}$ approaches $\tau_{HP\text{-}P}$ (12 min *vs* 10 min; see Table 2). Thus, e/cRAG fails to hold HP-CEs in the presence of Mn^{2+}. (2) On the other hand, if $k_1 = k_2$, i.e., the two rates are comparable, the observed $t_{HP\text{-}R}$ should be somewhat slower than $t_{HP\text{-}p}$, but the two lifetimes should be of the same order of magnitude. Clearly, the c/cRAG-catalyzed excision in Mn^{2+} fits into this profile (Table 2). (3) If $k_2 << k_1$, the rate-limiting step is the release of the hairpin, the lifetime measured by FRET is expected to be much slower than the one measured by electrophoresis ($\tau_{HP\text{-}p} << \tau_{HP\text{-}R}$). This appears to be the case in the cleavage reactions catalyzed by e/cRAG in Mg^{2+}, where $t_{HP\text{-}R}$ is at least 6 times slower than $\tau_{HP\text{-}P}$ (Table 2).

The role of metal ion cofactor in RAG-mediated cleavage reaction has been studied extensively (summarized in chapter 1) and has been implicated in affecting the RAG structure, RAG-RSS interaction, most importantly, the catalysis step of RAG-mediated cleavage on RSS site. Here in this study, by comparing the dissociation kinetics of HP-CEs in the presence of Mg^{2+} and Mn^{2+}, and their behavior in the context of other parameters, such as different forms of RAG proteins, single or coupled reaction, I provide unequivocal evidence that Mg^{2+} also function to

maintain CEC stability and promote HP-CEs retention. Our study further substantiated the important role of Mg^{2+} as a physiological cation in regulating V(D)J recombination throughout the process, from enforcing coupled cleavage of a synaptic complex by following 12/23 rule, to maintain post-cleavage complex stability in terms of HP-CEs retention. However, our observation contrasts with the previous finding that SEs are retained in SEC synaptic complex, regardless of the cation used. (28, 49) (31). The possible reason underneath these two seemingly controversial findings is that, the intrinsically high stability of SEC makes it less influenced by the type of cation present than that of the much labile CEC. Nevertheless, the sensitive nature of our fluorescence-based measurement allows us to assess a very broad dynamic range and to distinguish different levels of association between the RAGs and recombination intermediates under various conditions, which will then help to evaluate the effect of various factors on the stability of these associations *in situ*.

Besides our successful attempt to reveal the weak binding between HP-CEs with CEC, I also observed variation of binding affinities in the presence of different cations, by the fluorescence anisotropy measurement (Figure 4A). Mn^{2+} was found to induce the highest binding affinity of RAG and RSS (K_d = 3.9 nM), while Mg^{2+} and Ca^{2+} show comparable but much lower binding (K_d =13.5 nM or 14.5 nM, respectively). This is the first demonstration that Mn^{2+} induces stronger

binding and may partially explain the very aggressive nature of Mn^{2+}. Noted that the calculated K_d here of c/c RAG binding to 12RSS were somewhat different (much lower) from the K_d in two different anisotropy analyses, i.e., 41 nM and 28 nM reported by Ciubotaru et al and Zhao et al. Noted that the K_d in those two studies were determined for the interaction between cRAG1 and RSS, rather than cRAG1/cRAG2 as in our study, substantiating the notion that the presence of cRAG2 can significantly promote cRAG1 interaction with RSS. (Shuying Zhao, 2009, JMB) On the other hand, K_d for RAG-RSS binding was also determined by EMSA, where the K_d for cRAR1 binding is 123 nM, and the K_d for cRAR1/cRAG2 binding is 25nM. The K_d generated based on EMSA are slightly higher than the K_d obtained by anisotropy, which is likely attribute to the overestimation of binding affinity by EMSA, resulting from the separation of the bound complex from the free probe during the relatively harsh electrophoresis step. So the anisotropy measurement in our study seems to generate the most reliable K_d for c/cRAG-RSS interaction, and provide strong evidence that this interaction is metal ion dependent. Although the physiological role of metal ion on V(D)J recombination remains elusive, our *in vitro* biochemical studies on this issue definitely put forward a new potential regulatory mechanism of V(D)J recombination *in vivo*, where metal ion, depending on its content or concentration, may modulate the fidelity and efficiency of V(D)J recombination.

Table 1. Protein nomenclature

Category	Name	Protein Description
RAG1	cRAG1	core RAG1 (384-1008)
	eRAG1	E649A core RAG1 mutant (384-1008)
	dRAG1	D600A core RAG1 mutant (384-1008)
RAG2	cRAG2	core RAG2 (1-387)
RAG1-RAG2	c/cRAG	cRAG1/cRAG2
	e/cRAG	eRAG1/cRAG2
	d/cRAG	dRAG1/cRAG2

Table 2 Kinetics of the production and release of HP-CEs

Cleavage	RAG	Cation	$\tau_{HP\text{-}p}$[a] (min)	$\tau_{HP\text{-}R}$[b] (min)
Single	c/cRAG	Mn^{2+}	60 ± 5	120 ± 6
	e/cRAG	Mn^{2+}	10 ± 2	τ_1 12 ± 3; τ_2=370 ± 30[c]
	e/cRAG	Mg^{2+}	60 ± 4	400 ± 14
Coupled	c/cRAG	Mn^{2+}	ND[d]	186 ±10
	c/cRAG	Mg^{2+}	ND	>600
	e/cRAG	Mn^{2+}	ND	τ_1 12 ± 2; τ_2=380 ± 25[c]
	e/cRAG	Mg^{2+}	ND	>600

[a]: Lifetime of HP-CE production, a measure of the rate of HP-CE production. The number given was calculated from the kinetic analysis of HP-CE production, as exemplified in Fig. 5A.

[b]: Lifetime obtained from FRET or anisotropy, a measure of the rate of HP-CE release, as exemplified in Fig. 5A.

[c]: Bi-phasic kinetics, in which $\tau\tau_1$ is relevant to HP-CE release whereas τ_2 may be caused by the generation of additional band as it is not correlated with $\tau_{HP\text{-}p}$, i.e., HP-CE production rate (see Fig. 5A).

[d]: Not determined.

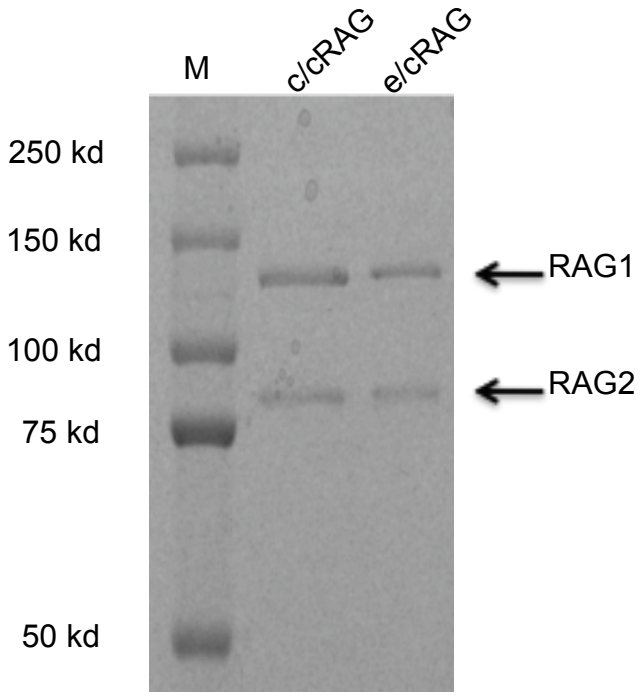

Figure 1. Visualization of c/cRAG and e/cRAG on SDS-PAGE, revealed by Coomassie blue staining.

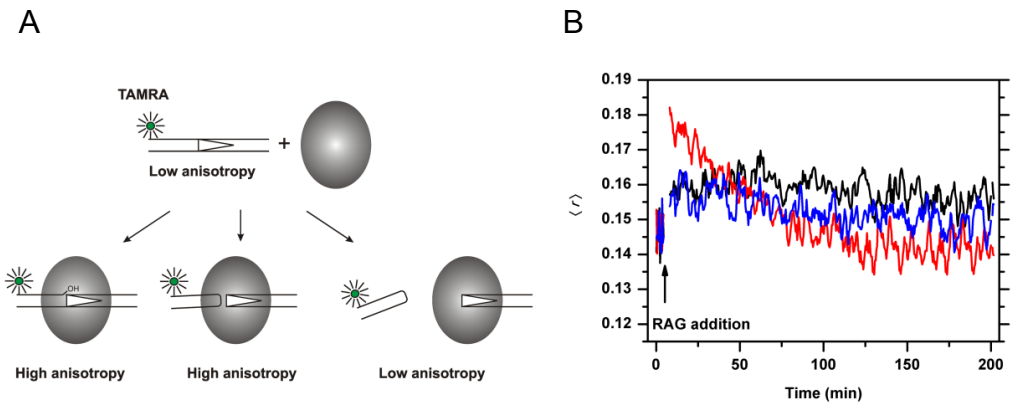

Figure 2. Real-time analysis of RAG-RSS interactions using fluorescence-Anisotropy.

(A) Schematic illustration of the expected changes in fluorescence anisotropy due to interactions between RAG and the 5'-TAMRA labeled 12RSS. The anisotropy signal increases once the RAG protein binds to the 12RSS. The elevated anisotropy signals are maintained after RAG-mediated nicking or excision, as long as the HP-CEs remain in the CEC. The release of HP-CEs from the CEC results in the reduction of the anisotropy signal.

(B) Cation-dependent changes in FRET experiment during RAG-RSS interactions. The anisotropy profiles of c/cRAG interactions with the TAMRA-labeled 12RSS are affected by the cation present in the cleavage reaction, i.e., Ca^{2+} (blue), Mg^{2+} (black) or Mn^{2+} (red).

A

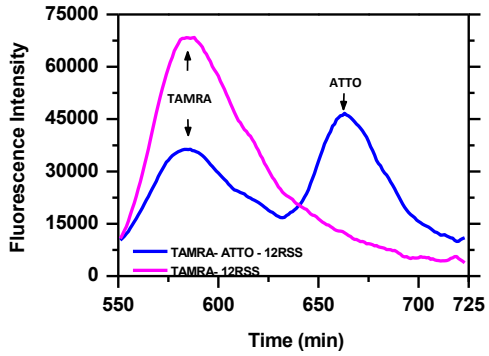
75000
60000
45000
30000
15000
0
Fluorescence Intensity
TAMRA
ATTO
TAMRA- ATTO - 12RSS
TAMRA- 12RSS
550
600
650
700
725
Time (min)

B

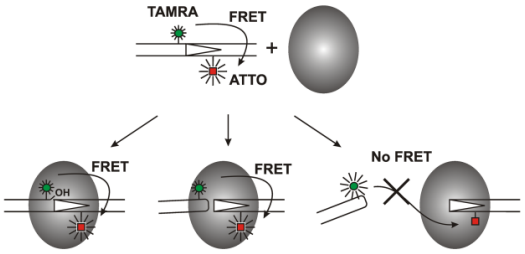
TAMRA
FRET
+
ATTO
FRET
OH
FRET
No FRET

C

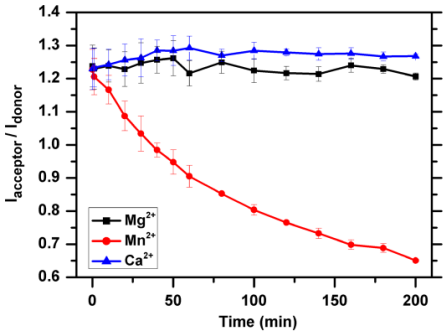
1.4
1.3
1.2
1.1
1.0
0.9
0.8
0.7
0.6
I acceptor / I donor
Mg2+
Mn2+
Ca2+
0
50
100
150
200
Time (min)

Figure 3. Real-time analysis of RAG-RSS interactions using FRET techniques

(A) Emission spectral of TAMRA-12RSS and TAMRA-ATTO-12RSS, the presence of ATTO results in a reduction of TAMRA intensity and the appearance of ATTO emission peak.

(B) Schematic representation of the FRET changes that result from RAG-mediated interactions with the TAMRA-ATTO doubly labeled 12RSS. The FRET signal remains unchanged during nicking (left) and hairpin formation (middle), as long as the HP-CEs are kept within the coding end complex (CEC) at close proximity with signal ends (SEs). The release of the HP-CEs from the CEC (right) results in an increase in donor (TAMRA), and a reduction in acceptor (ATTO), producing a reduction in FRET efficiency.

(B) c/cRAG mediated single cleavage reactions in the presence of different cations revealed by FRET. The ratio of acceptor to donor ($I_{acceptor}$ / I_{donor}) is compared among the cleavage reactions in the presence of Ca^{2+} (blue), which does not support cleavage, Mg^{2+} (black), which causes nicking only, or Mn^{2+} (red), which allows the uncoupled cleavage. The results are presented as an average of three replicates with the standard deviation (SD).

A

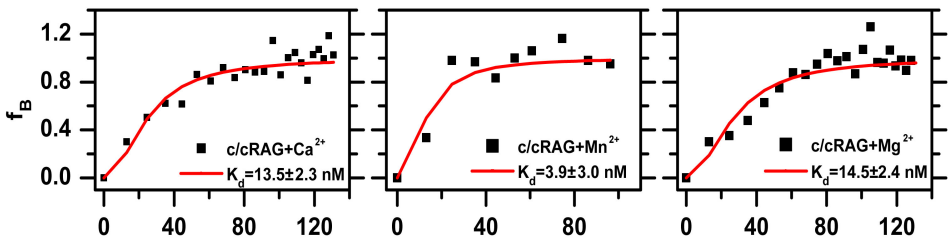
1.2
0.8
0.4
0.0
f_B
c/cRAG+Ca^{2+}
K_d=13.5±2.3 nM
c/cRAG+Mn^{2+}
K_d=3.9±3.0 nM
c/cRAG+Mg^{2+}
K_d=14.5±2.4 nM
0
40
80
120
RAG (nM)

B

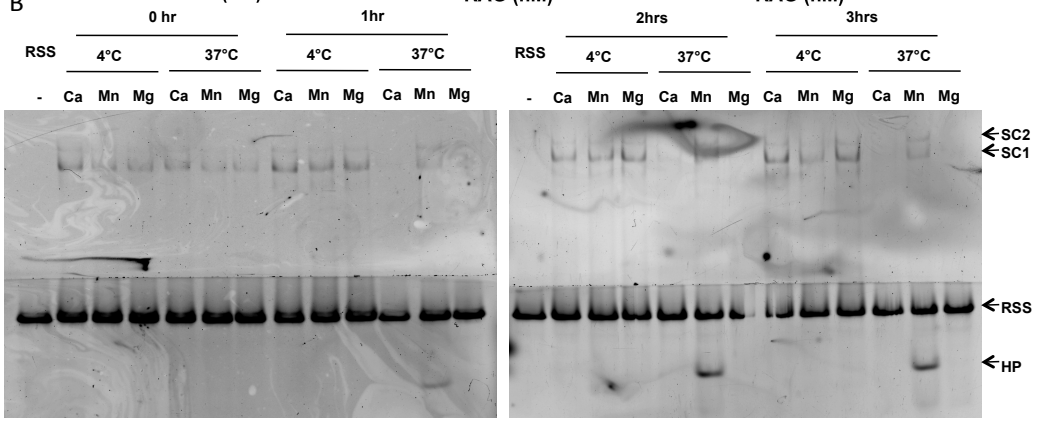
0 hr
1hr
2hrs
3hrs
RSS
4°C
37°C
- Ca Mn Mg Ca Mn Mg Ca Mn Mg Ca Mn Mg
SC2
SC1
RSS
HP

Figure 4. Comparison of the binding affinity of RAG and RSS in the presence of three cations

(A) Determination of the binding affinity (K_d) between c/cRAG and 12RSS in the presence of Ca^{2+} (left), Mn^{2+} (middle), and Mg^{2+} (right). The fraction of bound 12RSS (f_B) was calculated from fluorescence anisotropy data obtained with 5'-labeled TAMRA 12RSS as described in the supplemental information. The red lines represent the fit to a model that assumes a 1:2 binding stoichiometry, from which I obtained the dissociation constant of the complex (see supplemental information).

(B) RAG-RSS interactions analyzed by Electrophoretic Mobility Shift Assay (EMSA). c/cRAG was incubated with TAMRA-12RSS at 4 °C or 37 °C for the time indicated in the figure, in the presence of either Ca^{2+} or Mn^{2+} or Mg^{2+}. The first lane in each gel shows the intact 12RSS without RAG. The arrows point to the bands corresponding to the DNA-protein complexes (SC1 and SC2), the free 12RSS probe (RSS) and the hairpin (HP). Note the presence of DNA-protein complexes at 37°C after 3 hrs of incubation in the presence of Mn^{2+}.

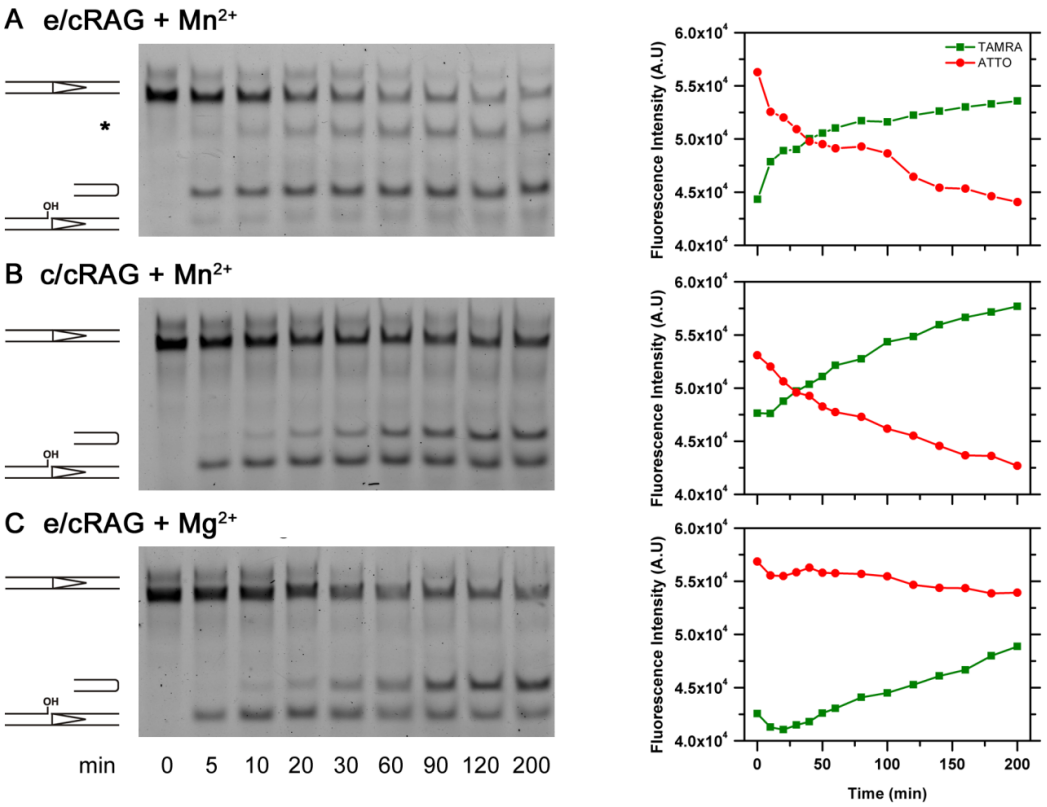
A e/cRAG + Mn2+
B c/cRAG + Mn2+
C e/cRAG + Mg2+
OH
min 0 5 10 20 30 60 90 120 200
TAMRA
ATTO
Fluorescence Intensity (A.U)
Time (min)

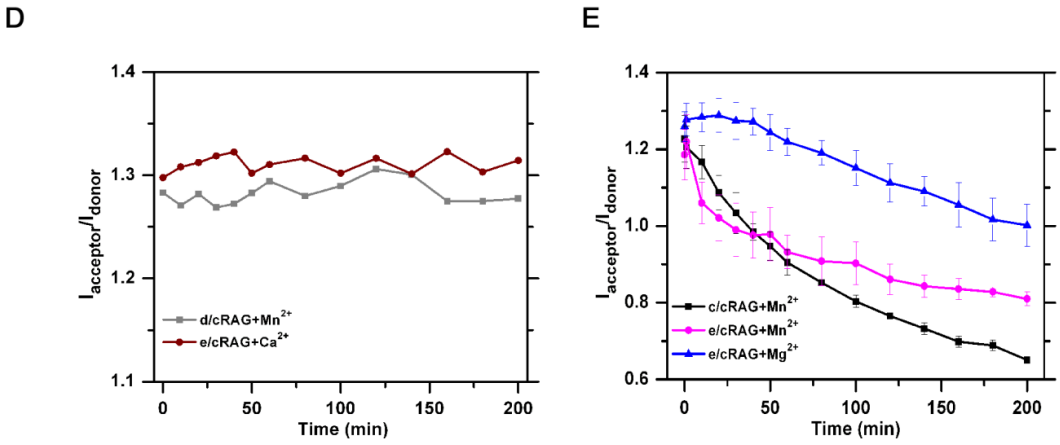
D
E
Iacceptor/Idonor
d/cRAG+Mn2+
e/cRAG+Ca2+
c/cRAG+Mn2+
e/cRAG+Mn2+
e/cRAG+Mg2+
Time (min)

Figure 5. Time-course assessment of cleavage reactions with different cations by both denaturing gel electrophoresis and FRET analysis. Left: Examination of the recombination intermediates, nicked ends and HP-CEs by denaturing gel electrophoresis, which are generated by (A) e/cRAG in Mn^{2+}, (B) c/cRAG in Mn^{2+}, (C) e/cRAG in Mg^{2+}. * denotes a non-specific band. Right: Results of FRET experiments under the same conditions as in the Left, showing the emission intensities of TAMRA (red) and ATTO (green) as a function of time. (D) FRET signals ($I_{acceptor}$ / I_{donor}) in reactions containing the catalytic inactive d/cRAG mutant in Mn^{2+} (gray line) or the gain-of-function e/cRAG in Ca^{2+} (red line). (E) FRET signals ($I_{acceptor}$ / I_{donor}) obtained from the cleavage reactions shown in (A-C): e/cRAG in Mn^{2+} (magenta), c/cRAG in Mn^{2+} (black) and e/cRAG in Mg^{2+} (blue).

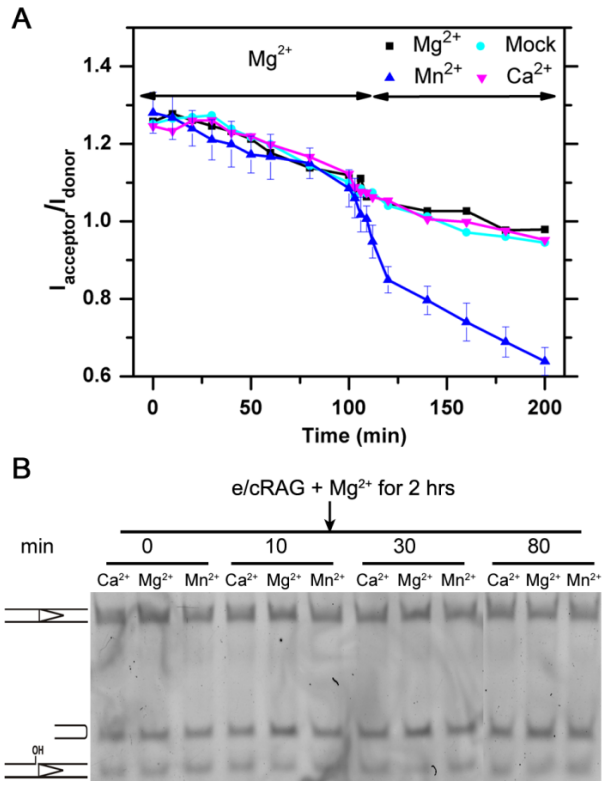
A
Mg2+
Mg2+
Mock
Mn2+
Ca2+
1.4
1.2
1.0
0.8
0.6
Iacceptor/Idonor
0
50
100
150
200
Time (min)
B
e/cRAG + Mg2+ for 2 hrs
min
0
10
30
80
Ca2+ Mg2+ Mn2+ Ca2+ Mg2+ Mn2+ Ca2+ Mg2+ Mn2+ Ca2+ Mg2+ Mn2+
OH

Figure 6. The influence of HP-CE release by different cations.

(A) FRET changes over the course of cation addition. The reaction was initiated with e/cRAG in Mg^{2+} and incubated for 2 hours, after which Mg^{2+} (black), Ca^{2+} (magenta), or Mn^{2+} (blue) were added. A mock treatment is shown in cyan.

(B) Denaturing gel electrophroresis analysis of HP-CE production after the step-wise addition of different cations. The different bands (from top to bottom) represent the intact RSS, hairpin, and nicked DNA. All reactions were initiated by e/cRAG in Mg^{2+} and incubated for 2 hrs, after which the different cations described in the figure were added to the reaction. The times represent the incubation time after cation addition.

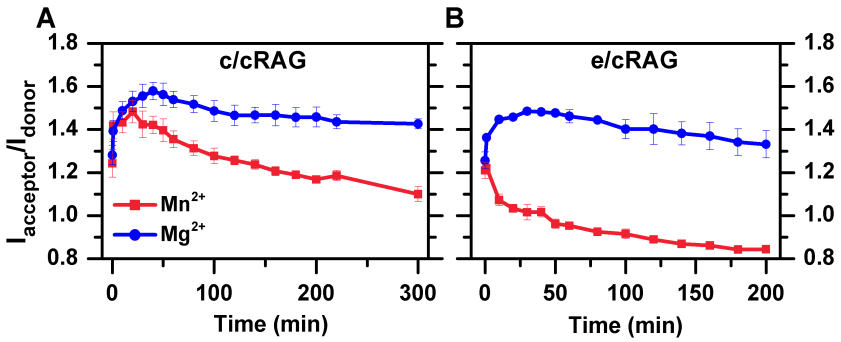

Figure 7. FRET profiles of coupled cleavage reactions catalyzed by (A) c/cRAG or (B) e/cRAG in the presence of HMGB1 and unlabeled 23RSS under Mg^{2+} (blue) or Mn^{2+} (red).

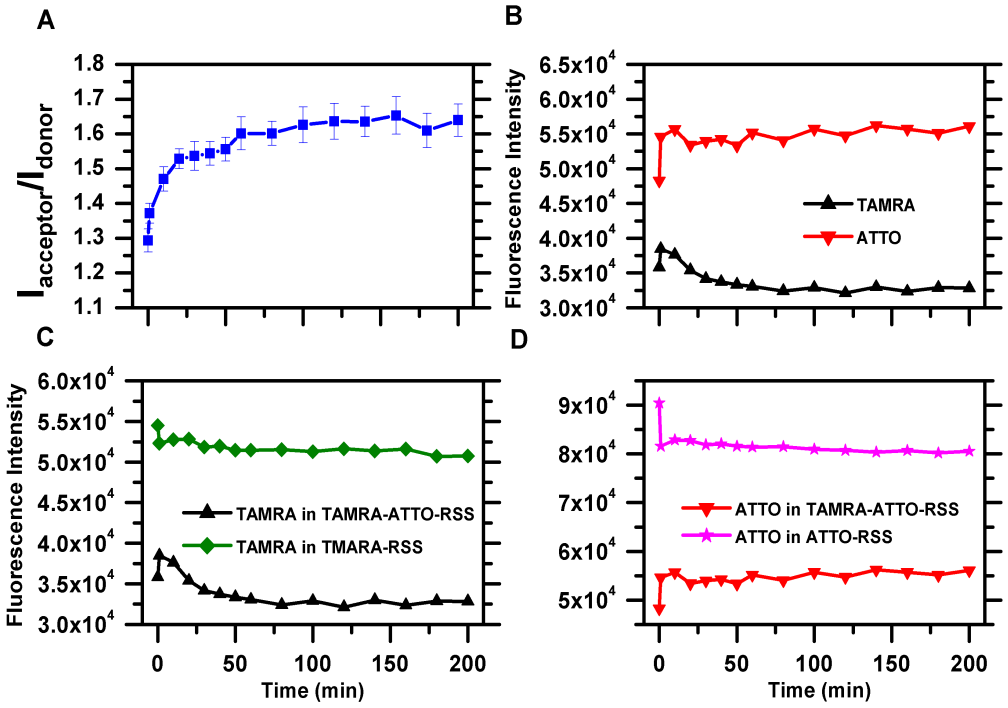
A
B
C
D
$I_{acceptor}/I_{donor}$
Fluorescence Intensity
TAMRA
ATTO
TAMRA in TAMRA-ATTO-RSS
TAMRA in TMARA-RSS
ATTO in TAMRA-ATTO-RSS
ATTO in ATTO-RSS
Time (min)

Figure 8. Confirmation of the initial increase of the ratio, $I_{acceptor}/I_{donor}$, as FRET change in coupled reaction

(A) Change of $I_{acceptor}/I_{donor}$ in the reaction mediated by e/cRAG in the presence of Ca^{2+} using TAMRA-ATO RSS.

(B) The corresponding changes of the emission intensities of TAMRA (black) and ATTO (red) observed in the above reaction.

(C) The fluorescence intensity was monitored for the single labeled 12RSS, TAMRA-12RSS (green), under the same reaction condition for TAMRA-ATTO 12RSS, and was compared to the TAMRA (black in C) intensity changes of the dual labeled 12RSS. The emission intensities TAMRA-12RSS stay quite constant, in contrast to the changes observed in the dual-labeled 12RSS, such as the gradual decrease observed in dual probe.

(D) The fluorescence intensity was monitored for the single labeled 12RSS, ATTO-12RSS (magenta), under the same reaction condition for TAMRA-ATTO 12RSS, and was compared to the ATTO (red in D) intensities of the dual labeled 12RSS, respectively. The intensity of single ATTO-12RSS also stays quite constant, in contrast to the changes observed in the dual-labeled 12RSS.

Reference

1. Ingersoll CM, Strollo CM (2007) Steady-State Fluorescence Anisotropy To Investigate Flavonoids Binding to Proteins. *J. Chem. Educ.* 84:1313.

2. Lakowicz JR (2006) *Principles of Fluorescence Spectroscopy* (Springer). 3rd Ed.

3. Anderson BJ, Larkin C, Guja K, Schildbach JF (2008) Using Fluorophore-labeled Oligonucleotides to Measure Affinities of Protein-DNA Interactions. *Methods Enzymol* 450:253–272.

4. Stryer L, Haugland RP (1967) Energy transfer: a spectroscopic ruler. *Proc. Natl. Acad. Sci. U.S.A.* 58:719–726.

5. Uster PS (1993) In situ resonance energy transfer microscopy: monitoring membrane fusion in living cells. *Meth. Enzymol.* 221:239–246.

6. Schatz DG, Oettinger MA, Baltimore D (1989) The V(D)J recombination activating gene, RAG-1. *Cell* 59:1035–1048.

7. Oettinger MA, Schatz DG, Gorka C, Baltimore D (1990) RAG-1 and RAG-2, adjacent genes that synergistically activate V(D)J recombination. *Science* 248:1517–1523.

8. van Gent DC et al. (1995) Initiation of V(D)J recombination in a cell-free system. *Cell* 81:925–934.

9. Rooney S, Chaudhuri J, Alt FW (2004) The role of the non-homologous end-joining pathway in lymphocyte development. *Immunol. Rev.* 200:115–131.

10. Schatz DG, Oettinger MA, Schlissel MS (1992) V(D)J Recombination: Molecular Biology and Regulation. *Annual Review of Immunology* 10:359–383.

11. Gellert M (2002) V(D)J RECOMBINATION: RAG PROTEINS, REPAIR FACTORS, AND REGULATION*. *Annual Review of Biochemistry* 71:101–132.

12. Fugmann SD, Lee AI, Shockett PE, Villey IJ, Schatz DG (2000) The RAG proteins and V(D)J recombination: complexes, ends, and transposition. *Annu. Rev. Immunol* 18:495–527.

13. Lu H et al. (2008) A Biochemically Defined System for Coding Joint Formation in V(D)J Recombination. *Mol Cell* 31:485–497.

14. Landree MA, Wibbenmeyer JA, Roth DB (1999) Mutational analysis of RAG1 and RAG2 identifies three catalytic amino acids in RAG1 critical for both cleavage steps of V(D)J recombination. *Genes Dev* 13:3059–3069.

15. Kriatchko AN, Anderson DK, Swanson PC (2006) Identification and Characterization of a Gain-of-Function RAG-1 Mutant. *Mol Cell Biol* 26:4712–4728.

16. Bergeron S, Anderson DK, Swanson PC (2006) RAG and HMGB1 proteins: purification and biochemical analysis of recombination signal complexes. *Meth. Enzymol.* 408:511–528.

17. Santagata S, Aidinis V, Spanopoulou E (1998) The effect of Me2+ cofactors at the initial stages of V(D)J recombination. *J. Biol. Chem* 273:16325–16331.

18. Shlyakhtenko LS et al. (2009) Molecular mechanism underlying RAG1/RAG2 synaptic complex formation. *J. Biol. Chem* 284:20956–20965.

19. Kriatchko AN, Bergeron S, Swanson PC (2008) HMG-box domain stimulation of RAG1/2 cleavage activity is metal ion dependent. *BMC Mol. Biol* 9:32.

20. van Gent DC, Hiom K, Paull TT, Gellert M (1997) Stimulation of V(D)J cleavage by high mobility group proteins. *EMBO J* 16:2665–2670.

21. Pavlicek JW, Lyubchenko YL, Chang Y (2008) Quantitative analyses of RAG-RSS interactions and conformations revealed by atomic force microscopy. *Biochemistry* 47:11204–11211.

22. Jones JM, Gellert M (2001) Intermediates in V(D)J recombination: A stable RAG1/2 complex sequesters cleaved RSS ends. *Proceedings of the National Academy of Sciences* 98:12926 –12931.

23. Grundy GJ et al. (2009) Initial Stages of V(D)J Recombination: The Organization of RAG1/2 and RSS DNA in the Postcleavage Complex. *Molecular Cell* 35:217–227.

CHAPTER 3

REGULATION OF V(D)J RECOMBINATION BY RAG RECOMBINASE - CHARACTERIZATION OF THE FRAME-SHIFT RAG2 MUTANT USING FLUORESCENCE-BASED MEASUREMENTS

Introduction

PCC (Post-cleavage complex) stability is thought to be directly related to the selection of appropriate repair pathway in V(D)J recombination, for its ability to properly retain and transfer the RAG-induced double strand breaks (DSBs) to the repair machinery. (1, 2). Various factors have been postulated to alter PCC stability, such as mutations in RAG, alteration in RSS heptamer and coding flanks, or mutations of DSB sensor or repair proteins, such as Ataxia telangiectasia mutated (ATM) and NHEJ factors etc. (3–5). Given the feasibility of using fluorescence-based detection techniques to quantify PCC stability (detailed in the Chapter 2), I decided to directly investigate a long-standing unresolved question on a RAG2 mutant, frame shift core RAG2 mutant (hereafter referred to as fsRAG2).

fsRAG2 is implicated in causing increased end resolution by aberrant repair pathways, such as alternative-NHEJ and homologous repair (HR) (1, 4). Notably, the aberrant end joining in the presence of fsRAG2 happens to both signal ends (SEs) and HP-CEs, which suggests that CEC and SEC both may be affected by this mutant. On the other

hand, in the NHEJ-deficient background, signal joints are more robustly rescued by the alternative-NHEJ than the rescue of coding joints, 100% to 50%, indicating that fsRAG2 mutant may affect CEC and SEC at different levels or with different regulatory systems (1, 4), which seems paradoxical to the fact that CEC and SEC actually refers to the same RAG complex and only differs in their retained ends, which in theory should handle HP-CEs and SEs similarly. Nevertheless, the exact molecular mechanism of fsRAG2-induced aberrant V(D)J recombination remains undefined, and a less stable PCC associated with fsRAG2 was blamed to be the underlying culprit, however, no direct biochemical evidence was reported. Here I took advantage of the fluorescence-based system to monitor in real time the RAG-mediated cleavage reaction in the presence of fsRAG2. Our highly sensitive and non-disruptive system allows us to characterize the molecular mechanism of the reaction containing fsRAG2, e.g., through direct comparison of fsRAG2 and cRAG2, I can reveal any abnormalities associated with this mutant, and I can determine whether or how fsRAG2 affects the PCC stability. In addition, to entertain the possibility that CEC and SEC might be influenced differently by fsRAG2, I sought to investigate the stability of both CEC and SEC in the same cleavage reaction conditions using the fluorescence-based monitoring system. My analyses will shed light on the mechanistic basis of fsRAG2-associated aberrant V(D)J recombination. Furthermore, such analysis also provides us with

more confidence to examine many other factors that might influence the efficiency and fidelity of V(D)J recombination.

Materials and Methods

Protein purification

Maltose binding protein (MBP) tagged core RAG1 (residues 384-1008) and core RAG2 (residues 1-387) proteins were co-expressed in 293T cells using the Plus/Lipofectamine reagent (Invitrogen, Carlsbad, CA). Other MBP-fused RAG proteins were also prepared, a gain-of-function RAG1 mutant E649A (eRAG1, 384-1008) (6), and a frame shift RAG2 mutant (fsRAG2) (1), in which the C-terminus 22 amino acids of core RAG2 is replaced by another 27 novel amino acids. Four combinations of wild type or mutant RAG1 and RAG2 were co-expressed in 293T cells, which are listed in Table I, along with the nomenclatures of these proteins. The expressed proteins were purified following the procedure described by Bergeron *et al.* (7). The protein concentration was measured with the Nanodrop Spectrophotometer (Thermo SCIENTIFIC, Wilmington, DE) and verified by SDS-PAGE, in which no bands other than RAG1 and RAG2 were visible, as shown in Figure 1. The same amount of RAG proteins was used in the binding or cleavage reactions unless descried otherwise.

DNA The sequence of the DNA substrate used in this study are shown below: 12RSS Top: 5'-TATCAGCTGATAGCTAACACAGTGCTACAGA-CTGGAACAAAAACCCTGCT-3'; 12RSS bottom: 5'-AGCAGGGTTTTTG-T-TC-CAGTCTGTAGCACTGTGTTAGCTATCAGCTGATC-3'; 23RSS top: 5'-ATCGAAGTACCAGTAGCACAGTGGTAGTACGCGTCTGTCTGGCTG-

TACAAAAACCATGGATCCT-3'; 23RSS bottom: 5'-AGGATCCATGGTT-TTTGTACAGCCAGACAGACGCGTACTACCACTGTGCTACTGGTACTT-CGAT-3'. The 12RSS top strand was labeled with TAMRA, either at 5'-end, or internally at the 3rd nucleotides (T) 5' to the heptamer. The 12RSS bottom strand used in the FRET experiment was labeled with ATTO647N (hereafter referred to as ATTO) at the spacer region, 6th nucleotides (T) 3' to the nonamer. And the 12RSS probe used for signal end complex (SEC) study is labeled with TAMRA at 5'end of the bottom strand. The fluorescence labeled-DNA nucleotides were obtained from IBA BioTAGnology (Göttingen, Germany) and the unlabeled ones from Integrated DNA Technologies Inc. (Coralville, IA). 12RSS top strand with the internal labeled TAMRA was annealed to the ATTO-labeled bottom strand and were purified by native polyacrylamide gel electrophoresis to remove any residual single-stranded DNA. The dually labeled 12RSS oligonucleotide substrates were examined in the FRET experiments while the 5' end-TAMRA-labeled (both top and bottom) 12RSS substrates were analyzed by the fluorescence anisotropy. As controls for analyzing fluorescence quenching effect, the singly labeled substrates were obtained by annealing the internal labeled TAMRA strand to the unlabeled bottom strand or the unlabeled top strand to the ATTO labeled bottom strand.

***In vitro* cleavage assay**

The cleavage reaction of the fluorescence-labeled 12RSS (20 nM) was catalyzed by RAG proteins (65 nM) in 10 ml reaction containing 10 mM Tris-HCl [pH 7.5], 50 mM NaCl and 100 μg/μl BSA in Mn^{2+} (0.2 mM) and Mg^{2+} (2.5 mM). The reaction inactive for cleavage was also included as a control, i.e., the same probe incubated in the same reaction buffer, except with Ca^{2+} (2.5 mM) or using the catalysis-defective RAG1 mutant (dRAG1) paired with cRAG2. For the coupled cleavage reactions, HMGB1 protein (30 ng/μl, Sigma-Aldrich) and 23RSS (150 nM) were included. The reaction mixture was incubated at 37°C for various times as indicated in the figures, and stopped by adding 10 ml denaturing loading dye containing 90% formamide for denaturation at 95°C and quick chill on ice before being loaded onto a 16% Tris-Borate-EDTA-7 M urea-polyacrylamide gel. After electrophoresis, the gel was imaged on a Typhoon scanner (GE Healthcare) with laser excitation at 532 nm and emission filter of 580 nm to detect TAMRA fluorescence or use laser excitation at 633 nm and emission filter of 670 nm to detect ATTO fluorescence.

Electrophoretic Mobility Shift Assay (EMSA)

EMSA was performed to analyze the interactions between RAG proteins and RSS. Samples were prepared as described for the *in vitro* cleavage assay. The reaction was stopped by adding 5 μl 100% glycerol for every 10 μl reaction, and the sample was immediately loaded onto 4% native gel (with 19:1 acrylamide: bisacrylamide). Samples were subjected

to electrophoresis at 200 V, 4°C for 2.5 hours. The resulting gel was imaged on the Typhoon scanner (GE Healthcare) to detect either TAMRA or ATTO fluorescence.

Fluorescence anisotropy.

A Photon Technology International QuantaMaster-4/2005SE Spectrofluorometer was used for all fluorescence experiments. A 3 mm × 3 mm quartz micro-cuvette with a 50 ml-sample chamber was used in all measurements, and temperature was controlled by a circulating water bath and set at 37°C except where noted. The fluorophore-labeled sample is excited by a polarized beam light, which allows photo-selection of a fraction of fluorophores that are properly oriented relative to the incoming light. The anisotropy is defined as $\langle r \rangle = (I_{VV} - GI_{VH})/(I_{VV}+2GI_{VH})$, where I is the fluorescent intensity, V and H reflects the vertical and horizontal orientation by which the emission and excitation polarizer is mounted. The factor G is defined as, I_{HV}/I_{HH}, the intensity ratio of the vertical emission to horizontal emission when the sample is excited with horizontal polarized light. G factor is dependent on the monochromator wavelength and slit width and is used to correct for polarization-dependent effects in detection sensitivity. The excitation and the emission wavelengths were set at 510 nm and 580 nm, and data was acquired every 10 seconds. Background correction was applied to all the measurements. The anisotropy of the 5'-TAMRA-labeled 12RSS in the appropriate buffer (with cations indicated in the figures) was measured before and after the addition of RAG proteins.

The temperature was maintained at 37°C for the duration of the experiment (~3 hours). The final concentration of all the components was the same as used in the *in vitro* cleavage reactions. At the end of cleavage reactions, SDS was added to liberate DNA from protein association, where the anisotropy of free HP-CEs is lower than the free probe or DNA with a nick.

Fluorescence Resonance Energy Transfer (FRET)

The same instrument and setting are used for FRET experiment as those in fluorescence anisotropy measurement. Samples were excited at 510 nm, except in the control experiments with ATTO-only RSS, where the excitation wavelength was set at 600 nm. Sample reactions were assembled as described for the *in vitro* cleavage assay, except that sample components were scaled up five-fold so that the final concentration of all the components was the same as used in the *in vitro* cleavage reaction. The FRET efficiency of the TAMRA-ATTO-labeled 12RSS probe was measured before and after adding the purified RAG proteins. Emission scans were recorded every 10 min during the first hour and then every 20 min for another 2 hours. The ratio $I_{acceptor}$ /I_{donor} was calculated from the peak intensities of the acceptor and donor, and used as a measure of the FRET efficiency. Note that the ratio, $I_{acceptor}$ /I_{donor}, does not represent the actual FRET efficiency, which should be $I_{acceptor}$ /(I_{donor} + $I_{acceptor}$), where the FRET efficiency is highly sensitive to donor-acceptor distance. Because I did not attempt to obtain the distance

information between donor-acceptor, rather we focused on the relative comparison of the FRET efficiency changes, and thus the ratio $I_{acceptor}$ /I_{donor} was used instead as a measure of FRET efficiency for its simplicity.

The experiment involving a temperature ramp was conducted on the cleavage reaction initiated by e/cRAG or e/fsRAG in Mg^{2+} at 37°C for 1 hour followed by a temperature increase to 55°C over 15 min. The emission intensities of TAMRA and ATTO were monitored over the temperature-ramp once every 2°C, and then every 20 min over the next 1 hour.

Data fitting.

Kinetic traces of FRET and fluorescence anisotropy experiment were fitted using the program embedded in OriginPro8, to either a mono-exponential decay ($I_{acceptor}$ /I_{donor} = A*exp*(-t/τ)+A_∞), In these equations, t represents time, τ represents the dissociation lifetime, and A_∞ represents the $I_{acceptor}$ /I_{donor} ratio where all generated HP-CEs is liberated from the RAG complex. Because in some reactions, HP-CEs was not completely released by the end of 3 hours acquisition time, meaning the lifetime is longer than 3 hours, the parameter A_∞ was determined by either adding a denaturing agent (0.5% SDS) at the end of the experiment, or by increasing the temperature to 55 °C to dissociate all hairpins. Both methods yield the same value, which was used as a fixed parameter in the fitting procedures.

Result

Comparison of CEC stability between cRAG2 and fsRAG2

As I discussed in chapter 2, RAG1 E649A mutant (eRAG1) as a gain-of-function mutant, allows single cleavage in the presence of Mg^{2+}. So I paired eRAG1 with fsRAG2 together (e/fsRAG), and compared the HP-CEs retention pattern in single reaction catalyzed by either e/cRAG or e/fsRAG in the presence of Mg^{2+} using FRET technique. As shown in Figure 2A, except for the initial drastic drop of the ratio $I_{acceptor}/I_{donor}$ (which will be discussed in detail in next section), FRET signal decreased at the same rate for cRAG2 and fsRAG2, suggesting that the stability of CEC formed with a single 12RSS is not significantly affected by the fsRAG2 mutant. The fsRAG2 does not seem to affect the cleavage activity either, as c/cRAG and c/fsRAG display comparable rate and level of HP-CEs formation, as shown in Figure 2B. Thus, this finding indicates fsRAG2 and cRAG2 display comparable degree of PCC stability.

To rule out the possibility that the lack of apparent differences between fsRAG2 and cRAG2 in our PCC stability analysis might have been attributed to the insensitivity of our detection system, I attempted to amplify the difference by applying a temperature-challenging release assay, which was described by Roth's group in their attempt to assess the SEC stability (3). Specifically, I first incubated the single cleavage reaction mediated by either e/cRAG or e/fsRAG at 37°C for one hour, a period of time sufficient to generate a significant amount of HP-CEs for subsequent

analysis. Then, the temperature was ramped to 55°C over a period of 15 min, and the reaction was maintained at 55°C for another 2 hours. FRET signal was continuously recorded during and after the temperature increase. As shown in Figure 2C, the rapid FRET drop upon temperature increase reflected the total release of newly generated HP-CEs and it happened almost simultaneously and at a similar temperature range for both reactions. This finding argues against the scenario of a less stable CEC that is formed in the presence of fsRAG2, where the FRET drop would happen earlier and at a lower temperature. Notably, there is a slight rise in the $I_{acceptor}$ /I_{donor} ratio during the temperature increase occurring in both RAG-containing reaction as well as in the probe only reaction, possibly due to the temperature-induced differential change in the quantum yield of TAMRA and ATTO fluorophores. This data further substantiates our earlier finding that in the single cleavage reaction, the CEC composed of the fsRAG2 displays a similar level of stability as compared to the one containing cRAG2.

To test the influence of fsRAG2 on HP-CEs retention under a more physiological condition, coupled reactions mediated by e/cRAG and e/fsRAG were also compared (Figure 3A, red and pink). Specifically, in coupled reaction containing e/cRAG, the FRET signal initially increases due to potential DNA bending (as discussed in chapter 2, Figure 7) and then gradually decays due to the release of HP-CEs. The above pattern of FRET changes was greatly altered in the presence of e/fsRAG, such that

an initial instant FRET drop occurred before the FRET increase caused by DNA bending. However, the FRET decay rate at later stage was indistinguishable between the two. The similar results were again observed when I tested coupled reactions that paired cRAG1 together with either cRAG2 or fsRAG2 (Figure 3A, black and blue). Notably, similar to c/cRAG, in the presence of the partner 23RSS and HMGB1, c/fsRAG can form a synaptic complex onto the labeled 12RSS, revealed by the upper shifted bands in EMSA as shown in Figure 3B, which indicates that fsRAG2 does not interfere with the synapsis formation. To summarize, regardless of the mysterious nature of the initial sharp FRET decrease and the content of partner RAG1, reactions containing cRAG2 or fsRAG2 show similar HP-CEs release rate, indicating that fsRAG2 does not seem to destabilize the CEC formed with either single RSS or paired RSSs, although both our study and others have shown that the paired-CEC is intrinsically more stable than the single-CEC (compare Figure 3A to Figure 2A) (8).

Evidence for the unique FRET pattern in RAG-mediated reactions containing fsRAG2 mutant

Although the PCC stability is not affected by fsRAG2, the initial rapid FRET drop associated only with fsRAG2 in both single reaction and coupled reaction raised great interest. To elucidate the role of fsRAG2 in mediating this unique FRET change pattern and to determine whether this change is assocated with actual hairpin formation, I replaced Mg^{2+} with

Ca^{2+} in e/fsRAG mediated single reaction to allow specific binding, or tested single reaction catalyzed by c/fs RAG protein together with Mg^{2+} to allow only nicking. In both cases, I observed the initial drastic signal reduction (Figure 4), together with the fact that this drop was observed at the very beginning of the reaction where no HP-CEs is formed yet, it implies that the FRET reduction was not caused by the actual cleavage, i.e., not due to HP-CEs formation and the subsequent release from CEC. However, the reduction of $I_{acceptor}/I_{donor}$ is completely unexpected since the distance between donor and acceptor is not supposed to undergo such drastic increase upon RAG binding. To ensure that the observed reduction is a real change of FRET efficiency, rather than the result of RAG-induced differential quenching of the donor or acceptor fluorophores, I measured the fluorescence intensity changes of single-labeled probes (TAMRA-labeled strand paired with an unlabeled strand or ATTO-labeled strand paired with an unlabeled strand) in a time-dependent manner under the same reaction condition as shown in Fig. 3A, Ca^{2+} and e/fsRAG. The result from single-labeled probe was compared with the intensity profile of the corresponding fluorophore in the doubly-labeled probe, as shown in Figure 5. The fluorescence intensity of the singly labeled probes displayed a rather constant profile over time, and did not exhibit the initial changes observed in the doubly-labeled probe (Figure 5). Thus, the reduction of ATTO in the doubly-labeled probe was indeed caused by a reduction in energy transfer efficiency, which could be either caused by orientation

alteration between donor and acceptor upon RAG interaction, or by actual distance increase between donor and acceptor. However, the latter scenario is less likely since the distance increase reflected by the drastic FRET reduction only happens when the two DNA strands that contain TAMRA and ATTO are significantly separated (melted), which requires a tremendous amount of energy and seems inconceivable to be induced by protein binding. Regardless of the actual cause, the FRET change seems unique to the presence of fsRAG2. It is known that RAG2 is the regulatory subunit of the RAG recombinase and can directly influence the recognition and interaction of RAG1 to a RSS thereby increase the specificity of RAG1 binding. Therefore, fsRAG2 mutant seems to modulate the RAG1 and 12RSS interaction in such way that the structure of RAG-RSS complex containing fsRAG2 is strikingly different from the one formed by cRAG2. Meanwhile, the TAMRA-ATTO labeled 12RSS probe used in our study may be highly sensitive to this conformational change, either because of the labeling position (especially ATTO labeling at the spacer region) or because of the choice of fluorophores (ATTO is a relative large molecule and is probably more prone to sense any conformational change), or the combination of both. To test these scenarios, I designed a different FRET 12RSS probe (hereafter referred to as ATTO-TAMRA-12RSS), where the choice of donor and acceptor is still the same but the labeling position is opposite to the previous one, with ATTO labeled at the coding flank 5' of heptamer and TAMRA at the spacer region, since

TAMRA is a relatively small molecule and may not be as sensitive as ATTO. When I applied the new probe in reaction containing c/fsRAG and Mg^{2+}, except that the FRET signal of free probe is considerably higher than the previous one, the initial drastic FRET reduction was again observed (Figure 6), which is identical to the previous findings, and further substantiate the unique feature of fsRAG2 in conferring this unusual structure. This finding indicates that the observed FRET drop is not unique to one particular fluorophore, but rather sensitive to the relative position of the two fluorophores upon interactions with fsRAG2 containing RAG. This finding suggests fsRAG2 may confer a structure of the RAG-pre-cleavage complex very different from the one formed by c/cRAG. Also, the labeling position, 3^{rd} nucleotide 5' to heptamer on the top strand and the 6^{th} nucleotide 3' to nonamer on the bottom strand, seems to be sensitive to the conformational change caused by fsRAG2, providing additional information on the contact site of RAG binding when fsRAG2 is present. Regardless of the detailed mechanism of FRET reduction, the unique structural change observed in fsRAG2 upon its interaction with RSS is of great interest for further investigation.

Further examination of the unusual RAG-12RSS complex associated with fsRAG2

Our FRET-based real time monitoring system reveals a unique structure of the pre-cleavage complex in the presence of fsRAG2. To further examine this structure, I applied both EMSA and fluorescence

anisotropy to characterize any possible distinct features associated with fsRAG2 in terms of the pre-cleavage complex formation and RAG-RSS interaction. In EMSA studies, with the same input of various RAG1/RAG2 combinations (Figure 1), a higher intensity band at the position of SC1 (Singe Complex 1, one of the complexes formed upon RAG binding to a single RSS, which is possibly composed of two RAG1 and one RAG2) was observed in reactions containing either e/fsRAG or c/fsRAG. Furthermore, a band migrating much slower than the conventional SC2 (Single Complex 2, which is composed of two RAG1 and two RAG2) also appeared when fsRAG2 was present, as shown in Figure 7C. The above phenotype was observed similarly in either Mg^{2+} or Ca^{2+} containing reaction, suggesting that regardless of the metal ion cofactor, fsRAG2 promotes more RAG-RSS complex formation, which is possibly due to stronger binding. In addition, fsRAG also renders the formation of larger RAG-RSS complex, which runs much slower than the conventional SC2 complex and is probably composed of more RAG1 or fsRAG2 protein in the complex. Indeed, when I applied fluorescence anisotropy to monitor the aforementioned reactions, a significantly higher anisotropy signal was observed in e/fsRAG than that in e/cRAG, in the presence of Ca^{2+}, as shown in Fig. 7B, in consistent with the EMSA study. Moreover, our binding affinity measurement performed by fluorescence anisotropy revealed that the binding constant for e/cRAG and e/fsRAG in Ca^{2+} is 14.7 ± 5.4 nM and 3.9 ± 3.5 nM, respectively. Thus, fsRAG2 paired with cRAG1

or eRAG1, can confer a larger and more stable pre-cleavage complex when assembled at the 12RSS. It is conceivable that such complex render a DNA structure significantly different from the one formed by the RAG-12RSS containing cRAG2. Notably, the large amount of complex formed in the presence of fsRAG2 diminished in the time dependent manner (Figure 8), which is possibly due to the HP-CEs formation and subsequent release as well as the intact 12RSS release. Taken together, the unique pre-cleavage complex induced by fsRAG2 exerts no influence on the CEC stability.

Comparison of SEC stability in the presence or absence of fsRAG2

Our finding of lack alteration of the CEC stability by fsRAG2 does not support the previous speculation, which attributed the increased aberrant joining associated with fsRAG2 to its destabilizing action on the PCC. However, as we know, PCC is composed of two subunits, CEC and SEC, which may not behave in a similar way. Even though the CEC stability is not influenced by fsRAG2, the SEC may respond differently. To entertain this possibility, I decided to examine the stability of SEC using fluorescence anisotropy. The probe for SEC study is a 50 bp 12RSS substrate (12RSS-TAMRA-1) that has the identical sequence to the one used earlier in assessing HP-CEs retention (TAMRA-12RSS). This 12RSS probe, however, is now labeled with TAMRA at 5' of bottom strand, which is five base pairs apart from the nonamer region. Possible scenarios are listed in Figure 9 for different outcomes, in which 12RSS-TAMRA-1 is

applied in RAG-mediated reactions, the free probe has a relatively low $\langle r \rangle$, binding to RAG proteins of various combinations will induce an elevated $\langle r \rangle$. After the RAG-mediated production of HP-CEs and blunt-SEs, if SEs are stably retained in the RAG-PCC, $\langle r \rangle$ remains constant, on the other hand, if SEs is gradually released from SEC, $\langle r \rangle$ decays.

I first compared SEs retention in the reactions catalyzed by either c/cRAG or c/fsRAG, and found that $\langle r \rangle$ presents a faster decay, i.e., shorter lifetime, in c/fsRAG than in c/cRAG, $\tau_{SE\text{-}R}$=680±30 min *vs* $\tau_{SE\text{-}R}$=454±13 min, respectively, despite less SEs generation in c/fsRAG mediated reaction, as shown in Figure 10 A and B. Our finding support the idea that fsRAG2 renders the formation of a less stable SEC, which may account for its aberrant phenotype. Notably, the lifetime generated for SEs release is much longer than those generated in HP-CEs retention, substantiating the previous finding that the SEC is more stable than CEC.

Discussion

Possible dual abnormalities associated with fsRAG2

Our finding that fsRAG2 renders a less stable SEC is consistent with the previous speculation on this issue. But a compromised SEC stability is not the only abnormality related to fsRAG2. I provide strong evidence that fsRAG2 also promotes an unique pre-cleavage complex assembly featured with higher binding affinity and possible larger RAG-RSS complexes, which is significantly different from the one formed by its non-mutated cRAG2 counterpart. As a matter of fact, the structural change of the pre-cleavage complex in the presence of fsRAG2 is so evident that it can be readily sensed by our FRET measurement, which is a highly powerful and sensitive technique and is capable of detecting such structural alteration, while no other assays by far can do so. Furthermore, the positions of donor-acceptor labeling on our FRET probe provide additional information on the binding surface of cRAG1 to a RSS when fsRAG2 is present, which differs from the one displayed by cRAG2.

Therefore, for the first time, I raised the possibility that in addition to the decreased PCC stability, an unusual pre-cleavage complex, might also attributes to the aberrant end resolution associated with fsRAG2, which of course requires subsequent in-depth examination. Thus, the aberrant joining associated with fsRAG2 may be caused by either abnormal pre-cleavage complex or less stable SEC, which however, are not mutually exclusive. Notably, in the presence of fsRAG2, both CEs and SEs are

prone to be repaired by aberrant pathways, although the rate of joining formation is much lower in CEs than that in SEs. Based on our study that no detectable impairment of CEC stability was observed in fsRAG2, so the aberrant CEs resolution is probably only caused by the abnormal pre-cleavage complex. On the other hand, aberrant signal joint formation may be induced by both unusual pre-cleavage complex and less stable SEC, and the combination of the two induces higher tendency and much severe aberrant joining of SEs. The detailed mechanisms under these scenarios remain to be defined. However, the evidence of full length RAG1 interaction with Ku (9) offers additional support for the role of RAG complex in collaborating and communicating with the NHEJ DNA repair machinery. Although core RAG1 was used in our study, the different partner RAG2, cRAG2 vs fsRAG2, may still affect the selection of DNA repair pathways, switching between the appropriate classic-NHEJ to the error-prone alternative pathways. The dissection of biochemical characteristic of fsRAG2 raises the possibility that abnormality associated with pre-cleavage complex may also affect the final end joining, and puts forward another parameter for future screening of the joining-deficient RAG mutant. Also, it provide us with more confidence of the advantages and strength of our fluorescence based system, which paves the way for future examinations of any parameters that might affect the efficiency and fidelity of V(D)J recombination.

Comparison of CEC and SEC stability under the same detection system

Our fluorescence-based measurements, for the first time, allow us to compare the stability of SEC and CEC in the same system, with accurate kinetic measurement. This opens a new possibility in the study of RAG biochemistry and enables detailed elucidation of the mechanism underlying the asymmetric nature of PCC in holding HP-CEs versus SEs. Three possible scenarios can be deprived based on the parallel comparison between SEC and CEC stability, which are listed below: 1) CEC and SEC stability is uniformly influenced by certain participating factor, e.g. RAG mutations, RSS mutations, metal ion cofactors etc., and such factor can simultaneously destabilize or stabilize CEC and SEC, which suggests that the RAG recombinase retains CEs and SEs in a highly orchestrated manner, despite of their intrinsically different stability (10). 2) CEC and SEC stability is differentially affected by a certain factor, which suggests that PCC retain CEs and SEs in completely unrelated manners. In another word, RAG may hold CEs and SEs with different mechanisms and a certain factor can cause the release of one end but have no influence on the other end. If this is indeed the case, it will shed light on the question why CEs and SEs have such different fate after they are generated. 3) How CEC and SEC stability is impacted under certain condition, uniformly or differentially, may also be dependent upon the individual factor that initiates the change, hypothetically, Mn^{2+} may induce

destabilization of both SEC and CEC, while a RSS mutant may only affect CEC stability without any disturbance on SEC stability. This will provide additional information on the role of each of these factors in retaining the SEC or CEC stability.

By exploring the feature of fsRAG2-containing reactions using the fluorescence based techniques, I demonstrated that fsRAG2 shows no influence on CEC stability, rather it causes a less stable SEC, suggesting that HP-CEs and SEs are retained in the RAG complex in different manners when fsRAG2 is present, which is consistent with scenario 2). Whether the different influence on CEC and SEC stability is unique to fsRAG2 or it is intrinsic nature of this process is of considerate interest and requires more extensive future investigations. However, it is well known that, even in the physiological V(D)J recombination, HP-CEs and SEs have very different fate after RAG-mediated cleavage. HP-CEs are processed and modified extensively before prompt resolution, while the precise SEs joining happens after a significant delay (11, 12). Even more so, processing and joining of SEs and HP-CEs requires different DNA repair proteins (13). In addition, the notion of HP-CEs and SEs are handled differently was also implicated in the study of NBS1 (4), which is a component of alternative-NHEJ (14, 15). NBS1 was directly involved in the aberrant repair of HP-CEs by the alternative-NHEJ, meanwhile, it greatly suppressed the alternative-NHEJ mediated repair of SEs (4). Together, others and I demonstrate that SEC and CEC have distinct properties and

can differentially respond to certain factor, i.e. fsRAG2, NBS1, which provides important insights into the mechanistic basis for the different fate of HP-CEs and SEs.

Table 1. Protein nomenclature

Category	Name	Protein Description
RAG1	cRAG1	core RAG1 (384-1008)
	eRAG1	E649A core RAG1 mutant (384-1008)
RAG2	cRAG2	core RAG2 (1-387)
	fsRAG2	Frame-shift core RAG2 mutant
RAG1-RAG2	c/cRAG	cRAG1/cRAG2
	e/cRAG	eRAG1/cRAG2
	c/fsRAG	
	e/fsRAG	eRAG1/fsRAG2

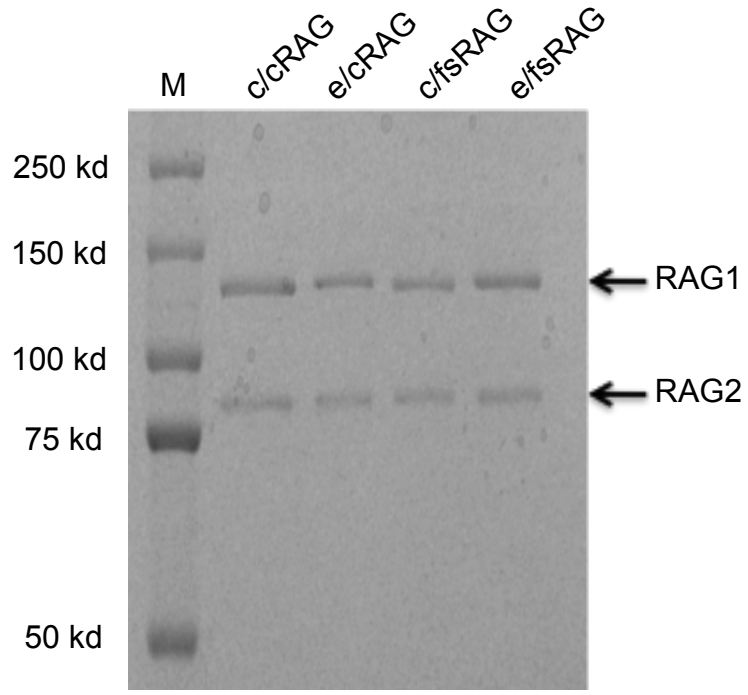

Figure 1. Visualization of various RAG preparations on SDS-PAGE, revealed by Coomassie blue staining. (A) Different core RAG combinations, including cRAG1, cRAG2, eRAG1, fsRAG2.

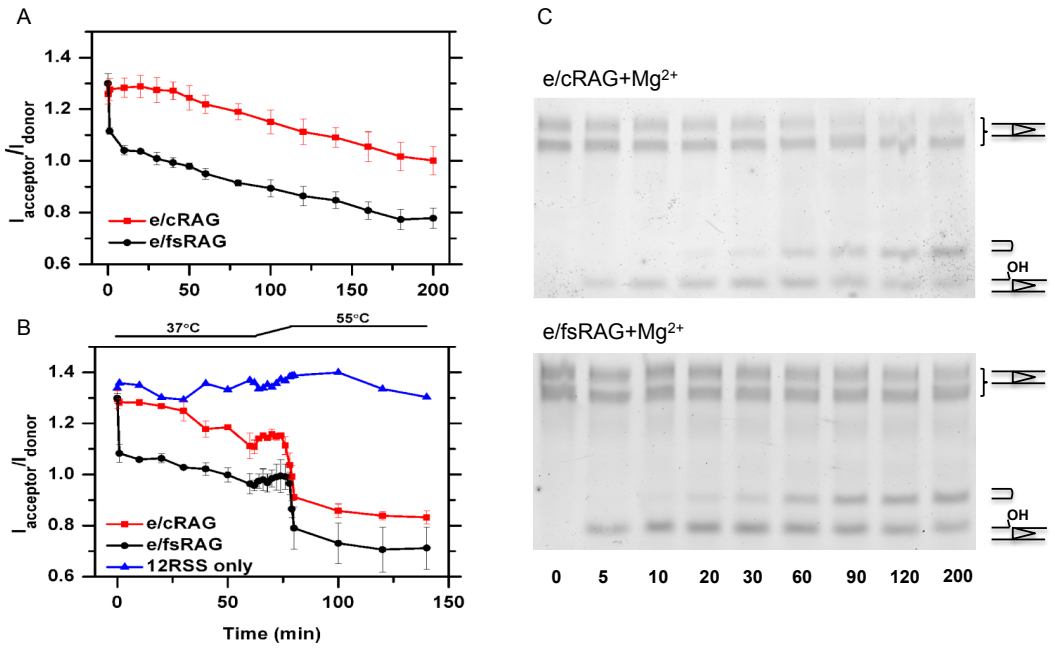

Figure 2. Unique FRET profiles conferred by the presence of fsRAG2.

(A) FRET profiles of E-RAG (red) and e/fsRAG (black) in single cleavage reactions in the presence of Mg^{2+}.

(B) The retention of HP-CEs in CEC under different temperatures. e/cRAG (red) or e/fsRAG (black) was initially incubated in Mg^{2+} at 37°C for 1 hour. The temperature was then ramped up to 55°C over a period of 15 min, and then kept constant at 55°C for 1 hour. A control with 12RSS only (blue) was used to rule out possible temperature-dependent changes in FRET due to changes in the fluorescence efficiencies of the dyes.

(C) Comparison between e/cRAG and e/fsRAG on the kinetics of recombination cleavage reaction made at the TAMRA-ATTO 12RSS.

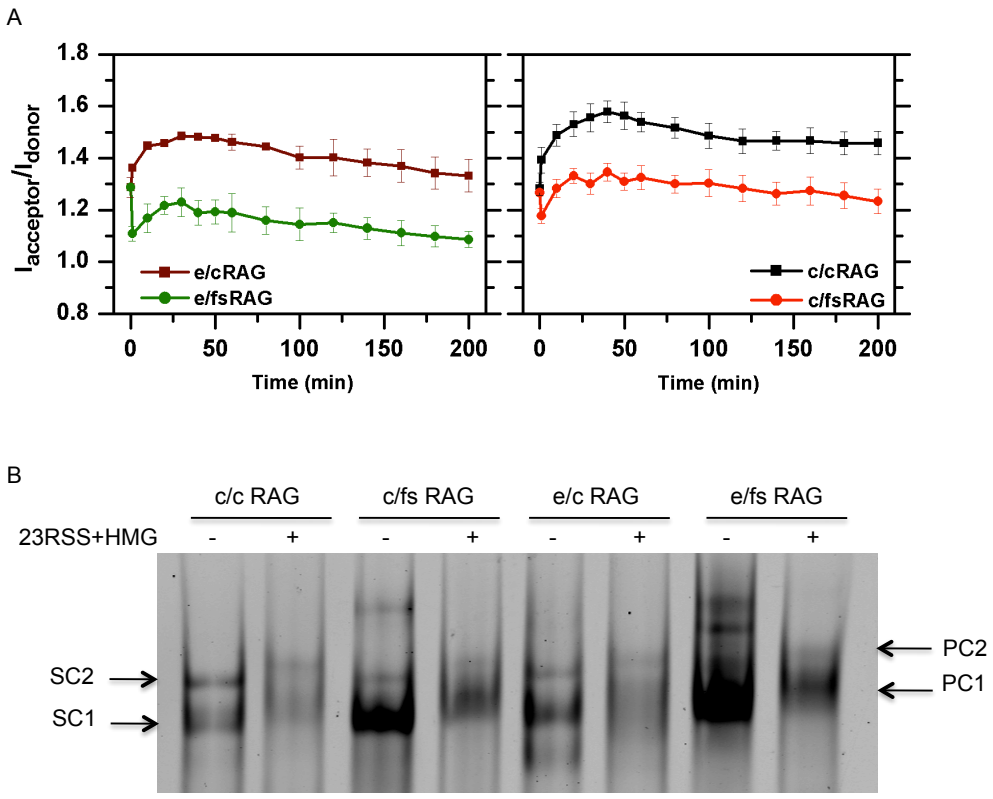

Figure 3. Comparison of FRET pattern in coupled reactions in the presence or absence of fsRAG2

(A) FRET profiles of the coupled cleavage reactions initiated by c/cRAG (black), e/cRAG (red), c/fsRAG (blue) and e/fsRAG (magenta) in the presence of unlabeled 23RSS, HMGB1 and Mg^{2+}.

(B) EMSA analysis of RAG-12RSS interactions in single reaction or coupled reactions. The major shifted bands present in lanes 2 and 4 (marked with bracket), are at the position higher than the SC1, reflecting paired complexes

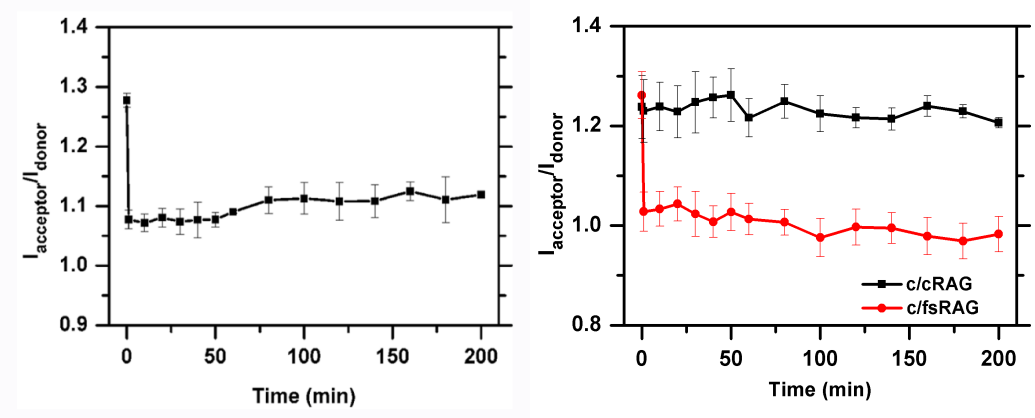

Figure 4. Evidence for a unique FRET pattern associated with fsRAG2.

(A) FRET profile of RAG-12RSS interactions induced by e/fsRAG in Ca^{2+}. (B) Fluorescence anisotropy of TAMRA-12RSS before and after the addition of e/cRAG (red) or e/fsRAG. (black). (C) Gel mobility shift assay (EMSA) analysis of the TAMRA-12RSS with various RAG combinations in the presence of Ca^{2+} or Mg^{2+}. The various reactions, after being assembled at 37°C for 0.5-1 min, were immediately analyzed by EMSA, in which only the shifted DNA-protein complexes, but not the free probe, are shown here. The arrows point to SC1 and SC2 RAG-RSS complexes, as well as some slower mobility complexes denoted by *.

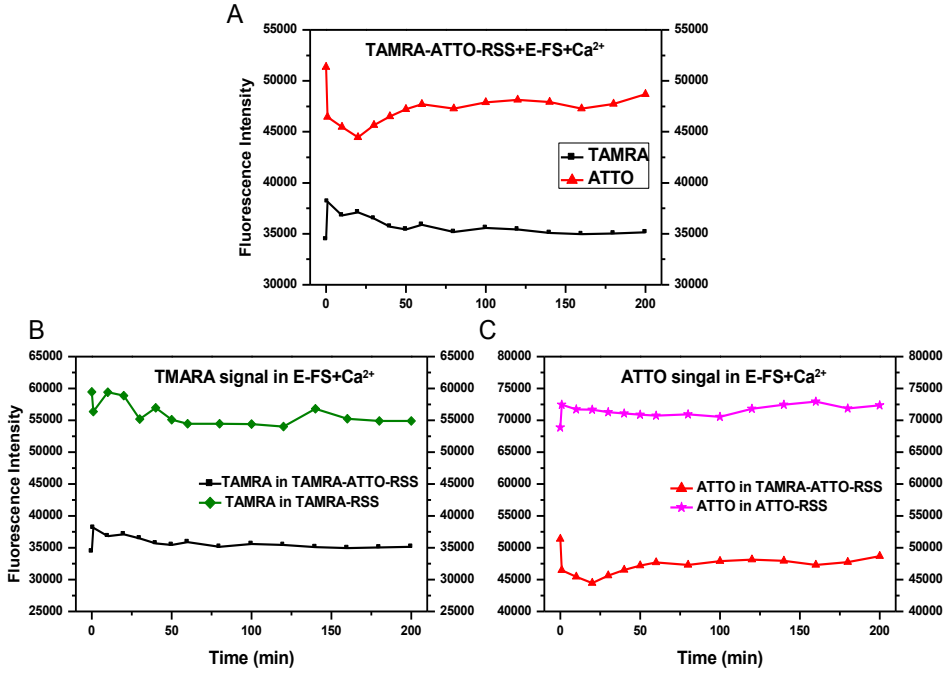
A
TAMRA-ATTO-RSS+E-FS+Ca2+
Fluorescence Intensity
TAMRA
ATTO
B
TMARA signal in E-FS+Ca2+
TAMRA in TAMRA-ATTO-RSS
TAMRA in TAMRA-RSS
Time (min)
C
ATTO singal in E-FS+Ca2+
ATTO in TAMRA-ATTO-RSS
ATTO in ATTO-RSS
Time (min)

Figure 5. Confirmation of the initial decrease of the ratio, $I_{acceptor}/I_{donor}$, as FRET change in the presence of fsRAG2

(A) Emission intensity of TAMRA (black squares) and ATTO (red triangles) in the doubly-labeled 12RSS in the presence of e/fsRAG and Ca2+ showing an initial rapid decrease in FRET. (B) Fluorescence intensity of TAMRA in the doubly-labeled probe (black squares) and singly-labeled 12RSS (green diamonds) in the presence of e/fsRAG and Ca2+. (C) Fluorescence intensity of ATTO in the doubly-labeled probe (red triangles) and singly-labeled 12RSS (magenta stars) in the same reaction conditions. The fluorescence intensities of TAMRA-12RSS and ATTO-12RSS were rather constant throughout the incubation, indicating that the changes observed with the doubly-labeled RSS samples are due to FRET change.

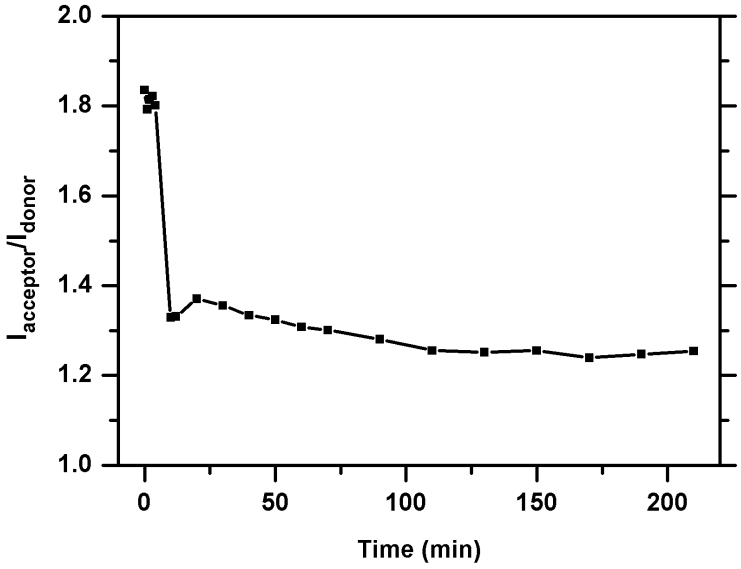

Figure 6. Confirm the unique FRET change with a new ATTO-TAMRA-12RSS probe, in the single reaction mediated by c/fsRAG in the presence of Mg^{2+}

A

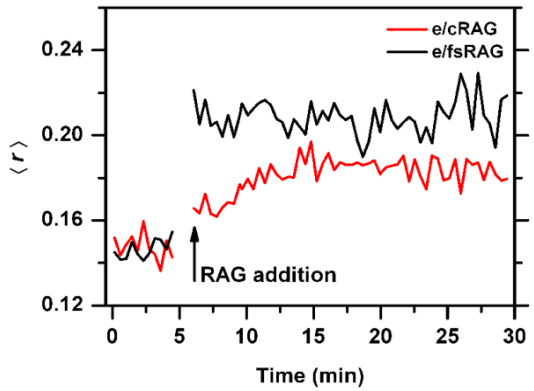
e/cRAG
e/fsRAG
0.24
0.20
0.16
0.12
⟨r⟩
RAG addition
0
5
10
15
20
25
30
Time (min)

B

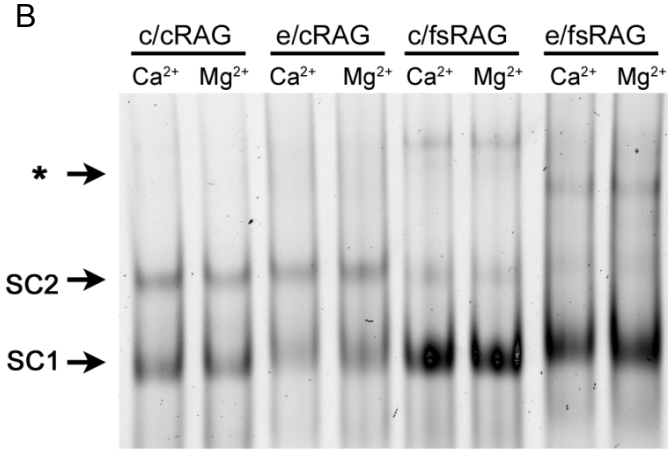
c/cRAG
e/cRAG
c/fsRAG
e/fsRAG
Ca2+
Mg2+
Ca2+
Mg2+
Ca2+
Mg2+
Ca2+
Mg2+
*
SC2
SC1

Figure 7. Characterization of the unique phenotype associated with fsRAG2

(A) Fluorescence anisotropy of TAMRA-12RSS before and after the addition of e/cRAG (red) or e/fsRAG. (black).

(B) Gel mobility shift assay (EMSA) analysis of the TAMRA-12RSS with various RAG combinations in the presence of Ca2+ or Mg2+. The various reactions, after being assembled at 37°C for 0.5-1 min, were immediately analyzed by EMSA, in which only the shifted DNA-protein complexes, but not the free probe, are shown here. The arrows point to SC1 and SC2 RAG-RSS complexes, as well as some slower mobility complexes denoted by *.

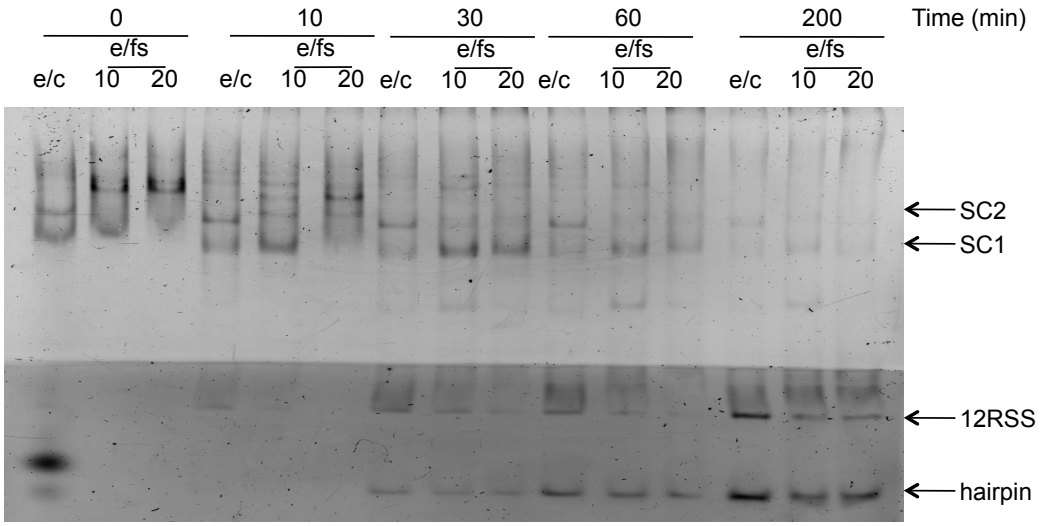

Figure 8. Time course RAG-RSS interactions analyzed by Electrophoretic Mobility Shift Assay (EMSA) , in the presence or absence of fsRAG2.

c/cRAG or c/fsRAG was incubated with TAMRA-12RSS at 37 °C for the time indicated in the figure, in the presence of Mg^{2+}. The arrows point to the bands corresponding to the DNA-protein complexes (SC1 and SC2), the free 12RSS probe (RSS) and the hairpin (HP).

Two doses of e/fsRAG,10 µl and 20 µl, were tested and compared to e/cRAG, the amount of which is comparable with 10 µl of e/fsRAG.

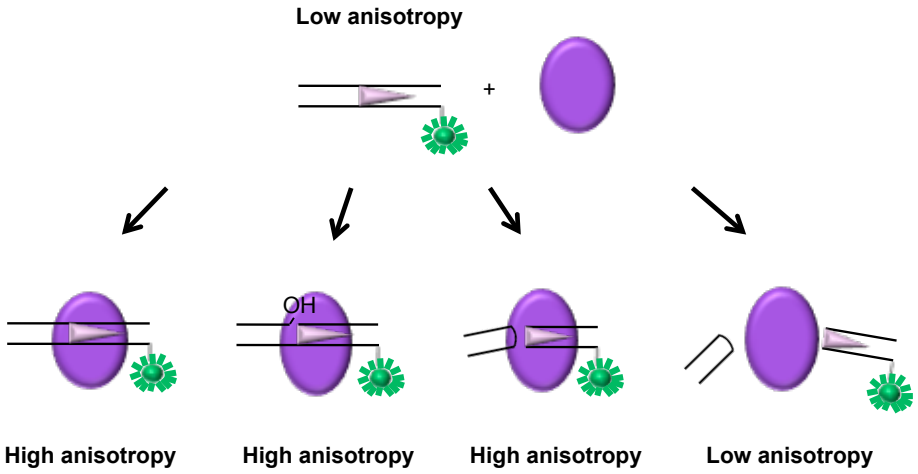

Figure 9. Possible outcomes of SEC stability under various conditions. 12RSS-TAMRA probe alone displays a lower anisotropy, binding of this probe to RAG increases anisotropy. Three conditions will retain a elevated $\langle r \rangle$, i.e. intact 12RSS remain bound to the RAG, nicked-product remain bound to the RAG, cleaved SEs retained in SEC. Both intact 12RSS release and SEs release will result in a the reduction of $\langle r \rangle$.

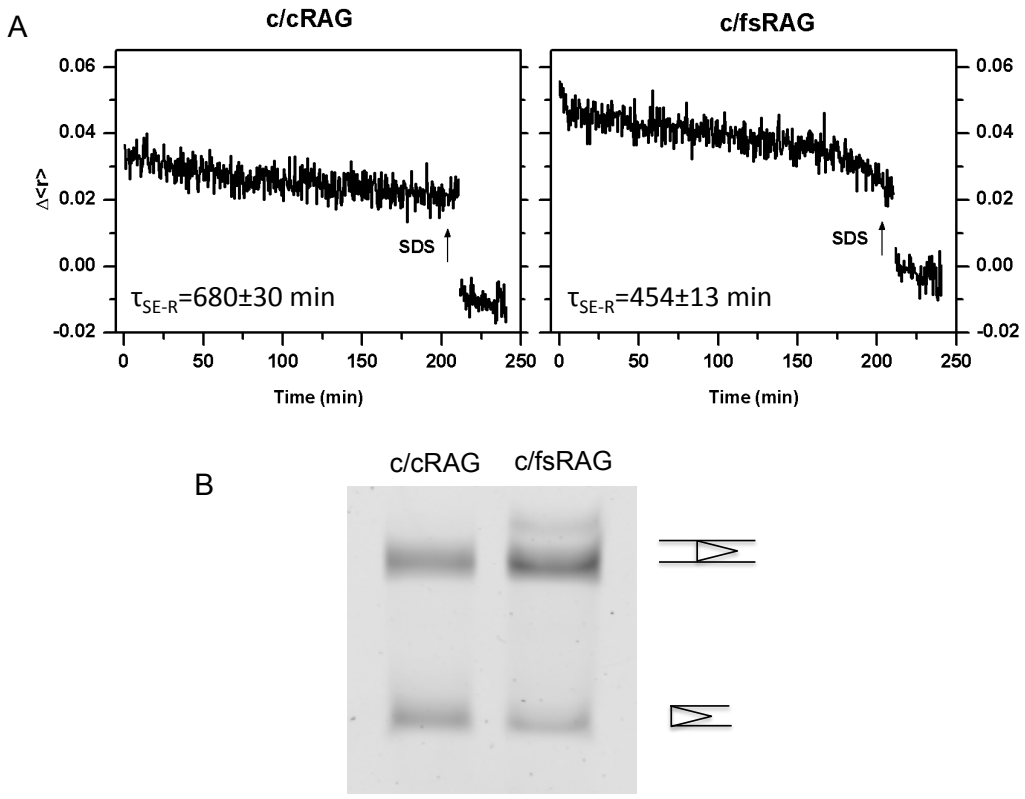

Figure 10. SEC stability in the presence of fsRAG2 or cRAG2.

(A) Anisotropy analysis of SEs retention in SEC in c/cRAG and c/fsRAG-catalyzed reactions. The lifetimes of the SEs release are listed.

(B) Electrophoresis analysis of the SEs generation.

Reference

1. Corneo B et al. (2007) Rag mutations reveal robust alternative end joining. *Nature* 449:483–486.

2. Qiu JX, Kale SB, Yarnell Schultz H, Roth DB (2001) Separation-of-function mutants reveal critical roles for RAG2 in both the cleavage and joining steps of V(D)J recombination. *Mol. Cell* 7:77–87.

3. Arnal SM, Holub AJ, Salus SS, Roth DB (2010) Non-consensus heptamer sequences destabilize the RAG post-cleavage complex, making ends available to alternative DNA repair pathways. *Nucleic Acids Res* 38:2944–2954.

4. Deriano L, Stracker TH, Baker A, Petrini JHJ, Roth DB (2009) Roles for NBS1 in alternative nonhomologous end-joining of V(D)J recombination intermediates. *Mol. Cell* 34:13–25.

5. Bredemeyer AL et al. (2006) ATM stabilizes DNA double-strand-break complexes during V(D)J recombination. *Nature* 442:466–470.

6. Kriatchko AN, Anderson DK, Swanson PC (2006) Identification and Characterization of a Gain-of-Function RAG-1 Mutant. *Mol Cell Biol* 26:4712–4728.

7. Bergeron S, Anderson DK, Swanson PC (2006) RAG and HMGB1 proteins: purification and biochemical analysis of recombination signal complexes. *Meth. Enzymol.* 408:511–528.

8. Shlyakhtenko LS et al. (2009) Molecular mechanism underlying RAG1/RAG2 synaptic complex formation. *J. Biol. Chem* 284:20956–20965.

9. Raval P, Kriatchko AN, Kumar S, Swanson PC (2008) Evidence for Ku70/Ku80 association with full-length RAG1. *Nucleic Acids Research* 36:2060 –2072.

10. Jones JM, Gellert M (2001) Intermediates in V(D)J recombination: A stable RAG1/2 complex sequesters cleaved RSS ends. *Proceedings of the National Academy of Sciences* 98:12926 –12931.

11. Helmink BA, Sleckman BP (2012) The Response to and Repair of RAG-Mediated DNA Double-Strand Breaks. *Annual Review of Immunology* 30:null.

12. Agrawal A, Schatz DG (1997) RAG1 and RAG2 Form a Stable Postcleavage Synaptic Complex with DNA Containing Signal Ends in V(D)J Recombination. *Cell* 89:43–53.

13. Roth DB (2003) Restraining the V(D)J recombinase. *Nat. Rev. Immunol.* 3:656–666.

14. Della-Maria J et al. (2011) hMre11/hRad50/Nbs1 and DNA ligase III{alpha}/XRCC1 act together in an alternative non-homologous end joining pathway. *J Biol Chem*. Available at: http://www.ncbi.nlm.nih.gov/pubmed/21816818 [Accessed August 23, 2011].

15. Williams GJ, Lees-Miller SP, Tainer JA (2010) Mre11-Rad50-Nbs1 conformations and the control of sensing, signaling, and effector responses at DNA double-strand breaks. *DNA Repair* 9:1299–1306.

CHAPTER 4

REGULATION OF V(D)J RECOMBINATION BY RAG RECOMBINASE - THE IMPORTANCE OF FULL LENGTH RAG2 IN FORMING PRE-CLEAVAGE AND IN STABILIZING POST-CLEAVAGE COMPLEX

Introduction

The RAG-mediated reaction has been recapitulated in the cell-free system, where recombinant RAG1 and RAG2 proteins are necessary and sufficient to catalyze the site-specific cleavage on the RSS containing DNA substrate (1). By far, most biochemical characterizations (including our previous studies) have been relying on the core RAG1 and core RAG2, the smallest functional truncated RAG mutants, because they are more easily purified as soluble and functional forms and their cleavage activity is generally more efficient (2). However, non-core regions of RAG proteins are indispensible for physiological V(D)J recombination. For example, replacing full length RAG2 (flRAG2, see table 1 for nomenclature) with core RAG2 (cRAG2), the cRAG2-knock in mice displayed severe genome instability and elevated tendency for lymphoid neoplasm (3). The underlying mechanism of this abnormality was attributed to an significantly increased level of aberrant repair of RAG DSB (3). Furthermore, mutations found in non-core region of both RAG1 and RAG2 have been implicated in various immune deficiency diseases, e.g. Severe Combined Immunodeficiency (SCID) and Omenn Syndrome (OS) (2). Because non-core regions of RAG recombinase play such an

essential role in physiological V(D)J recombination as well as in lymphocyte development, it is of great importance to explore the biochemical nature and function of flRAG1 and flRAG2. By far, the error-prone outcome associated with core RAG has been speculated for their severe defect in forming a stable post cleavage complex (PCC), for example, compared to the core RAG1 and core RAG2 proteins, the full length RAG1 promotes the holding of hairpin coding ends in PCC (4) while the full length RAG2 helps retain signal ends in PCC (3). However, these studies relied mostly on gel electrophoresis or physical isolation of the PCC complex, which were narrowly focused and failed to reveal the real-time interactions between RAG and intact RSS or the subsequent SEs and CEs.

As detailed in the Chapter 2, I have successfully developed a system that monitors the RAG-mediated cleavage reaction in real time, which allows us to make quantitative comparisons among various parameters that might influence the reaction. As detailed in Chapter 3, the characterization of a well-known frame-shift RAG2 mutant (fsRAG2) in our real-time monitoring system revealed several unique features associated with this mutant, i.e. it promotes the assembly of an abnormal pre-cleavage complex and the formation of a less stable SEC. However, the CEC stability was found indistinguishable between fsRAG2 and cRAG2, which may reflect an artifact due to the intrinsic instability of core forms RAG2.

The importance of RAG non-core regions in physiological V(D)J recombination and the concern of erroneous outcome associated with core RAG together prompted us to extend our study to full length RAG, under a more physiological condition such as in coupled reaction in the presence of Mg^{2+}. I first focused on the flRAG2, which is expressed at a higher level than flRAG1 and thus is easier to purify. I then compared the cleavage activity, binding characteristics to RSS, as well as the CEC and SEC stability in coupled reactions containing either cRAG2 or flRAG2 paired with cRAG1. Notably, during *in vivo* V(D)J recombination, instead of binding to a bare DNA which is frequently used in *most in vitro* biochemical studies, physiological RAG actually targets at the chromosome, where the DNA is tightly packaged in conjunction with histone proteins. As discussed in Chapter 1, flRAG2 has a plant homeodomain (PHD) at its C-terminus non-core region, which is known to directly interact with a modified chromatin that has high levels of tri-methylation at Lysine 4 on histone 3 (H3K4me3). This interaction directs the recruitment of RAG2 to the chromosome, and determine the chromosome accessibility of *in vivo* V(D)J recombination (5). So in order to make our study more physiological relevant, I also took into consideration a chromatin element. A synthesized H3K4me3 peptide was included in the RAG mediated reactions and was tested for its influence on the aforementioned parameters, i.e. binding characteristics, cleavage activity and the stability of CEC and SEC. Because our fluorescence

based monitoring system is highly sensitive, I can detect slight differences of RAG-RSS interaction mediated by full length RAG or core RAG in various situations.

Through fluorescence based-biochemistry characterization, I will shed light on the essential role of full length RAG in the physiological V(D)J recombination and how non-core regions of RAG fine tune the RAG activity throughout the reaction. Our study will be a big step forward in unveiling the underlying mechanism of physiological V(D)J recombination.

Materials and Methods

Protein purification

Maltose binding protein (MBP) tagged core RAG1 (residues 384-1008) and core RAG2 (residues 1-387) proteins were co-expressed in 293T cells using the Plus/Lipofectamine reagent (Invitrogen, Carlsbad, CA). Core RAG1 is also co-expressed with full length RAG2 in 293T cells. The expressed proteins were purified following the procedure described by Bergeron *et al.* (6). The protein concentration was measured with the Nanodrop Spectrophotometer (Thermo SCIENTIFIC, Wilmington, DE) and verified by SDS-PAGE, in which no bands other than RAG1 and RAG2 were visible, as shown in Figure 1. The same amount of RAG proteins was used in the binding or cleavage reactions unless descried otherwise.

DNA substrates

The sequence of the DNA substrate used in this study are shown below: 12RSS Top: 5'-TATCAGCTGATAGCTAACACAGTGCTACAGA-CTGGAACAAAAACCCTGCT-3'; 12RSS bottom: 5'-AGCAGGGTTTTTG-T-TC-CAGTCTGTAGCACTGTGTTAGCTATCAGCTGATC-3'; 23RSS top: 5'-ATCGAAGTACCAGTAGCACAGTGGTAGTACGCGTCTGTCTGGCTG-TACAAAAACCATGGATCCT-3'; 23RSS bottom: 5'-AGGATCCATGGTT-TTTGTACAGCCAGACAGACGCGTACTACCACTGTGCTACTGGTACTT-CGAT-3'. The 12RSS top strand was labeled with TAMRA at 5'-end and paired with unlabeled bottom strand, the purified double strand DNA were analyzed by the fluorescence anisotropy. The fluorescence labeled-DNA

nucleotides were obtained from IBA BioTAGnology (Göttingen, Germany) and the unlabeled ones from Integrated DNA Technologies Inc. (Coralville, IA).

***In vitro* cleavage assay**

The coupled cleavage reaction of the fluorescence-labeled 12RSS (20 nM) was catalyzed by RAG proteins (65 nM) in 10 ml reaction containing 10 mM Tris-HCl [pH 7.5], 50 mM NaCl and 100 μg/μl BSA in Mn^{2+} (0.2 mM) and Mg^{2+} (2.5 mM), HMGB1 protein (30 ng/μl, Sigma-Aldrich) and 23RSS (150 nM). To enhance the cleavage activity in the presence flRAG2, DMSO is supplemented to the reactions with a final concentration 5%. The reaction mixture was incubated at 37°C for various times as indicated in the figures, and stopped by adding 10 ml denaturing loading dye containing 90% formamide for denaturation at 95°C and quick chill on ice before being loaded onto a 16% Tris-Borate-EDTA-7 M urea-polyacrylamide gel. After electrophoresis, the gel was imaged on a Typhoon scanner (GE Healthcare) with laser excitation at 532 nm and emission filter of 580 nm to detect TAMRA fluorescence.

Fluorescence anisotropy.

A Photon Technology International QuantaMaster-4/2005SE Spectrofluorometer was used for all fluorescence experiments. A 3 mm × 3 mm quartz micro-cuvette with a 50 ml-sample chamber was used in all measurements, and temperature was controlled by a circulating water bath and set at 37°C except where noted. The fluorophore-labeled sample

is excited by a polarized beam light, which allows photo-selection of a fraction of fluorophores that are properly oriented relative to the incoming light. The anisotropy is defined as $\langle r \rangle = (I_{VV} - GI_{VH})/(I_{VV}+2GI_{VH})$, where I is the fluorescent intensity, V and H reflects the vertical and horizontal orientation by which the emission and excitation polarizer is mounted. The factor G is defined as, I_{HV}/I_{HH}, the intensity ratio of the vertical emission to horizontal emission when the sample is excited with horizontal polarized light. G factor is dependent on the monochromator wavelength and slit width and is used to correct for polarization-dependent effects in detection sensitivity. The excitation and the emission wavelengths were set at 510 nm and 580 nm, and data was acquired every 10 seconds. Background correction was applied to all the measurements. The anisotropy of the 5'-TAMRA-labeled 12RSS in the appropriate buffer (with cations indicated in the figures) was measured before and after the addition of RAG proteins. The temperature was maintained at 37°C for the duration of the experiment (~3 hours). The final concentration of all the components was the same as used in the *in vitro* cleavage reactions. At the end of cleavage reactions, SDS and proteinase K were added to liberate DNA from protein association, where the anisotropy of free HP-CEs is lower than the free probe or DNA with a nick.

Data fitting.

Kinetic traces of FRET and fluorescence anisotropy experiment were fitted using the program embedded in OriginPro8, to a mono-

exponential decay ($I_{acceptor}$ /I_{donor} = A*exp*(-t/τ)+A_∞), In these equations, t represents time, τ represents the dissociation lifetime, and A_∞ represents the $I_{acceptor}$ /I_{donor} ratio where all generated HP-CEs is liberated from the RAG complex. Because in some reactions, HP-CEs was not completely released by the end of 3 hours acquisition time, meaning the lifetime is longer than 3 hours, the parameter A_∞ was determined by adding a denaturing agent (0.5% SDS and proteinase K) at the end of the experiment. Both methods yield the same value, which was used as a fixed parameter in the fitting procedures.

Result

Reveal the difference between flRAG2 and cRAG2 mediated reaction by anisotropy and FRET experiment

Based on our previous studies in Chapter 2, that FRET experiment and anisotropy experiment measure the same kinetics of HP-CEs retention. Since SEs retention can only be monitored via anisotropy experiment, I then sought to record both CEC and SEC stability using fluorescence anisotropy. First, I performed a time-course *in vitro* cleavage reaction in c/cRAG or c/flRAG mediated coupled reactions in the presence of Mg^{2+}. As shown in the left panel of Figure 2, the hairpin generation kinetics of the two reactions are similar, with the lifetime $\tau_{HP\text{-}R}$ = 60 min. However, the overall activity was slightly higher in c/cRAG-induced cleavage than that of c/flRAG, because c/cRAG generates more HP-CEs after 3 hours incubation (Left panel of Figure 2A, B). The comparison of the cleavage activity between c/cRAG and c/flRAG has long been studied and the results were somewhat inconsistent, probably due to the use of different RAG constructs as well as the different purification procedure, and most importantly, due to the variations in the experimental condition of cleavage reactions, such as salt concentration, with or without BSA, with or without DMSO, etc (7, 8). So it is relatively difficult to make a cross comparison among all these studies. However, in our study, as long as the condition in *in vitro* cleavage reaction is consistent with the subsequent anisotropy measurements, I can normalize the difference of hairpin

generation when I determine the HP-CEs release rate, which is additional strength of my system. I then examined the HP-CEs association within CEC in coupled reaction by fluorescence anisotropy. To minimize any variations from different experiments, the changes in anisotropy during the cleavage reaction were expressed as $\Delta \langle r \rangle$, which is defined by subtracting free probe $\langle r \rangle$ from the $\langle r \rangle$ upon RAG addition over the course of cleavage reaction. In this case, RAG binding to intact 12RSS can cause an increase in $\Delta \langle r \rangle$ over the free probe, and thus $\Delta \langle r \rangle$ after RAG binding is higher than 0. On the other hand, the generation and subsequent release of HP-CEs from CEC results in a decrease of $\Delta \langle r \rangle$, and the complete release of all HP-CEs by SDS/proteinase K treatment in the end of the incubation is supposed to generate a negative $\Delta \langle r \rangle$ over the control, because the size of HP-CEs are smaller than the non-cleaved or nicked 12RSS substrates, and thus the $\langle r \rangle$ is smaller. The changes of $\Delta \langle r \rangle$ over the reaction course was fitted into a mono-exponential decay and the $\Delta \langle r \rangle$ of free HP-CEs after SDS/ProK treatment was used as an “offset” (the critical points value) to calculate the $\tau_{HP\text{-}R}$. As shown in the right panel of Figure 2, upon RAG addition, the initial $\Delta \langle r \rangle$ in c/flRAG mediated reactions is significantly lower than the $\Delta \langle r \rangle$ observed in the c/cRAG reactions, indicating c/flRAG confers a lower binding affinity to the RSS than that of c/cRAG. Our observation is consistent with the previous EMSA data, which shows that the combination of cRAG1 and flRAG2 resulted in a lower level of paired

complexes, and the underlying mechanism has been attributed to the RAG2 C-terminus mediated destabilizing of RAG-RSS interaction (especially with the coding flank) (9). Regardless of the different initial binding affinities, the decay of $\Delta \langle r \rangle$ in c/flRAG is faster than that in c/cRAG, suggesting that the CEC containing flRAG2 is less stable and HP-CEs is more readily released from CEC than the reaction containing cRAG2. On one hand, the less stable CEC in the presence of flRAG2 seems to match to the lower binding affinity under the same condition. This hypothesis, however, assumes that the interaction between RAG and RSS in the pre-cleavage complex is similar with the interaction of RAG and HP-CEs in the CEC. On the other hand, the finding that flRAG2 confers a less stable CEC is in stark contrast with the previous SEC studies (3), which will be discussed in detail in the next section.

The difference in CEC stability between c/cRAG and c/flRAG containing reaction will be verified in the FRET experiment under the same conditions.

I then extended our study to a more physiological condition by including a chromatin element, H3K4me3 peptide. H3K4Me3 has been reported to promote RAG-mediated RSS cleavage at both nicking and hairpinning steps (8), and it can also greatly increase the formation of RAG-RSS pre-cleavage complex (8, 9). Remarkably, the stimulation can be achieved both *in cis* (tethered to RSS or reconstitute a chromatin on RSS substrate) and *in trans* (free H3K4me3 peptide). However, the effect

of H3K4me3 on CEC stability has not been addressed. I reasoned that our system offers an excellent approach to examine the role of H3K4me3 through out the RAG-mediated reaction in the presence or absence of flRAG2. Indeed, when H3K4Me3 peptide was present in the reaction catalyzed by c/flRAG on fluorophore-labeled RSS substrates, but not c/cRAG (Figure 2B and 2C, Figure 3B), I found a significant increase in the initial fluorescence anisotropy with an overall longer lifetime (compared $\tau_{HP\text{-}R}$=255±5 min to $\tau_{HP\text{-}R}$=198±8 min), as shown in Figure 2 and Figure 3, which reflects the protein association at the probe. This finding clearly indicates that the PHD-binding H3K4Me3 can significantly enhance the HP-CE retention by the flRAG2-containing CEC-PR. Also in line with the previous reports (53, 54), the formation of more c/flRAG-12RSS complexes was induced by H4K4me3 peptide as well, since an enhancement in the initial anisotropy was found upon addition of c/flRAG to the reaction containing the peptide (Figure 2C). Thus, I provide the direct evidence that the H3K4me3 peptide can stabilize both pre-cleavage and post-cleavage RAG complexes. The kinetics of HP-CEs production and release is summarized in Table 1.

Comparison of the stability of SEC in the presence of cRAG2 and flRAG2

I then sought to determine SEC stability in c/cRAG or c/flRAG mediated reactions. The 12RSS-TAMRA (probe for the SEC study) was incubated in coupled reactions catalyzed by either c/cRAG or c/flRAG, and

monitored by fluorescence anisotropy. $\Delta \langle r \rangle$ was again used to reflect the RAG-12RSS interaction at the beginning of the reaction, and the changes of RAG-SEs/12RSS interaction during the reaction process. Consistent with our previous finding using TAMRA-12RSS (probe for the CEC study), c/flRAG mediated reaction again displays a lower $\Delta \langle r \rangle$, which further proves that c/flRAG binds to RSS with a less affinity than that of c/cRAG. Despite the initial lower binding, $\Delta \langle r \rangle$ remains barely unchanged over the reaction course in the presence of flRAG2, which is significantly different from the pattern observed in c/cRAG, where an initial higher $\Delta \langle r \rangle$ rapidly decays, as shown in Figure 4A. Consistent with the previous finding, c/flRAG generate slightly less SEs compared to c/cRAG (Figure 4B). The decay of $\Delta \langle r \rangle$ indicates the release of SEs from SEC in the presence of cRAG2, while a constant $\Delta \langle r \rangle$ in flRAG2 represents a relatively stable SEC. Our finding using a more sensitive detection system substantiates the finding by the Roth's group, that SEC composed of flRAG2 is more stable then the one with cRAG2, The kinetic of SE release is summarized in Table 1.

Discussion

A more stable SEC in the presence of flRAG2

Using the fluorescence anisotropy, I found that as compared to the cRAG2, the flRAG2 confers a somewhat unstable CEC, but a rather stable SEC. Although seemingly contradictory, this finding again highlights the asymmetric feature of the RAG in dealing with coding ends versus signal ends. This feature was also evident in our analysis of fsRAG2, as described in Chapter 2, where fsRAG2 exert no influence on CEC stability but renders a less stable SEC. Notably, unlike the flRAG2, both cRAG2 and fsRAG2 are considered as mutant forms of RAG2, and these two mutants seem to share similar influence on the SEC stability, by conferring poor retention of SEs in SEC. Our findings substantiate the importance of non-core region of RAG2 in maintaining the SEC stability. Furthermore, I also provide the first parallel comparison of the two forms of RAG2 mutants, cRAG2 and fsRAG2, in their influences on both CEC and SEC. The demonstration of less stable SECs of these RAG2 mutants provide mechanistic explanation of their abnormal phenotypes observed *in vivo*, such as elevated aberrant rearrangement (cRAG2 and fsRAG2), compromised genomic stability and high propensity for lymphoid neoplasm (cRAG2) in mice carrying these RAG2 mutants (3, 10, 11).

Less stable CEC in the presence of RAG2?

The appropriate time window and strength of HP-CE association with the CEC may be a key for optimal resolution of newly generated HP-

CEs, although the structural basis of this association and its functional connection to ultimate end resolution pathways remains to be defined. I demonstrated that the flRAG2 causes faster HP-CEs release than that of the cRAG2, reflecting the weak binding between HP-CEs and CEC in the presence of the flRAG2. This finding draws a contrast with the SEC comparison and is also contradictory with the general idea that flRAG2 should function to stabilize post-cleavage complex, as compared to cRAG2.

Notably, the physiological target for RAG2 recognition is the modified chromatin DNA that has high level of tri-methylation on H3K4, and the binding is through the C-terminal PHD domain of flRAG2 (7, 8). The cross talk between the RAG2-PHD domain with a epigenetic signal at chromosomal loci ensures the correct targeting of RAG2, i.e., according to the presence of appropriate chromosomal modifications. Furthermore, it was suggested that the PHD-dependent inhibition of RAG-mediated cleavage is a check-point to minimize the illegitimate RAG activity (9). On the other hand, most *in vitro* RAG-mediated cleavage reaction has been relying on the RSS substrate without a chromatin component, including ours. Thus, the use of bare DNA substrate in the reactions containing flRAG2 fail to establish the correct interaction with the PHD domain and therefore may not reflect the genuine influence or function of flRAG2 in these reactions. If this were indeed the case, we should not be surprised by our demonstration of a labile CEC conferred by flRAG2. In another

word, without an appropriate form of target DNA, the c/flRAG displays no advantage over c/cRAG in preserving the CEC stability. Moreover, a further reduced CEC stability in the flRAG2 compared to the cRAG2, might reflect an abnormal in vitro artifact of RAG-RSS when the PHD domain fails to target the appropriate partner, H3K4me3. Therefore, it is important to take into consideration the chromatin component when we characterize the role of flRAG2 in their interaction with recombination substrates or recombination ends.

Indeed, the addition of H3K4me3 peptide into c/flRAG mediated reactions significantly increases the binding affinity between RAG and RSS, and more importantly, induces a better HP-CEs retention in CEC. Although flRAG2 seems to render a less stable CEC *in vitro*, we would still expect it to develop a very stable CEC in the physiological conditions, when it is surrounded by H3K4me3 and is able to exerts more stringent regulation over the RAG-mediated cleavage reaction as well as the subsequent end joining, through the interaction with chromatin. Therefore, a stable CEC and a stable SEC are both essential *in vivo* for the transfer of the ends to an appropriate repair pathway, which ultimately ensure the efficiency and fidelity of V(D)J recombination and also minimize the genome instability.

Table 1. Protein nomenclature

Category	Name	Protein Description
RAG1	cRAG1	core RAG1 (384-1008)
RAG2	cRAG2	core RAG2 (1-387)
	flRAG2	full length RAG2 (1-528)
RAG1-RAG2	c/cRAG	cRAG1/cRAG2
	c/flRAG	eRAG1/cRAG2

Table 2 Kinetics of the production and release of HP-CEs

Labeled ends	RAG	Cation	$\tau_{HP\text{-}p}$[a] (min)	$\tau_{HP\text{-}R}$[b] (min)
HP-CEs[c]	c/cRAG	Mg^{2+}	60 ± 4	231 ± 5
	c/flRAG	Mg^{2+}	62 ± 3	198 ± 8
	c/flRAG+peptide	Mg^{2+}	52 ± 4	255 ± 5
SEs[d]	c/cRAG	Mg^{2+}	60 ± 4	680 ± 30
	c/flRAG	Mg^{2+}	62 ± 3	454 ± 13

[a]: Lifetime of HP-CE production determined by electrophoresis. The number given was calculated from the kinetic analysis of HP-CE production, as exemplified in Figure 2.

[b]: Lifetime obtained from anisotropy, a measure of the rate of HP-CE release, as shown in Figure 2 and 4.

[c]: Determine the HP-CEs production and release rate, TAMRA is labeled at the coding flanks.

[d]: Determine the SEs production and release rate, TAMRA is labeled at the signal ends.

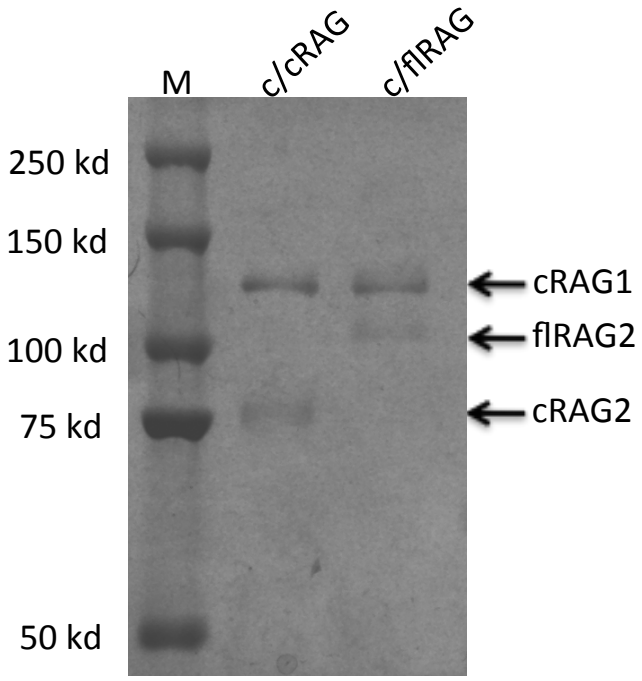

Figure 1. Visualization of RAG proteins on SDS-PAGE, revealed by coomassie blue staining, shown here is cRAG1 paired with either cRAG2 or flRAG2.

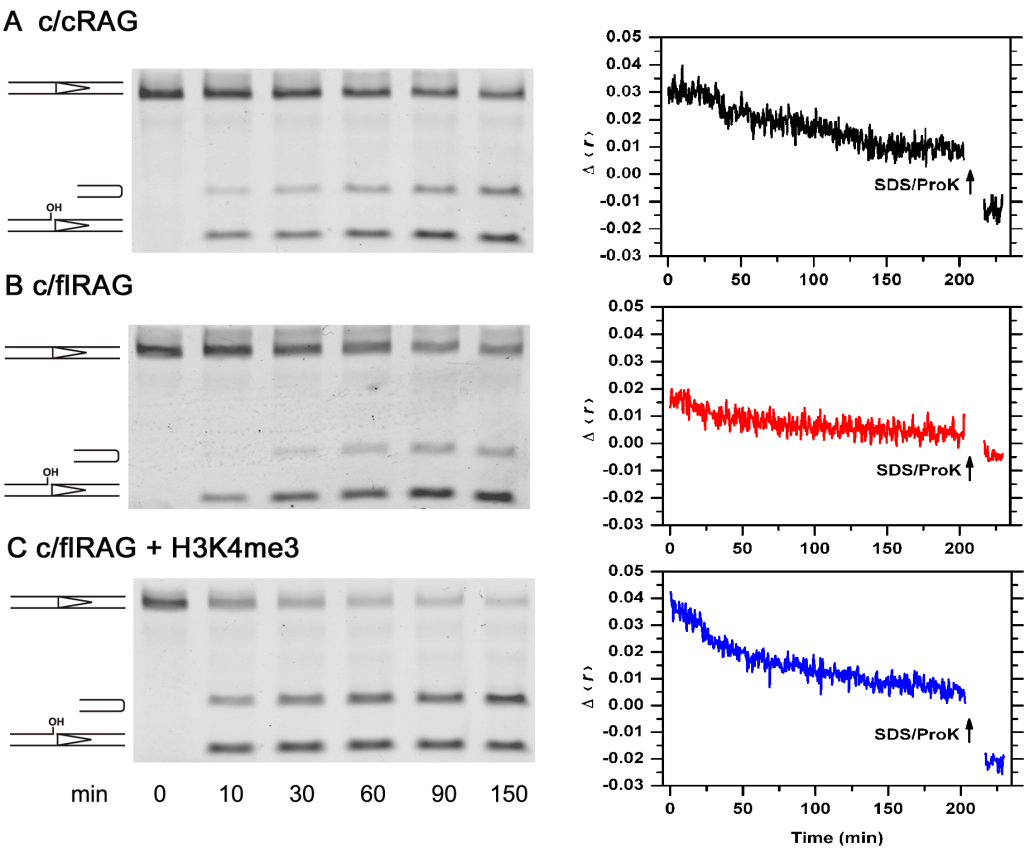
A c/cRAG
OH
B c/flRAG
OH
C c/flRAG + H3K4me3
OH
min 0 10 30 60 90 150
0.05
0.04
0.03
0.02
0.01
0.00
-0.01
-0.02
-0.03
Δ ⟨r⟩
SDS/ProK
0 50 100 150 200
Time (min)

Figure 2.

Assessment of HP-CE production and association with CEC-PR composed of c/c RAG or c/flRAG in the coupled cleavage reactions with Mg2+ and HMGB1.

(A) Cleavage reactions catalyzed by c/cRAG; (B) Cleavage reactions catalyzed by c/flRAG; and (C) Coupled reaction mediated by c/flRAG in the presence of H3K4me4. Left panel: time-course analysis of cleavage intermediates, including nicked and hairpin products, revealed by denaturing gel electrophoresis. Right panel: real-time monitoring of cleavage reactions by fluorescence anisotropy. Results of anisotropy are displayed as changes of Δ〈r〉over a function of time. Δ〈r〉is obtained by subtracting the〈r〉of free probe (A, B) or free probe plus peptide (C) from the〈r〉upon RAG and HMGB1 addition. After monitoring fluorescence anisotropy for 3 hours, SDS/ProK was added into the reaction mixture to disrupt the protein-DNA complex and liberate the DNA.

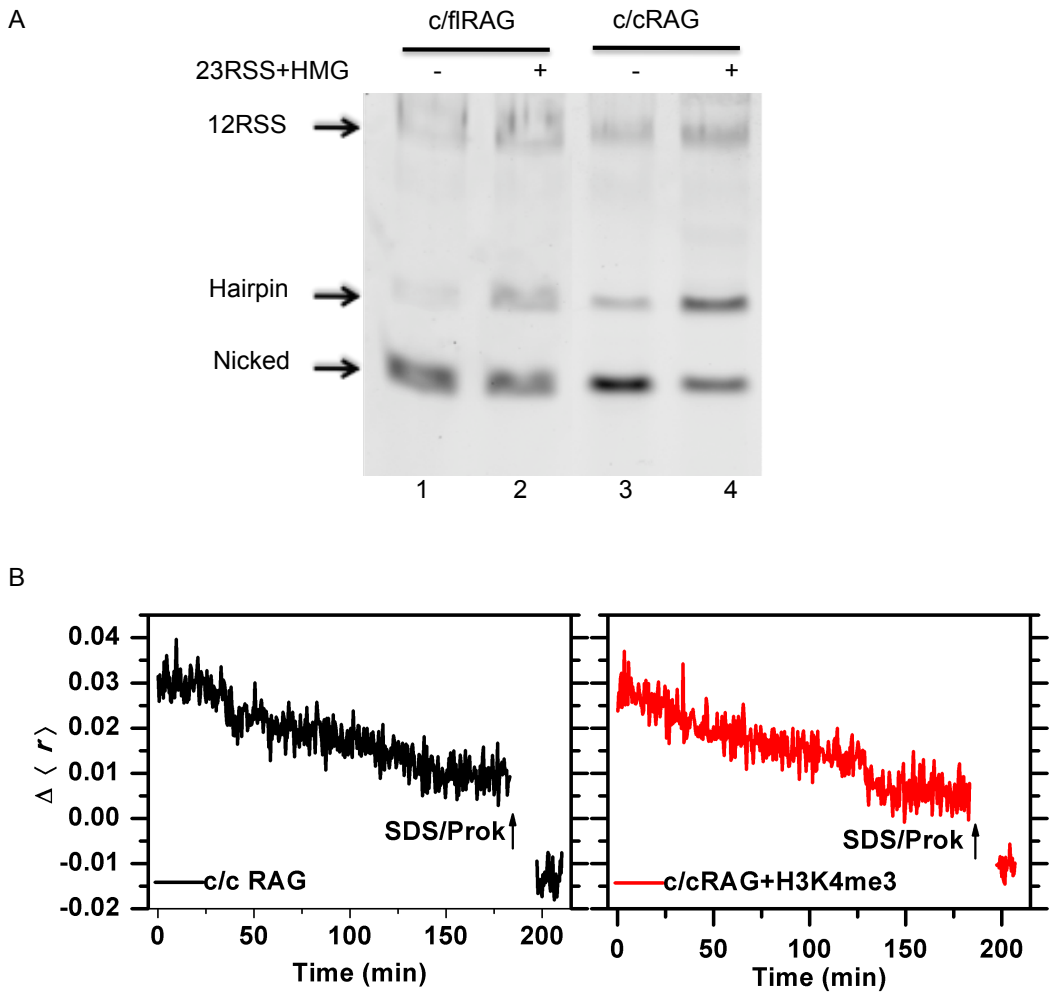

Figure 3. The effect of H3K4me3 on c/cRAG mediated reaction.

(A) In vitro cleavage reactions mediated by c/fl RAG or c/cRAG, in the absence (lanes 1 and 3) or presence of partner 23RSS and HMGB1 (lanes 2 and 4).

(B) Effect of H3K4me3 peptide on c/cRAG-mediated coupled cleavage reaction, analyzed by fluorescence anisotropy. Left, w/o H3K4me3 peptide. Right, with H3K4me3 peptide. The lifetime τHP-R is indicated in each graph.

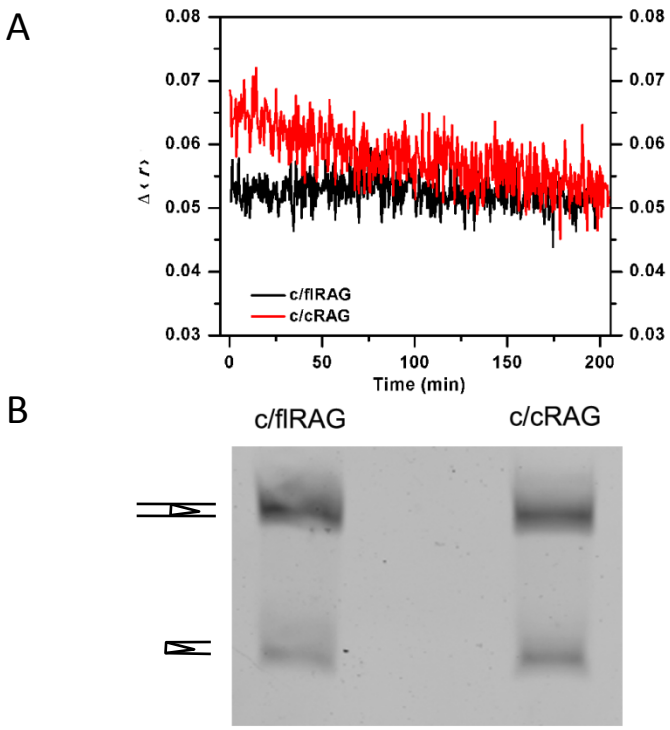

Figure 4. Comparison of SEC stability in reactions catalyzed by either c/flRAG or c/cRAG, revealing the role of flRAG2 in retaining the SEs.

(A) SEs retention in SEC analyzed by fluorescence anisotropy.

(B) *In vitro* cleavage reaction mediated by c/flRAG and c/cRAG, revealed by electrophoresis.

Reference

1. van Gent DC et al. (1995) Initiation of V(D)J recombination in a cell-free system. *Cell* 81:925–934.

2. Schatz DG, Swanson PC (2011) V(D)J Recombination: Mechanisms of Initiation. *Annual Review of Genetics* 45:167–202.

3. Deriano L et al. (2011) The RAG2 C terminus suppresses genomic instability and lymphomagenesis. *Nature* 471:119–123.

4. Kumar S, Swanson PC (2009) Full-length RAG1 promotes contact with coding and intersignal sequences in RAG protein complexes bound to recombination signals paired in cis. *Nucleic Acids Res* 37:2211–2226.

5. Ji Y et al. (2010) The In Vivo Pattern of Binding of RAG1 and RAG2 to Antigen Receptor Loci. *Cell* 141:419–431.

6. Bergeron S, Anderson DK, Swanson PC (2006) RAG and HMGB1 proteins: purification and biochemical analysis of recombination signal complexes. *Meth. Enzymol.* 408:511–528.

7. Liu Y, Subrahmanyam R, Chakraborty T, Sen R, Desiderio S (2007) A plant homeodomain in RAG-2 that binds Hypermethylated lysine 4 of histone H3 is necessary for efficient antigen-receptor-gene rearrangement. *Immunity* 27:561–571.

8. Shimazaki N, Tsai AG, Lieber MR (2009) H3K4me3 Stimulates the V(D)J RAG Complex for Both Nicking and Hairpinning in trans in Addition to Tethering in cis: Implications for Translocations. *Molecular Cell* 34:535–544.

9. Grundy GJ, Yang W, Gellert M (2010) Autoinhibition of DNA cleavage mediated by RAG1 and RAG2 is overcome by an epigenetic signal in V(D)J recombination. *Proceedings of the National Academy of Sciences* 107:22487 –22492.

10. Corneo B et al. (2007) Rag mutations reveal robust alternative end joining. *Nature* 449:483–486.

11. Deriano L, Stracker TH, Baker A, Petrini JHJ, Roth DB (2009) Roles for NBS1 in alternative nonhomologous end-joining of V(D)J recombination intermediates. *Mol. Cell* 34:13–25.

CHAPTER 5

DIRECT REGULATIONS OF PROTEIN LEVEL BETWEEN RAG1 AND RAG2

Introduction

RAG can generate double strand breaks during the rearrangement of immunoglobulin and T cell receptor gene, which is a essential process during V(D)J recombination and normal lymphocyte development. RAG1 or RAG2-deficient mice completely lack mature T and B cells, blocking the lymphocyte development at very early stage (1, 2) However, in addition to initiating site-specific excision at antigen receptor gene loci, RAG has also been shown to cause DSB at other sites by recognizing illegitimate cryptic RSS or certain DNA structure (3–5). The effect of the abnormal and excessive RAG activity is detrimental to genome integrity and to an animal as a whole, which includes susceptibility to recombination-induced translocation, and increased propensity of lymphoid malignancy, as well as growth retardation and early death of an animal (6). Considering the possible deleterious effect associated with the RAG recombinase, The RAG recombinase has to be stringently controlled both temporally and spatially throughout the lymphopoiesis as well as the cell cycle.

The regulatory mechanisms on RAG expression are reviewed in Chapter1. Briefly, RAG expression is generally restricted to T and B cells and the transcription of RAG mRNA occurs in two waves. Many regulatory factors have been identified to regulate the level of RAG mRNA along

lymphocyte development (7, 8). In addition, RAG2 can also be regulated at the post-translational level in a cell cycle dependent manner. Phosphorylation by CyclineA/cdk2 at T490 residue leads to the subsequent proteasome-mediated degradation through an Skp2/SCF poly-ubiquitinination pathway. The cell cycle-dependent destruction of RAG2 couples V(D)J recombination to the cell cycle control and to the selection of appropriate DNA repair pathways, which ensures the high efficiency and high fidelity of recombination events (9–11).

Notably, RAG1 has a RING domain in its amino terminal non-core region and thus is a potential E3 ligase (12). *In vitro* assays showed that the target of RAG1 E3 ligase includes RAG1 itself, RAG2, KPNA, Histone 3, etc (12–15). However, the *in vivo* pathway and substrates associated with RAG1 E3 ligase remain largely elusive. Considering the close relationship between RAG1 and RAG2 in V(D)J recombination (16, 17), it is conceivable to suspect that RAG2 might be modified and regulated by RAG1. To this end, previous work in our lab tried to manipulate the expression of both RAG1 and RAG2 in order to detect any regulations between the two proteins. A pre-B cell line with dual regulatory mechanisms of RAG1 vs RAG2 was developed, where RAG1 is regulated through a tetracycline-inducible system and RAG2 is under the control of a temperature sensitive system. More specifically, a pre-B cell lines transformed with temperature-sensitive Abelson-leukemia virus (ts-Abl), designated as ts-Abl-pre-B cells, was used to modulate the RAG2

expression through temperature manipulation (18, 19). In a non-inducible condition, the ts-Abl-pre-B cells were maintained at 33°C, upon temperature increase to 39°C, v-Abl is inactivated, which leads to cell cycle arrest, up-regulation of endogenous RAG1 and RAG2 and the onset of recombination at the immunoglobulin light chain loci (18). Notably, the RAG2 protein could be readily detected upon v-abl inactivation, but the endogenous RAG1 protein were barely found, despite its apparent activity on light chain rearrangement (20), which may be attributed to the extremely low levels or labile nature of RAG1. However, the concurrent regulation of RAG1 and RAG2 through v-Abl inactivation/reactivation makes it impossible to study the influence of RAG1 or RAG2 exerting on each other. So a separate system for regulation of RAG1 expression, a tetracycline-inducible system was introduced into the aforementioned ts-Abl-pre-B cells, where expression of the EGFP-RAG1 fusion gene and the transcription activator tTA gene are under the control of a tetracycline responsive/regulatory element (TRE), see Figure 1 for details. Removal of tetracycline (-Tet) from the culture medium results in the binding of tTA protein to the TRE, leading to a transcriptional up-regulation of tTA itself and EGFP-RAG1 expression in the transfected cells (21, 22). Thus, through temperature sensitive- and tetracycline-inducible system, RAG1 and RAG2 can be regulated independent of each other, which made it possible to reveal any cross-regulation between RAG1 and RAG2, as any influence on each other would disrupt their individual expression pattern

following their own inducible system. With the help of this elegant system, it was found that RAG2 level is significantly reduced upon EGFP-RAG1 induction (Figure 2), and the suppression occurs in the post-transcriptional manner, possibly by promoting RAG2 degradation. Indeed, direct comparison of the half-life of RAG2 with or without RAG1 revealed that induced RAG1 facilitate the degradation of endogenous RAG2. The biochemical pathway responsible for the down-regulation of RAG2 by RAG1 was not determined, but a proteasome inhibitor, epoxomicin, was shown to block the RAG2 reduction in the dose-dependent manner, raising the possibility that RAG2 is tagged for degradation by RAG1 E3 ligase through a proteasome mediated pathway. Interestingly, other than epoxomicin, other proteasome inhibitors tested such as MG-132 and clasto-lactacystin-β-lactone show no prevention of RAG2 reduction, suggesting the presence of other possible pathways.

Regardless of the exact mechanism, RAG1 seems to directly modulate the RAG2 expression level in a pre-B cell background. To further dissect whether this phenotype is unique to lymphocytes or it is a another regulatory property intrinsic to RAG1 and RAG2, I decided to extend this study to a completely different system, where various forms RAG1 and RAG2 were transiently transfected into a non-lymphocyte cell lines, and their expression level were monitored.

Material and methods

Transient transfection of RAG1 and RAG2 constructs into 293T cell line

293T cells were transiently transfected with various combinations of RAG1 and RAG2, i.e., flRAG1 only, flRAG2 only, fRAG1+ fRAG2, fRAG1+ cRAG2, cRAG1+ fRAG2 or cRAG1+cRAG2, where 1:1 ratio of RAG1 to RAG2 plasmids was used. Given the extremely low level of fRAG proteins in the transfected cells, I also adjusted the plasmid ratio in some experiments. In particular, the ratio of fRAG1 to cRAG2 and fRAG2 to cRAG1 was made at 4 while fRAG1 to fRAG2 was at 4:4, as compared to the amount of crag constructs. Forty-eight hours later, cells were harvested, counted and lysed in SDS-PAGE loading buffer at defined number of cells per microliter of the buffer.

Serum deprivation experiment conducted in NIH 3T3 cell line

Three forms of RAG2, i.e. cRAG2, fRAG2 and TRAG2 were tranfected into NIH3T3 cells, either by themselves or co-transfected with cRAG1 or fRAG1 plasmids. 1 ug of cRAG1 or cRAG2 were used for each transfection, while 4 ug of fRAG1, fRAG2 or TRAG2 plasmid were used due to the extremely low level of fRAG, especially fRAG1. 12 hours after transfection, cells were subjected to serum deprivation for 48 hours by incubating in DMEM medium containing 0.5% serum. Same transfections were also conducted in the serum-rich condition, where the cells were maintained in DMEM medium with 10% serum after transfection.

Westernblot

Cells were collected and directly boiled at 95°C in 1xSDS-PAGE loading buffer (loaded with an equal cell number per lane for the transiently transfected 293T cells) were separated on 10% SDS-PAGE and then blotted onto nitrocellular membranes (Millipore Inc.). The membranes were incubated with primary antibodies specific to MBP (Neomarkers), RAG1 (Cell signaling), or tubulin (Santa Cruz) overnight at 4°C. The proteins recognized by the primary antibodies were revealed by HRP-conjugated secondary anti-Rabbit, anti-Rabbit or anti-Mouse (Sigma) antibodies followed by chemiluminesence detection (Pierce).

Result

Reduction of full length RAG2 by full-length RAG1 in 293T cells

I first examined the level of RAG proteins in 293T cells that were transiently transfected with various combination of core and full-length RAG1 and RAG2 constructs that contain the MBP tag, as detailed in Material & Methods. As shown in Figure 3A, the co-transfection with cRAG1 and cRAG2 constructs results in the highest level of both cRAG1 and cRAG2 proteins among all the various combinations. However, the co-transfection of fRAG1 with fRAG2 yielded almost undetectable levels of RAG proteins. Interestingly, when fRAG1 paired with cRAG2 or cRAG1 with fRAG2, these full-length RAG proteins could be readily detectable, which is consistent with the previous notion that co-transfection with core RAG can increase the stability of the partner RAG protein. To make more quantitative comparison, I increased fRAG constructs at the ratio four times of cRAG plasmids, and compared to the level in the cells transfected with single fRAG1 or fRAG2 constructs (also four times of the cRAG) as input controls. Again, the presence of cRAG1 and cRAG2 was found to increase the level of fRAG2 and fRAG1 proteins, respectively, as compared to the single transfection (Figure 3B, comparing lane 2 and 3 to 5 and 6). However, the co-transfection of fRAG1 and fRAG2 resulted in a a very low level of RAG1 or essentially undetectable RAG2, both of which were significantly reduced in comparison to the single transfection (Figure 3B, lane 4 to lane 5 and 6). This finding indicates that the presence of

fRAG1 can cause great reduction in fRAG2 while the fRAG2 can also result in some diminishment of fRAG1. Thus, N-terminal RAG1 and possibly C-terminal region of RAG2 and is important for their mutual down-regulation, which seems to occur beyond developing lymphocytes.

Cell-cycle independent regulation of fRAG2 by fRAG1

Given the well-known cell-cycle dependent RAG2 degradation, I asked the question whether this down-regulation of fRAG2 by fRAG1 is mediated through a cell cycle-dependent manner. Toward this end, we tested the RAG expression level in cells arrested at G1-phase. Specifically, various RAG combinations were transfected into NIH3T3 cell lines, which is known to be responsive to the serum-deprivation to undergo G1-phase arrest. Twelve hours after transfection, cells were maintained in serum-free (0.5%) medium to induce cell cycle arrest at the G1 phase. Meanwhile, a T490A RAG2 mutant is also included in the comparison because it was shown to be resistant to the cell cycle-mediated RAG2 degradation (9). As a control, the same sets of transfection were performed without the serum deprivation step. Again, to balance the level of core RAG and full length RAG, the a 1:4 ratio of core RAG to full length RAG DNA transfection was applied in both serum rich and serum deprived reactions in the co-transfection, as well as in the single transfection controls, i.e., the amount of DNA for full length RAG is 4 times of core RAG DNA. As shown in Figure 4, flRAG1-mediated reduction of flRAG2 was observed in both serum-containing and serum-

deprived cells (see lane 4-7 in both Fig. 5A & B), indicating the cell-cycle independence of the flRAG1-mediated regulation. Again, consistent with the finding in Figure 3B, no such reduction was seen in cRAG2 (Figure 4 lanes 1-3). Interestingly, for the T490A full-length RAG2 mutant, both cRAG1 and flRAG1 resulted in a comparable level of reduction in flRAG2, indicating an absence of flRAG1-specific effect in reducing this RAG2 mutant (Figure 4, lane 7-9, 14-15). Taken together, our data suggest that the flRAG1-induced reduction of flRAG2 is mediated through the non-core region of RAG2, independent of cell cycle progression, but possibly dependent on the T490 phosphorylation of the flRAG2.

Discussion

The RAG1/2 proteins are known to play a pivotal role in the formation of the adaptive immune system. Impaired control of their expression results in abnormal lymphocyte development and/or immunodeficiency. Several levels of RAG1/2 regulation have been identified during lymphocyte development, such as a stage-dependent transcriptional regulation of RAG1/2 genes and a cell-cycle dependent degradation of RAG2 proteins.

RAG2 protein is a very abundant protein inside the nucleus, and its expression fluctuates much more drastically than the RAG1 expression during different stages of B-cell and T-cell development (20, 23). Moreover, RAG2 displays genome-wide binding, which is directed to the H3K4me3-enriched chromatin, but independent of the RSS recognition or the antigen receptor gene loci (24). Together, the excessive RAG2 protein level and its broad binding mode, build a well-designed prerequisite platform to allow prompt onset of rearrangement once RAG1 is on board. Thus, when RAG1 enters a RAG2 binding site in the RSS site specific manner, the V(D)J recombination may occur. Although this strategy is advantageous for the generation of a diverse antigen receptor repertoire, it may also increase the chance of illegitimate cleavage at non-RSS loci mediated by RAG1, which can compromise of the genome stability. Therefore, the level of the RAG2 that is in an association with RAG1 must be stringently controlled at all times. It is well known that RAG2 is

subjected to a cell cycle-dependent degradation via a polyubiquitin-26S proteasome pathway (11). However, this type of degradation requires the export of RAG2 from the nucleus into cytoplasm. Indeed, it was shown that the phosphorylation of Thr490 leads to the translocation of RAG2 from nucleus into cytoplasm and the disruption of this phosphorylation by T490A mutation stabilizes the RAG2 pool in the nucleus, which prevents the cell-cycle dependent RAG2 diminishment (25). This regulation mechanism seems to only subject to the free form of RAG2 for targeted degradation as RAG1 shows no cell-cycle dependent oscillation. Thus, this cell-cycle dependent degradation pathway may precludes it from acting on the active RAG1/2 recombinase. On the other hand, RAG1/2 recombinase actually poses more danger to the genome than the RAG2 alone. To keep this danger to the minimal level, there may be another level of control, which results an immediate on-site shut-down of the recombinase activity. The RAG1-mediated degradation of RAG2, revealed in this study, may fit perfectly to this mission.

Our *in vitro* transient transfection system demonstrate that RAG2 is indeed down-regulated by RAG1, and this regulation requires the presence of non-core region of both RAG1 and RAG2, and is independent of cell cycle. This finding substantiates our earlier in vivo finding by using a dual-inducible RAG1/2 system. Taken together, I provided strong evidence for a novel mechanism to regulate the RAG2 level, besides the previously identified regulation mechanisms, i.e., developmental stage

dependent transcriptional regulation and cell-cycle dependent degradation. This new regulation has been shown at the post-translational level of the endogenous RAG2, which, however, needs to be verified in the transient transfection system.

The direct down-regulation of RAG2 by RAG1 naturally prompted us to consider the possibility of RAG1 functioning as an E3 ligase. RAG1 may either acts alone as E3 ligase as postulated by several groups (13–15), or recruit other E3-ligase, as discussed in the recent study by Swanson's group. In this study, the authors demonstrate that full length RAG1 interacts with VprBP directly, and the latter is known to be a component of multi-subunit cullin RING E3 ligase, VprBP/DDB1/Cul4A/Roc1 (VDCR) (26, 27). Furthermore, they found that the non-core region of full-length RAG1 could enhance the activity of VDCR in an *in vitro* ubiquitinylation assay. Based on these findings, this group concludes that through VprBP, RAG1 may recruit cullin RING E3 ligase to the recombination machinery for ubiquitination and subsequent degradation, although the endogenous substrate of RAG1-VDCR complex mediated ubiquitintion has not been identified. Our finding that RAG2 is down-regulated only by full length RAG1 but not core RAG1 is in line with this scenario, highlighting the essential role of the non-core region of the full length RAG1 in regulating RAG2 level, presumably by recruiting VprBP/DDB1/Cul4A/Roc1. If RAG2 is indeed subjective to this modification, it may promote rapid removal of RAG1/2- complexes,

including both pre-cleavage and post-cleavage complexes, which facilitate the sustainability of a very delicate level of active recombinase to carry out effective antigen receptor gene assembly without causing genome instability. According to this postulation, the RAG1-dependent RAG2 degradation is likely mediated through a proteasome pathway. I attempted to inhibit proteasome activity by using several proteosome inhibitors. The RAG1-mediated RAG2 degradation was found only inhibited by epoxomicin, which is a selective proteosome inhibitor by binding to the β5 subunit and inhibiting the chymotryptic activity of the 20S proteosome. The application of other commonly used proteasome inhibitors, such as MG-132, fail to retard the RAG1-mediated degradation of the endogenous RAG2. It is unclear whether RAG1 relies on the conventional 26S proteasome pathway or it collaborates with other pathways for the final degradation. Future studies will be needed to delineate the role of proteosome components in this regulation.

On the other hand, it is importantly to note that proteasomes are present and functional in both cytoplasm and nucleus, and the nuclear proteasome can directly target the nucleus proteins for degradation (28). It is possible that the inability of these proteasome inhibitors to delay RAG2 degradation may reflect the their inability of to act on the nuclear proteasome. If that were the case, the RAG1-mediated RAG2 degradation might be relying on a nuclear proteasome pathway, possibly 20S proteasome. The idea is compatible with our earlier argument that instead

of using the cytoplasm proteasome, a nuclear pathway may exist to ensure the on-site control of RAG2 level. However, further investigations are required to fully elucidate this possibility.

Although the exact pathway remains to be defined, the fact that RAG2 is subjected to direct RAG1 regulation is of considerable significance. RAG1 and RAG2 function tightly together to carry out V(D)J recombination and play a central role in lymphocyte development as well as the adaptive immune system. So the direct-regulation between the two seems conceptually suitable to fine-tune the activity of RAG recombinase, because it can influence the formation of recombination excision machinery, the stability of post-cleavage complex and subsequent transition into NHEJ-mediated end resolution process. Furthermore, the direct regulation introduces another check-point to quickly shut-down recombination machinery in the nucleus, and to reduce mis-targeting and/or to minimize transposition by restricting the level and the time-span of the unresolved SEC, even in the absence of cell cycle progression.

In the absence of tetracycline (-Tet)

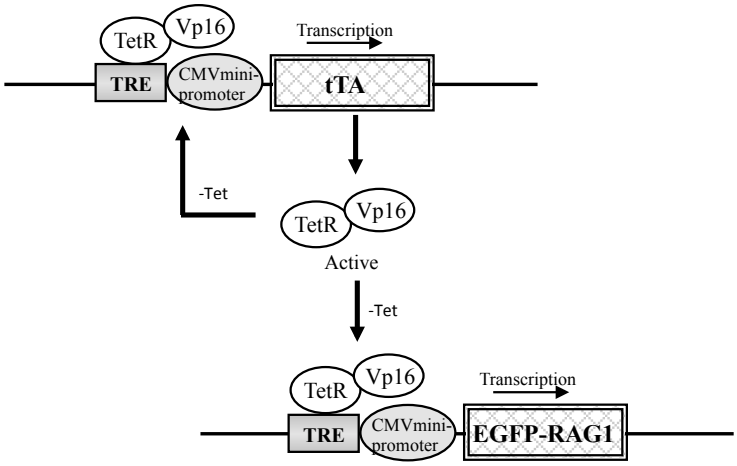

In the presence of tetracycline (+Tet)

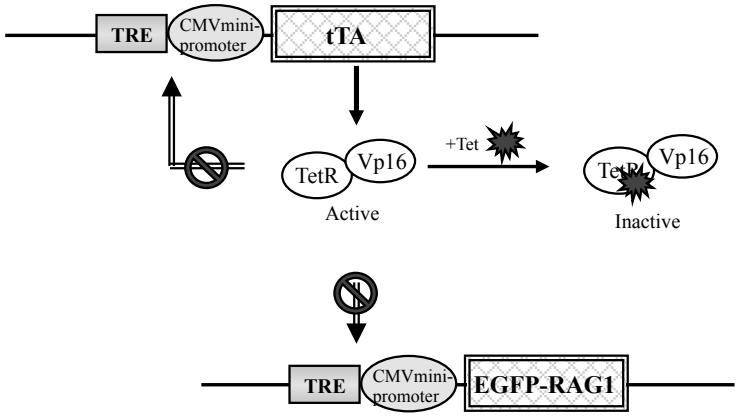

Figure 1. Tetracycline inducible system (Made by Zhi Li)

Activation of the transactivator tTA, a fusion protein consisting of the tet-repressor (tetR) and Vp16 activation domain, by removing tetracycline (-Tet) from the culture medium results in the binding of tTA to the tet-responsive element (TRE) and transcription of tTA and EGFP-RAG1 genes in the transfected cells. Inactivation of the tTA by adding tetracycline (+Tet) to the medium turns off the transcription of target genes.

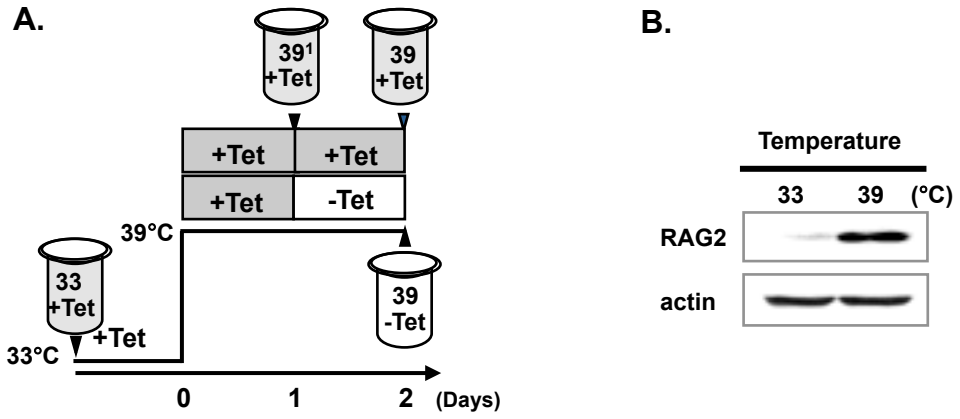

Figure 2. Reduction of RAG2 proteins in RAG1-inducing cells (Made by Zhi Li)

(A) Experimental design: cells were cultured at 33°C (33), 39°C for 1day (39^1), 39°C for 2 days (39) in the presence of tetracycline (+Tet). Or tetracycline was removed as indicated 1 day right before harvest (-Tet) while the cells were kept at 39°C for 2 days (39). Black arrows indicate harvesting points.

(B) Reduction of RAG2 proteins in RAG1-inducing cells. E4 and H10 cells were cultured at 39°C for 2 days in the presence (+Tet) or absence of tetracycline (-Tet) as described above. Total cell lysates were immunoblotted for EGFP-RAG1, RAG2, tTA and actin.

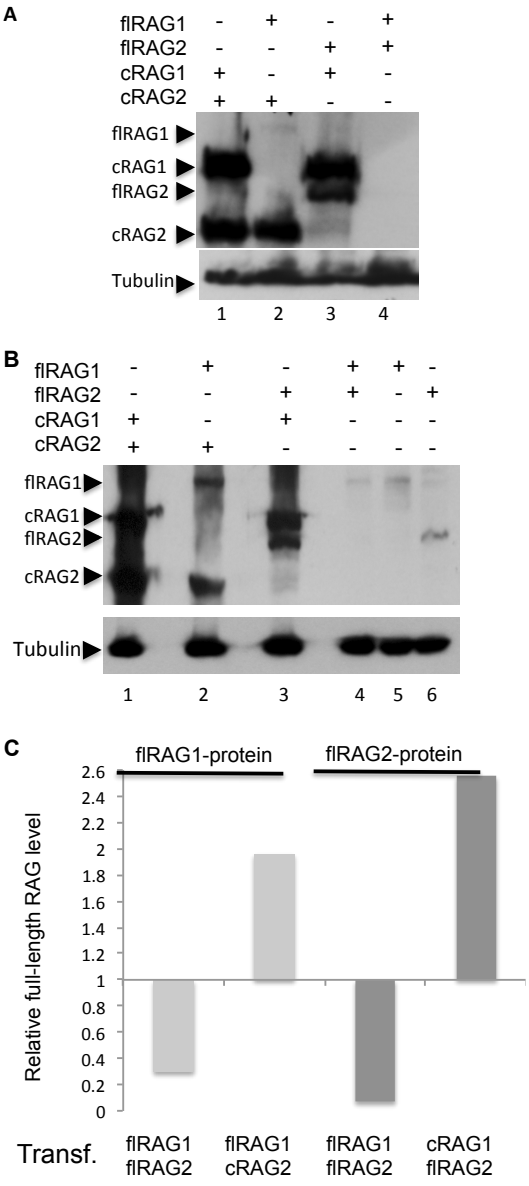
A
flRAG1 - + - +
flRAG2 - - + +
cRAG1 + - + -
cRAG2 + + - -
flRAG1
cRAG1
flRAG2
cRAG2
Tubulin
1 2 3 4
B
flRAG1 - + - + + -
flRAG2 - - + + - +
cRAG1 + - + - - -
cRAG2 + + - - - -
flRAG1
cRAG1
flRAG2
cRAG2
Tubulin
1 2 3 4 5 6
C
flRAG1-protein
flRAG2-protein
Relative full-length RAG level
2.6
2.4
2.2
2
1.8
1.6
1.4
1.2
1
0.8
0.6
0.4
0.2
0
Transf.
flRAG1 flRAG2
flRAG1 cRAG2
flRAG1 flRAG2
cRAG1 flRAG2

Figure 3. *In vitro* analysis of the regulation between RAG1 and RAG2. Various MBP-fused-RAG plasmid combinations were transfected into 293T cells and total cell lysates were immunoblotted for MBP and tubulin.

(A) Reduction of flRAG2 was observed in the presence of flRAG1 (lane 4) but not in cRAG1 (lane 3). cRAG and flRAG plasmids were transfected at 1:1 ratio (1ug). cRAG2 level is not influenced by cRAG1 or flRAG1.

(B) Comparison of the co-expression of RAG1/2 (lane 1-4) *versus* single transfection of flRAG1 or flRAG2 (lane 5 and 6). cRAG and flRAG plasmids were transfected at 1:4 ratio (1ug:4ug).

(C) Comparison of the ratio of the flRAG expression level in co-transfected cells *versus* in single transfected cells. Protein bands were quantitated by Imgae J program and the intensity of each band was normalized to the intensity of input control (tubulin).

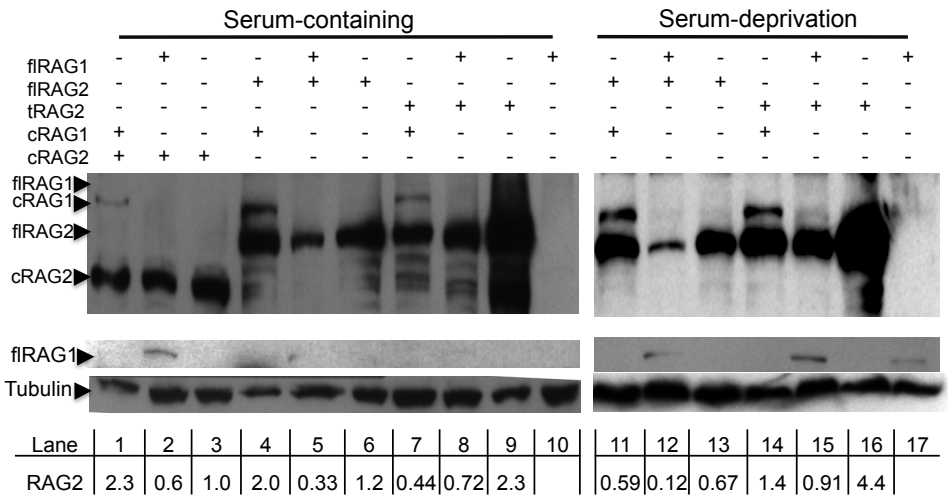

Figure 4. Cell-cycle independent flAG2 degradation mediated by flRAG1. Various MBP-fused-RAG plasmid combinations were transfected into NIH3T3 cells, which were subjected to serum depravation by incubating in the medium containing 0.5% serum for 48hs (lane 11-17). As a control, cells transfected with the same combinations of RAG plasmids were incubated in serum rich medium (lane 1-10). A mutant RAG2 plasmid is also included, tRAG2, which is defective in cell-cycle dependent RAG2 degradation. Total cell lysates were immunoblotted for MBP, RAG1 and tubulin. flRAG1 protein expression was confirmed with anti-RAG1 since it was not visible when probed with anti-MBP.

Reduction of flRAG2 was observed when co-expressed with flRAG1 in both serum-containing and serum-deprived condition (lane 5 and 12).

Protein bands were quantified by Image J and normalized to tubulin, and the relative intensity was shown below each lane.

Reference

1. Mombaerts P et al. (1992) RAG-1-deficient mice have no mature B and T lymphocytes. *Cell* 68:869–877.

2. Shinkai Y et al. (1992) RAG-2-deficient mice lack mature lymphocytes owing to inability to initiate V(D)J rearrangement. *Cell* 68:855–867.

3. Naik AK, Raghavan SC (2012) Differential reaction kinetics, cleavage complex formation, and nonamer binding domain dependence dictate the structure-specific and sequence-specific nuclease activity of RAGs. *J. Mol. Biol.* 415:475–488.

4. Zhang M, Swanson PC (2009) HMGB1/2 can target DNA for illegitimate cleavage by the RAG1/2 complex. *BMC Molecular Biology* 10:24.

5. Zhang M, Swanson PC (2008) V(D)J recombinase binding and cleavage of cryptic recombination signal sequences identified from lymphoid malignancies. *J. Biol. Chem.* 283:6717–6727.

6. Barreto V, Marques R, Demengeot J (2001) Early death and severe lymphopenia caused by ubiquitous expression of the Rag1 and Rag2 genes in mice. *Eur. J. Immunol.* 31:3763–3772.

7. Amin RH, Schlissel MS (2008) Foxo1 directly regulates the transcription of recombination-activating genes during B cell development. *Nat. Immunol.* 9:613–622.

8. Lazorchak AS, Schlissel MS, Zhuang Y (2006) E2A and IRF-4/Pip promote chromatin modification and transcription of the immunoglobulin kappa locus in pre-B cells. *Mol. Cell. Biol.* 26:810–821.

9. Li Z, Dordai DI, Lee J, Desiderio S (1996) A conserved degradation signal regulates RAG-2 accumulation during cell division and links V(D)J recombination to the cell cycle. *Immunity* 5:575–589.

10. Lee J, Desiderio S (1999) Cyclin A/CDK2 regulates V(D)J recombination by coordinating RAG-2 accumulation and DNA repair. *Immunity* 11:771–781.

11. Jiang H et al. (2005) Ubiquitylation of RAG-2 by Skp2-SCF links destruction of the V(D)J recombinase to the cell cycle. *Mol. Cell* 18:699–709.

12. Yurchenko V, Xue Z, Sadofsky M (2003) The RAG1 N-Terminal Domain Is an E3 Ubiquitin Ligase. *Genes Dev.* 17:581–585.

13. Jones JM, Gellert M (2003) Autoubiquitylation of the V(D)J Recombinase Protein RAG1. *PNAS* 100:15446–15451.

14. Simkus C, Makiya M, Jones JM (2009) Karyopherin alpha 1 is a putative substrate of the RAG1 ubiquitin ligase. *Molecular Immunology* 46:1319–1325.

15. Grazini U et al. (2010) The RING Domain of RAG1 Ubiquitylates Histone H3: A Novel Activity in Chromatin-Mediated Regulation of V(D)J Joining. *Molecular Cell* 37:282–293.

16. Oettinger MA, Schatz DG, Gorka C, Baltimore D (1990) RAG-1 and RAG-2, Adjacent Genes That Synergistically Activate V(D)J Recombination. *Science* 248:1517–1523.

17. McBlane JF et al. (1995) Cleavage at a V(D)J recombination signal requires only RAG1 and RAG2 proteins and occurs in two steps. *Cell* 83:387–395.

18. Chen YY, Wang LC, Huang MS, Rosenberg N (1994) An Active V-Abl Protein Tyrosine Kinase Blocks Immunoglobulin Light-Chain Gene Rearrangement. *Genes Dev.* 8:688–697.

19. Brown ML, Lew S, Chang Y (2000) The scid recombination-inducible cell line: a model to study DNA-PK-independent V(D)J recombination. *Immunology Letters* 75:21–26.

20. Lin WC, Desiderio S (1994) Cell Cycle Regulation of V(D)J Recombination-Activating Protein RAG-2. *PNAS* 91:2733–2737.

21. Gossen M, Bujard H (1992) Tight control of gene expression in mammalian cells by tetracycline-responsive promoters. *Proc. Natl. Acad. Sci. U.S.A.* 89:5547–5551.

22. Shockett P, Difilippantonio M, Hellman N, Schatz DG (1995) A Modified Tetracycline-Regulated System Provides Autoregulatory, Inducible Gene Expression in Cultured Cells and Transgenic Mice. *PNAS* 92:6522–6526.

23. Leu TM, Schatz DG (1995) rag-1 and rag-2 are components of a high-molecular-weight complex, and association of rag-2 with this complex is rag-1 dependent. *Mol. Cell. Biol.* 15:5657–5670.

24. Ji Y et al. (2010) The In Vivo Pattern of Binding of RAG1 and RAG2 to Antigen Receptor Loci. *Cell* 141:419–431.

25. Mizuta R, Mizuta M, Araki S, Kitamura D (2002) RAG2 Is Down-Regulated by Cytoplasmic Sequestration and Ubiquitin-Dependent Degradation. *J. Biol. Chem.* 277:41423–41427.

26. Kassmeier MD et al. (2011) VprBP binds full-length RAG1 and is required for B-cell development and V(D)J recombination fidelity. *EMBO J* advance online publication. Available at: http://dx.doi.org/10.1038/emboj.2011.455 [Accessed January 29, 2012].

27. McCall CM et al. (2008) Human Immunodeficiency Virus Type 1 Vpr-Binding Protein VprBP, a WD40 Protein Associated with the DDB1-CUL4 E3 Ubiquitin Ligase, Is Essential for DNA Replication and Embryonic Development. *Mol. Cell. Biol.* 28:5621–5633.

28. Von Mikecz A (2006) The Nuclear Ubiquitin-Proteasome System. *J Cell Sci* 119:1977–1984.

CHAPTER 6

CONCLUSIONS

V(D)J recombination is a elegant and sophisticated genetic process that assembles different gene segments to encode for the variable region of a antigen receptor (immunoglobulin or T cell receptor), therefore it primarily accounts for the enormous diversity of the antigen receptor repertoire, which is fundamental to the adaptive immune response. Notably, the generation of double strand breaks by RAG recombinase is prerequisite for a complete V(D)J recombination, despite the fact that double strand breaks are considered the most dangerous lesion to a cell and thus has to be resolved rapidly and appropriately. Furthermore, even though the double strand breaks are properly attended without causing danger to the cell, a functional rearrangement is frequently accompanied with several unsuccessful rearrangement events arising from the random end processing by the imprecise end-joining pathway, which can potentially compromise the genome integrity. Therefore, the diversity achieved by V(D)J recombination is at great expense of the genome stability. In order to maximize the diversity yet maintain the genome stability, V(D)J recombination has to be stringently controlled at various levels, as detailed in chapter1. Our studies introduce several new regulatory mechanisms into this already delicate regulatory network, 1) Mg^{2+}, as the physiological cation of V(D)J recombination, helps to stabilize the coding end complex, in addition to its well-known role that ensures the controlled cleavage

through synapsis formation. Thus, our finding extend the importance of metal ion cofactor in V(D)J recombination, i.e. it not only affects the structure of the pre-cleavage complex and the catalysis step, but also modulates the stability of post-cleavage complex. 2) The integrity of core RAG2 is essential for the correct assembly of the pre-cleavage complex as well as the sufficient retention of the signal ends in the signal end complex, because a frame-shift RAG2 mutant was found to induce an abnormal pre-cleavage complex and a less stable signal end complex, which may account for its high propensity of aberrant end joining. 3) The presence of non-core region of RAG2 enhances the stability of both CEC and SEC, which are necessary for the appropriate end repair. Our findings substantiate the indispensible role of non-core region of RAG recombinase to ensure the efficiency and fidelity of V(D)J recombination. 4) RAG2 protein level is directly controlled by RAG1 through a RAG1-mediated degradation manner, which provides a novel pathway to control the endogenous RAG2 protein, especially the RAG2 that are in close proximity with RAG1, possibly in the same complex, i.e. targeted destruction of the post-cleavage complex or signal end complex. My studies further enrich the idea that the *in vivo* V(D)J recombination is stringently regulated at multifaceted levels, and highlight the importance of the balance between the antigen receptors diversity and the genome stability during V(D)J recombination. Furthermore, I validate and develop several parameters (RAG recombinase, metal ion cofactor) and several

aspects (pre-cleavage complex assembly and post-cleavage complex stability) for future diagnosis of the potential defect in V(D)J recombination and thus is big step forward to understand and dissect the mechanism of V(D)J recombination. In addition, my studies pave the way to identify and characterize more factors that might potentially influence the fidelity and efficiency of V(D)J recombination.

REFERENCES

1. Cooper MD, Alder MN (2006) The Evolution of Adaptive Immune Systems. *Cell* 124:815–822.

2. Murphy KM, Travers P, Walport M (2007) *Janeway's Immunobiology (Immunobiology: The Immune System* (Garland Science). 7th Ed.

3. Hozumi N, Tonegawa S (1976) Evidence for somatic rearrangement of immunoglobulin genes coding for variable and constant regions. *Proc. Natl. Acad. Sci. U.S.A.* 73:3628–3632.

4. Alt FW, Baltimore D (1982) Joining of Immunoglobulin Heavy Chain Gene Segments: Implications from a Chromosome with Evidence of Three D-JH Fusions. *PNAS* 79:4118–4122.

5. Lewis S, Gellert M (1989) The mechanism of antigen receptor gene assembly. *Cell* 59:585–588.

6. Brack C, Hirama M, Lenhard-Schuller R, Tonegawa S (1978) A complete immunoglobulin gene is created by somatic recombination. *Cell* 15:1–14.

7. Early P, Huang H, Davis M, Calame K, Hood L (1980) An immunoglobulin heavy chain variable region gene is generated from three segments of DNA: VH, D and JH. *Cell* 19:981–992.

8. Lieber MR (2010) The Mechanism of Double-Strand DNA Break Repair by the Nonhomologous DNA End-Joining Pathway. *Annual Review of Biochemistry* 79:181–211.

9. Rooney S, Chaudhuri J, Alt FW (2004) The role of the non-homologous end-joining pathway in lymphocyte development. *Immunol. Rev.* 200:115–131.

10. Schatz DG, Swanson PC (2011) V(D)J recombination: mechanisms of initiation. *Annu. Rev. Genet.* 45:167–202.

11. Gellert M (2002) V(D)J RECOMBINATION: RAG PROTEINS, REPAIR FACTORS, AND REGULATION*. *Annual Review of Biochemistry* 71:101–132.

12. Oettinger MA, Schatz DG, Gorka C, Baltimore D (1990) RAG-1 and RAG-2, Adjacent Genes That Synergistically Activate V(D)J Recombination. *Science* 248:1517–1523.

13. Schatz DG, Oettinger MA, Baltimore D (1989) The V(D)J recombination activating gene, RAG-1. *Cell* 59:1035–1048.

14. van Gent DC et al. (1995) Initiation of V(D)J recombination in a cell-free system. *Cell* 81:925–934.

15. Hiom K, Gellert M (1997) A stable RAG1-RAG2-DNA complex that is active in V(D)J cleavage. *Cell* 88:65–72.

16. Mundy CL, Patenge N, Matthews AGW, Oettinger MA (2002) Assembly of the RAG1/RAG2 Synaptic Complex. *Mol Cell Biol* 22:69–77.

17. McBlane JF et al. (1995) Cleavage at a V(D)J recombination signal requires only RAG1 and RAG2 proteins and occurs in two steps. *Cell* 83:387–395.

18. van Gent DC, Mizuuchi K, Gellert M (1996) Similarities between initiation of V(D)J recombination and retroviral integration. *Science* 271:1592–1594.

19. van Gent DC, Hiom K, Paull TT, Gellert M (1997) Stimulation of V(D)J cleavage by high mobility group proteins. *EMBO J* 16:2665–2670.

20. Sawchuk DJ et al. (1997) V(D)J Recombination: Modulation of RAG1 and RAG2 Cleavage Activity on 12/23 Substrates by Whole Cell Extract and DNA-bending Proteins. *The Journal of Experimental Medicine* 185:2025 –2032.

21. Santagata S, Aidinis V, Spanopoulou E (1998) The effect of Me2+ cofactors at the initial stages of V(D)J recombination. *J. Biol. Chem* 273:16325–16331.

22. Bassing CH, Swat W, Alt FW (2002) The mechanism and regulation of chromosomal V(D)J recombination. *Cell* 109 Suppl:S45–55.

23. Lieber MR (2010) The Mechanism of Double-Strand DNA Break Repair by the Nonhomologous DNA End-Joining Pathway. *Annu. Rev. Biochem.* 79:181–211.

24. Helmink BA, Sleckman BP (2011) The Response to and Repair of RAG-Mediated DNA Double-Strand Breaks. *Annual Review of Immunology*. Available at: http://www.ncbi.nlm.nih.gov/pubmed/22224778 [Accessed March 24, 2012].

25. Mao Z, Bozzella M, Seluanov A, Gorbunova V (2008) Comparison of nonhomologous end joining and homologous recombination in human cells. *DNA Repair (Amst.)* 7:1765–1771.

26. Mao Z, Bozzella M, Seluanov A, Gorbunova V (2008) DNA repair by nonhomologous end joining and homologous recombination during cell cycle in human cells. *Cell Cycle* 7:2902–2906.

27. Lewis SM (1994) P nucleotides, hairpin DNA and V(D)J joining: making the connection. *Semin. Immunol.* 6:131–141.

28. Gilfillan S, Dierich A, Lemeur M, Benoist C, Mathis D (1993) Mice lacking TdT: mature animals with an immature lymphocyte repertoire. *Science* 261:1175–1178.

29. Downs JA, Jackson SP (2004) A means to a DNA end: the many roles of Ku. *Nat Rev Mol Cell Biol* 5:367–378.

30. Mari P-O et al. (2006) Dynamic assembly of end-joining complexes requires interaction between Ku70/80 and XRCC4. *Proceedings of the National Academy of Sciences* 103:18597 –18602.

31. Gottlieb TM, Jackson SP (1993) The DNA-dependent protein kinase: requirement for DNA ends and association with Ku antigen. *Cell* 72:131–142.

32. Yaneva M (1997) Interaction of DNA-dependent protein kinase with DNA and with Ku: biochemical and atomic-force microscopy studies. *The EMBO Journal* 16:5098–5112.

33. Meek K, Douglas P, Cui X, Ding Q, Lees-Miller SP (2007) trans Autophosphorylation at DNA-dependent protein kinase's two major autophosphorylation site clusters facilitates end processing but not end joining. *Mol. Cell. Biol* 27:3881–3890.

34. Mahaney BL, Meek K, Lees-Miller SP (2009) Repair of ionizing radiation-induced DNA double strand breaks by non-homologous end-joining. *Biochem J* 417:639–650.

35. Moshous D et al. (2001) Artemis, a Novel DNA Double-Strand Break Repair/V(D)J Recombination Protein, Is Mutated in Human Severe Combined Immune Deficiency. *Cell* 105:177–186.

36. Ma Y, Pannicke U, Schwarz K, Lieber MR (2002) Hairpin opening and overhang processing by an Artemis/DNA-dependent protein kinase complex in nonhomologous end joining and V(D)J recombination. *Cell* 108:781–794.

37. Lieber MR (2008) The mechanism of human nonhomologous DNA end joining. *J. Biol. Chem* 283:1–5.

38. Lu H et al. (2008) A Biochemically Defined System for Coding Joint Formation in V(D)J Recombination. *Mol Cell* 31:485–497.

39. Tsai C-L, Drejer AH, Schatz DG (2002) Evidence of a critical architectural function for the RAG proteins in end processing, protection, and joining in V(D)J recombination. *Genes & Development* 16:1934 – 1949.

40. Agrawal A, Schatz DG (1997) RAG1 and RAG2 Form a Stable Postcleavage Synaptic Complex with DNA Containing Signal Ends in V(D)J Recombination. *Cell* 89:43–53.

41. Qiu JX, Kale SB, Yarnell Schultz H, Roth DB (2001) Separation-of-function mutants reveal critical roles for RAG2 in both the cleavage and joining steps of V(D)J recombination. *Mol. Cell* 7:77–87.

42. Sekiguchi J, Whitlow S, Alt FW (2001) Increased Accumulation of Hybrid V(D)J Joins in Cells Expressing Truncated versus Full-Length RAGs. *Molecular Cell* 8:1383–1390.

43. Elkin SK, Matthews AG, Oettinger MA (2003) The C-terminal portion of RAG2 protects against transposition in vitro. *EMBO J* 22:1931–1938.

44. Neiditch MB, Lee GS, Landree MA, Roth DB (2001) RAG Transposase Can Capture and Commit to Target DNA before or after Donor Cleavage. *Mol Cell Biol* 21:4302–4310.

45. Swanson PC (2004) The bounty of RAGs: recombination signal complexes and reaction outcomes. *Immunol. Rev.* 200:90–114.

46. Posey JE, Pytlos MJ, Sinden RR, Roth DB (2006) Target DNA Structure Plays a Critical Role in RAG Transposition. *PLoS Biol* 4:e350.

47. Fugmann SD, Messier C, Novack LA, Cameron RA, Rast JP (2006) An ancient evolutionary origin of the Rag1/2 gene locus. *Proc. Natl. Acad. Sci. U.S.A.* 103:3728–3733.

48. Sebastian D. F (2010) The origins of the Rag genes—From transposition to V(D)J recombination. *Seminars in Immunology* 22:10–16.

49. Sakano H, H|[uuml]|ppi K, Heinrich G, Tonegawa S (1979) Sequences at the somatic recombination sites of immunoglobulin light-chain genes. *, Published online: 26 July 1979; | doi:10.1038/280288a0* 280:288–294.

50. Dreyfus DH, Jones JF, Gelfand EW (1999) Asymmetric DDE (D35E)-like sequences in the RAG proteins: implications for V(D)J recombination and retroviral pathogenesis. *Med. Hypotheses* 52:545–549.

51. Landree MA, Wibbenmeyer JA, Roth DB (1999) Mutational analysis of RAG1 and RAG2 identifies three catalytic amino acids in RAG1 critical for both cleavage steps of V(D)J recombination. *Genes Dev* 13:3059–3069.

52. Kim DR, Dai Y, Mundy CL, Yang W, Oettinger MA (1999) Mutations of acidic residues in RAG1 define the active site of the V(D)J recombinase. *Genes Dev* 13:3070–3080.

53. Max EE, Seidman JG, Leder P (1979) Sequences of Five Potential Recombination Sites Encoded Close to an Immunoglobulin Kappa Constant Region Gene. *PNAS* 76:3450–3454.

54. Ferrier P ed. *V(D)J Recombination* Available at: http://www.springerlink.com/content/978-1-4419-0296-2#section=641426&page=1 [Accessed March 23, 2012].

55. Schatz DG (2004) Antigen receptor genes and the evolution of a recombinase. *Semin. Immunol.* 16:245–256.

56. Jones JM, Gellert M (2004) The taming of a transposon: V(D)J recombination and the immune system. *Immunol. Rev.* 200:233–248.

57. Litman GW, Rast JP, Fugmann SD (2010) The origins of vertebrate adaptive immunity. *Nat. Rev. Immunol.* 10:543–553.

58. Fugmann SD, Lee AI, Shockett PE, Villey IJ, Schatz DG (2000) The RAG proteins and V(D)J recombination: complexes, ends, and transposition. *Annu. Rev. Immunol* 18:495–527.

59. Cuomo CA, Oettinger MA (1994) Analysis of regions of RAG-2 important for V(D)J recombination. *Nucleic Acids Res.* 22:1810–1814.

60. Silver DP, Spanopoulou E, Mulligan RC, Baltimore D (1993) Dispensable sequence motifs in the RAG-1 and RAG-2 genes for plasmid V(D)J recombination. *Proc. Natl. Acad. Sci. U.S.A.* 90:6100–6104.

61. Kirch SA, Sudarsanam P, Oettinger MA (1996) Regions of RAG1 protein critical for V(D)J recombination. *European Journal of Immunology* 26:886–891.

62. Steen SB, Han J-O, Mundy C, Oettinger MA, Roth DB (1999) Roles of the "Dispensable" Portions of RAG-1 and RAG-2 in V(D)J Recombination. *Molecular and Cellular Biology* 19:3010 –3017.

63. Dudley DD et al. (2003) Impaired V(D)J Recombination and Lymphocyte Development in Core RAG1-Expressing Mice. *J Exp Med* 198:1439–1450.

64. Deriano L et al. (2011) The RAG2 C terminus suppresses genomic instability and lymphomagenesis. *Nature* 471:119–123.

65. Akamatsu Y et al. (2003) Deletion of the RAG2 C Terminus Leads to Impaired Lymphoid Development in Mice. *PNAS* 100:1209–1214.

66. Liang H-E et al. (2002) The "dispensable" portion of RAG2 is necessary for efficient V-to-DJ rearrangement during B and T cell development. *Immunity* 17:639–651.

67. Huye LE, Purugganan MM, Jiang M-M, Roth DB (2002) Mutational analysis of all conserved basic amino acids in RAG-1 reveals catalytic,

step arrest, and joining-deficient mutants in the V(D)J recombinase. *Mol. Cell. Biol* 22:3460–3473.

68. Fugmann SD, Villey IJ, Ptaszek LM, Schatz DG (2000) Identification of two catalytic residues in RAG1 that define a single active site within the RAG1/RAG2 protein complex. *Mol. Cell* 5:97–107.

69. Dreyfus DH (2006) The DDE recombinases: diverse roles in acquired and innate immunity. *Ann. Allergy Asthma Immunol* 97:567–576; quiz 576–578, 602.

70. Beese LS, Steitz TA (1991) Structural basis for the 3'-5' exonuclease activity of Escherichia coli DNA polymerase I: a two metal ion mechanism. *EMBO J.* 10:25–33.

71. Lovell S, Goryshin IY, Reznikoff WR, Rayment I (2002) Two-metal active site binding of a Tn5 transposase synaptic complex. *Nat Struct Mol Biol* 9:278–281.

72. Allingham JS, Pribil PA, Haniford DB (1999) All three residues of the Tn10 transposase DDE catalytic triad function in divalent metal ion binding. *Journal of Molecular Biology* 289:1195–1206.

73. McMahan CJ, Difilippantonio MJ, Rao N, Spanopoulou E, Schatz DG (1997) A basic motif in the N-terminal region of RAG1 enhances V(D)J recombination activity. *Mol Cell Biol* 17:4544–4552.

74. Noordzij JG et al. (2000) N-Terminal Truncated Human RAG1 Proteins Can Direct T-Cell Receptor but Not Immunoglobulin Gene Rearrangements. *Blood* 96:203–209.

75. Santagata S et al. (2000) N-Terminal RAG1 Frameshift Mutations in Omenn's Syndrome: Internal Methionine Usage Leads to Partial V(D)J Recombination Activity and Reveals a Fundamental Role in Vivo for the N-Terminal Domains. *PNAS* 97:14572–14577.

76. Simkus C, Makiya M, Jones JM (2009) Karyopherin alpha 1 is a putative substrate of the RAG1 ubiquitin ligase. *Molecular Immunology* 46:1319–1325.

77. Arbuckle JL, Rahman NS, Zhao S, Rodgers W, Rodgers KK (2011) Elucidating the domain architecture and functions of non-core RAG1: The

capacity of a non-core zinc-binding domain to function in nuclear import and nucleic acid binding. *BMC Biochem* 12:23.

78. Schatz DG, Swanson PC (2011) V(D)J recombination: mechanisms of initiation. *Annu. Rev. Genet.* 45:167–202.

79. Jackson PK et al. (2000) The lore of the RINGs: substrate recognition and catalysis by ubiquitin ligases. *Trends Cell Biol.* 10:429–439.

80. Yurchenko V, Xue Z, Sadofsky M (2003) The RAG1 N-Terminal Domain Is an E3 Ubiquitin Ligase. *Genes Dev.* 17:581–585.

81. Grazini U et al. (2010) The RING Domain of RAG1 Ubiquitylates Histone H3: A Novel Activity in Chromatin-Mediated Regulation of V(D)J Joining. *Molecular Cell* 37:282–293.

82. Jones JM, Gellert M (2003) Autoubiquitylation of the V(D)J Recombinase Protein RAG1. *PNAS* 100:15446–15451.

83. Jones JM, Simkus C (2009) The roles of the RAG1 and RAG2 "non-core" regions in V(D)J recombination and lymphocyte development. *Arch. Immunol. Ther. Exp. (Warsz.)* 57:105–116.

84. Kassmeier MD et al. (2011) VprBP binds full-length RAG1 and is required for B-cell development and V(D)J recombination fidelity. *EMBO J* advance online publication. Available at: http://dx.doi.org/10.1038/emboj.2011.455 [Accessed January 29, 2012].

85. Ramón-Maiques S et al. (2007) The plant homeodomain finger of RAG2 recognizes histone H3 methylated at both lysine-4 and arginine-2. *Proceedings of the National Academy of Sciences* 104:18993 –18998.

86. Zhao S, Gwyn LM, De P, Rodgers KK (2009) A non-sequence specific DNA binding mode of RAG1 is inhibited by RAG2. *J Mol Biol* 387:744–758.

87. Akamatsu Y, Oettinger MA (1998) Distinct roles of RAG1 and RAG2 in binding the V(D)J recombination signal sequences. *Mol. Cell. Biol* 18:4670–4678.

88. Callebaut I, Mornon J-P (1998) The V(D)J recombination activating protein RAG2 consists of a six-bladed propeller and a PHD fingerlike

domain, as revealed by sequence analysis. *Cellular and Molecular Life Sciences* 54:880–891.

89. Liu Y, Subrahmanyam R, Chakraborty T, Sen R, Desiderio S (2007) A plant homeodomain in RAG-2 that binds Hypermethylated lysine 4 of histone H3 is necessary for efficient antigen-receptor-gene rearrangement. *Immunity* 27:561–571.

90. Matthews AGW et al. (2007) RAG2 PHD finger couples histone H3 lysine 4 trimethylation with V(D)J recombination. *Nature* 450:1106–1110.

91. Grundy GJ, Yang W, Gellert M (2010) Autoinhibition of DNA cleavage mediated by RAG1 and RAG2 is overcome by an epigenetic signal in V(D)J recombination. *Proceedings of the National Academy of Sciences* 107:22487 –22492.

92. Elkin SK et al. (2005) A PHD Finger Motif in the C Terminus of RAG2 Modulates Recombination Activity. *J. Biol. Chem.* 280:28701–28710.

93. West KL et al. (2005) A Direct Interaction between the RAG2 C Terminus and the Core Histones Is Required for Efficient V(D)J Recombination. *Immunity* 23:203–212.

94. Li Z, Dordai DI, Lee J, Desiderio S (1996) A conserved degradation signal regulates RAG-2 accumulation during cell division and links V(D)J recombination to the cell cycle. *Immunity* 5:575–589.

95. Lee J, Desiderio S (1999) Cyclin A/CDK2 regulates V(D)J recombination by coordinating RAG-2 accumulation and DNA repair. *Immunity* 11:771–781.

96. Jiang H et al. (2005) Ubiquitylation of RAG-2 by Skp2-SCF links destruction of the V(D)J recombinase to the cell cycle. *Mol. Cell* 18:699–709.

97. Zhang L, Reynolds TL, Shan X, Desiderio S (2011) Coupling of V(D)J recombination to the cell cycle suppresses genomic instability and lymphoid tumorigenesis. *Immunity* 34:163–174.

98. Jackson SP (2002) Sensing and Repairing DNA Double-Strand Breaks. *Carcinogenesis* 23:687–696.

99. Grawunder U et al. (1995) Down-regulation of RAG1 and RAG2 gene expression in PreB cells after functional immunoglobulin heavy chain rearrangement. *Immunity* 3:601–608.

100. Wilson A, Held W, MacDonald HR (1994) Two Waves of Recombinase Gene Expression in Developing Thymocytes. *J Exp Med* 179:1355–1360.

101. Chen Z et al. (2011) Transcription factors E2A, FOXO1 and FOXP1 regulate recombination activating gene expression in cancer cells. *PLoS ONE* 6:e20475.

102. Amin RH, Schlissel MS (2008) Foxo1 directly regulates the transcription of recombination-activating genes during B cell development. *Nat. Immunol.* 9:613–622.

103. Lazorchak AS et al. (2010) Sin1-mTORC2 suppresses rag and il7r gene expression through Akt2 in B cells. *Mol. Cell* 39:433–443.

104. Hsu L-Y, Liang H-E, Johnson K, Kang C, Schlissel MS (2004) Pax5 activates immunoglobulin heavy chain V to DJ rearrangement in transgenic thymocytes. *J. Exp. Med.* 199:825–830.

105. Zhang Z et al. (2006) Transcription factor Pax5 (BSAP) transactivates the RAG-mediated V(H)-to-DJ(H) rearrangement of immunoglobulin genes. *Nat. Immunol.* 7:616–624.

106. Hu H et al. (2006) Foxp1 is an essential transcriptional regulator of B cell development. *Nature Immunology* 7:819–826.

107. Kuo TC, Schlissel MS (2009) Mechanisms controlling expression of the RAG locus during lymphocyte development. *Curr. Opin. Immunol.* 21:173–178.

108. Schulz D et al. (2012) Gfi1b negatively regulates Rag expression directly and via the repression of FoxO1. *The Journal of Experimental Medicine* 209:187 –199.

109. Bednarski JJ et al. (2012) RAG-induced DNA double-strand breaks signal through Pim2 to promote pre–B cell survival and limit proliferation. *The Journal of Experimental Medicine* 209:11 –17.

110. Hikida M et al. (1998) Expression of Recombination Activating Genes in Germinal Center B Cells: Involvement of Interleukin 7 (IL-7) and the IL-7 Receptor. *J Exp Med* 188:365–372.

111. Liu Y, Zhang L, Desiderio S (2009) Temporal and spatial regulation of V(D)J recombination: interactions of extrinsic factors with the RAG complex. *Adv. Exp. Med. Biol.* 650:157–165.

112. Ji Y et al. (2010) The In Vivo Pattern of Binding of RAG1 and RAG2 to Antigen Receptor Loci. *Cell* 141:419–431.

113. Ramsden DA, McBlane JF, van Gent DC, Gellert M (1996) Distinct DNA sequence and structure requirements for the two steps of V(D)J recombination signal cleavage. *EMBO J* 15:3197–3206.

114. Akamatsu Y et al. (1994) Essential Residues in V(D)J Recombination Signals. *J Immunol* 153:4520–4529.

115. Ramsden DA, Baetz K, Wu GE (1994) Conservation of sequence in recombination signal sequence spacers. *Nucleic Acids Res* 22:1785–1796.

116. Nadel B, Tang A, Escuro G, Lugo G, Feeney AJ (1998) Sequence of the Spacer in the Recombination Signal Sequence Affects V(D)J Rearrangement Frequency and Correlates with Nonrandom Vκ Usage In Vivo. *The Journal of Experimental Medicine* 187:1495–1503.

117. Cuomo CA, Mundy CL, Oettinger MA (1996) DNA sequence and structure requirements for cleavage of V(D)J recombination signal sequences. *Mol Cell Biol* 16:5683–5690.

118. Arnal SM, Holub AJ, Salus SS, Roth DB (2010) Non-consensus heptamer sequences destabilize the RAG post-cleavage complex, making ends available to alternative DNA repair pathways. *Nucleic Acids Res* 38:2944–2954.

119. Montalbano A et al. (2003) V(D)J recombination frequencies can be profoundly affected by changes in the spacer sequence. *J. Immunol.* 171:5296–5304.

120. Feeney AJ, Tang A, Ogwaro KM (2000) B-cell repertoire formation: role of the recombination signal sequence in non-random V segment utilization. *Immunol. Rev.* 175:59–69.

121. Eastman QM, Leu TMJ, Schatz DG (1996) Initiation of V(D)J recombination in vitro obeying the 12/23 rule. *, Published online: 07 March 1996; | doi:10.1038/380085a0* 380:85–88.

122. Jones JM, Gellert M (2002) Ordered assembly of the V(D)J synaptic complex ensures accurate recombination. *The EMBO Journal* 21:4162–4171.

123. Jung D et al. (2003) Extrachromosomal recombination substrates recapitulate beyond 12/23 restricted VDJ recombination in nonlymphoid cells. *Immunity* 18:65–74.

124. Drejer-Teel AH, Fugmann SD, Schatz DG (2007) The beyond 12/23 restriction is imposed at the nicking and pairing steps of DNA cleavage during V(D)J recombination. *Mol. Cell. Biol. 2*7:6288–6299.

125. Cobb RM, Oestreich KJ, Osipovich OA, Oltz EM (2006) in *Advances in Immunology* (Academic Press), pp 45–109. Available at: http://www.sciencedirect.com/science/article/pii/S0065277606910025 [Accessed March 25, 2012].

126. Schatz DG, Oettinger MA, Schlissel MS (1992) V(D)J Recombination: Molecular Biology and Regulation. *Annual Review of Immunology* 10:359–383.

127. Feeney A (2010) Epigenetic regulation of V(D)J recombination. *Seminars in Immunology* 22:311–312.

128. Bergman Y, Cedar H (2010) Epigenetic control of recombination in the immune system. *Seminars in Immunology* 22:323–329.

129. del Blanco B, García V, García-Mariscal A, Hernández-Munain C (2011) Control of V(D)J Recombination through Transcriptional Elongation and Changes in Locus Chromatin Structure and Nuclear Organization. *Genetics Research International* 2011:1–10.

130. Cherry SR, Baltimore D (1999) Chromatin remodeling directly activates V(D)J recombination. *Proc. Natl. Acad. Sci. U.S.A.* 96:10788–10793.

131. Bergman Y, Cedar H (2010) Epigenetic control of recombination in the immune system. *Seminars in Immunology* 22:323–329.

132. Zhang M, Swanson PC (2009) HMGB1/2 can target DNA for illegitimate cleavage by the RAG1/2 complex. *BMC Molecular Biology* 10:24.

133. Rodgers KK et al. (1999) A dimer of the lymphoid protein RAG1 recognizes the recombination signal sequence and the complex stably incorporates the high mobility group protein HMG2. *Nucleic Acids Res* 27:2938–2946.

134. van Gent DC, Ramsden DA, Gellert M (1996) The RAG1 and RAG2 proteins establish the 12/23 rule in V(D)J recombination. *Cell* 85:107–113.

135. Shlyakhtenko LS et al. (2009) Molecular mechanism underlying RAG1/RAG2 synaptic complex formation. *J. Biol. Chem* 284:20956–20965.

136. Kriatchko AN, Bergeron S, Swanson PC (2008) HMG-box domain stimulation of RAG1/2 cleavage activity is metal ion dependent. *BMC Mol. Biol* 9:32.

137. Taccioli GE et al. (1993) Impairment of V(D)J Recombination in Double-Strand Break Repair Mutants. *Science* 260:207–210.

138. Gong C et al. (2005) Mechanism of nonhomologous end-joining in mycobacteria: a low-fidelity repair system driven by Ku, ligase D and ligase C. *Nature Structural & Molecular Biology* 12:304–312.

139. Lin WC, Desiderio S (1994) Cell Cycle Regulation of V(D)J Recombination-Activating Protein RAG-2. *PNAS* 91:2733–2737.

140. Weinstock DM, Jasin M (2006) Alternative pathways for the repair of RAG-induced DNA breaks. *Mol. Cell. Biol* 26:131–139.

141. Bennardo N, Cheng A, Huang N, Stark JM (2008) Alternative-NHEJ is a mechanistically distinct pathway of mammalian chromosome break repair. *PLoS Genet* 4:e1000110.

142. Iliakis G (2009) Backup pathways of NHEJ in cells of higher eukaryotes: Cell cycle dependence. *Radiotherapy and Oncology* 92:310–315.

143. Bentley J, Diggle CP, Harnden P, Knowles MA, Kiltie AE (2004) DNA Double Strand Break Repair in Human Bladder Cancer Is Error Prone and Involves Microhomology-Associated End-Joining. *Nucl. Acids Res.* 32:5249–5259.

144. Bennardo N, Cheng A, Huang N, Stark JM (2008) Alternative-NHEJ Is a Mechanistically Distinct Pathway of Mammalian Chromosome Break Repair. *PLoS Genet* 4.

145. Perrault R, Wang H, Wang M, Rosidi B, Iliakis G (2004) Backup pathways of NHEJ are suppressed by DNA-PK. *J. Cell. Biochem* 92:781–794.

146. Simsek D, Jasin M (2010) Alternative end-joining is suppressed by the canonical NHEJ component Xrcc4-ligase IV during chromosomal translocation formation. *Nat. Struct. Mol. Biol* 17:410–416.

147. Sawchuk DJ et al. (2004) Ku70/Ku80 and DNA-dependent Protein Kinase Catalytic Subunit Modulate RAG-mediated Cleavage. *Journal of Biological Chemistry* 279:29821 –29831.

148. Raval P, Kriatchko AN, Kumar S, Swanson PC (2008) Evidence for Ku70/Ku80 association with full-length RAG1. *Nucleic Acids Research* 36:2060 –2072.

149. Cui X, Meek K (2007) Linking double-stranded DNA breaks to the recombination activating gene complex directs repair to the nonhomologous end-joining pathway. *Proc. Natl. Acad. Sci. U.S.A* 104:17046–17051.

150. Lee GS, Neiditch MB, Salus SS, Roth DB (2004) RAG proteins shepherd double-strand breaks to a specific pathway, suppressing error-prone repair, but RAG nicking initiates homologous recombination. *Cell* 117:171–184.

151. Corneo B et al. (2007) Rag mutations reveal robust alternative end joining. *Nature* 449:483–486.

152. Deriano L, Stracker TH, Baker A, Petrini JHJ, Roth DB (2009) Roles for NBS1 in alternative nonhomologous end-joining of V(D)J recombination intermediates. *Mol. Cell* 34:13–25.

153. Bredemeyer AL et al. (2006) ATM stabilizes DNA double-strand-break complexes during V(D)J recombination. *Nature* 442:466–470.

154. Jones JM, Gellert M (2001) Intermediates in V(D)J recombination: A stable RAG1/2 complex sequesters cleaved RSS ends. *Proceedings of the National Academy of Sciences* 98:12926 –12931.

155. Ingersoll CM, Strollo CM (2007) Steady-State Fluorescence Anisotropy To Investigate Flavonoids Binding to Proteins. *J. Chem. Educ.* 84:1313.

156. Lakowicz JR (2006) *Principles of Fluorescence Spectroscopy* (Springer). 3rd Ed.

157. Anderson BJ, Larkin C, Guja K, Schildbach JF (2008) Using Fluorophore-labeled Oligonucleotides to Measure Affinities of Protein-DNA Interactions. *Methods Enzymol* 450:253–272.

158. Stryer L, Haugland RP (1967) Energy transfer: a spectroscopic ruler. *Proc. Natl. Acad. Sci. U.S.A.* 58:719–726.

159. Uster PS (1993) In situ resonance energy transfer microscopy: monitoring membrane fusion in living cells. *Meth. Enzymol.* 221:239–246.

160. Schatz DG, Oettinger MA, Baltimore D (1989) The V(D)J recombination activating gene, RAG-1. *Cell* 59:1035–1048.

161. Oettinger MA, Schatz DG, Gorka C, Baltimore D (1990) RAG-1 and RAG-2, adjacent genes that synergistically activate V(D)J recombination. *Science* 248:1517–1523.

162. Rooney S, Chaudhuri J, Alt FW (2004) The role of the non-homologous end-joining pathway in lymphocyte development. *Immunol. Rev.* 200:115–131.

163. Kriatchko AN, Anderson DK, Swanson PC (2006) Identification and Characterization of a Gain-of-Function RAG-1 Mutant. *Mol Cell Biol* 26:4712–4728.

164. Bergeron S, Anderson DK, Swanson PC (2006) RAG and HMGB1 proteins: purification and biochemical analysis of recombination signal complexes. *Meth. Enzymol.* 408:511–528.

165. Pavlicek JW, Lyubchenko YL, Chang Y (2008) Quantitative analyses of RAG-RSS interactions and conformations revealed by atomic force microscopy. *Biochemistry* 47:11204–11211.

166. Grundy GJ et al. (2009) Initial Stages of V(D)J Recombination: The Organization of RAG1/2 and RSS DNA in the Postcleavage Complex. *Molecular Cell* 35:217–227.

167. Helmink BA, Sleckman BP (2012) The Response to and Repair of RAG-Mediated DNA Double-Strand Breaks. *Annual Review of Immunology* 30:null.

168. Roth DB (2003) Restraining the V(D)J recombinase. *Nat. Rev. Immunol.* 3:656–666.

169. Della-Maria J et al. (2011) hMre11/hRad50/Nbs1 and DNA ligase III{alpha}/XRCC1 act together in an alternative non-homologous end joining pathway. *J Biol Chem*. Available at: http://www.ncbi.nlm.nih.gov/pubmed/21816818 [Accessed August 23, 2011].

170. Williams GJ, Lees-Miller SP, Tainer JA (2010) Mre11-Rad50-Nbs1 conformations and the control of sensing, signaling, and effector responses at DNA double-strand breaks. *DNA Repair* 9:1299–1306.

171. Schatz DG, Swanson PC (2011) V(D)J Recombination: Mechanisms of Initiation. *Annual Review of Genetics* 45:167–202.

172. Kumar S, Swanson PC (2009) Full-length RAG1 promotes contact with coding and intersignal sequences in RAG protein complexes bound to recombination signals paired in cis. *Nucleic Acids Res* 37:2211–2226.

173. Shimazaki N, Tsai AG, Lieber MR (2009) H3K4me3 Stimulates the V(D)J RAG Complex for Both Nicking and Hairpinning in trans in Addition

to Tethering in cis: Implications for Translocations. *Molecular Cell* 34:535–544.

174. Mombaerts P et al. (1992) RAG-1-deficient mice have no mature B and T lymphocytes. *Cell* 68:869–877.

175. Shinkai Y et al. (1992) RAG-2-deficient mice lack mature lymphocytes owing to inability to initiate V(D)J rearrangement. *Cell* 68:855–867.

176. Naik AK, Raghavan SC (2012) Differential reaction kinetics, cleavage complex formation, and nonamer binding domain dependence dictate the structure-specific and sequence-specific nuclease activity of RAGs. *J. Mol. Biol.* 415:475–488.

177. Zhang M, Swanson PC (2008) V(D)J recombinase binding and cleavage of cryptic recombination signal sequences identified from lymphoid malignancies. *J. Biol. Chem.* 283:6717–6727.

178. Barreto V, Marques R, Demengeot J (2001) Early death and severe lymphopenia caused by ubiquitous expression of the Rag1 and Rag2 genes in mice. *Eur. J. Immunol.* 31:3763–3772.

179. Lazorchak AS, Schlissel MS, Zhuang Y (2006) E2A and IRF-4/Pip promote chromatin modification and transcription of the immunoglobulin kappa locus in pre-B cells. *Mol. Cell. Biol.* 26:810–821.

180. Chen YY, Wang LC, Huang MS, Rosenberg N (1994) An Active V-Abl Protein Tyrosine Kinase Blocks Immunoglobulin Light-Chain Gene Rearrangement. *Genes Dev.* 8:688–697.

181. Brown ML, Lew S, Chang Y (2000) The scid recombination-inducible cell line: a model to study DNA-PK-independent V(D)J recombination. *Immunology Letters* 75:21–26.

182. Gossen M, Bujard H (1992) Tight control of gene expression in mammalian cells by tetracycline-responsive promoters. *Proc. Natl. Acad. Sci. U.S.A.* 89:5547–5551.

183. Shockett P, Difilippantonio M, Hellman N, Schatz DG (1995) A Modified Tetracycline-Regulated System Provides Autoregulatory,

Inducible Gene Expression in Cultured Cells and Transgenic Mice. *PNAS* 92:6522–6526.

184. Leu TM, Schatz DG (1995) rag-1 and rag-2 are components of a high-molecular-weight complex, and association of rag-2 with this complex is rag-1 dependent. *Mol. Cell. Biol.* 15:5657–5670.

185. Mizuta R, Mizuta M, Araki S, Kitamura D (2002) RAG2 Is Down-Regulated by Cytoplasmic Sequestration and Ubiquitin-Dependent Degradation. *J. Biol. Chem.* 277:41423–41427.

186. McCall CM et al. (2008) Human Immunodeficiency Virus Type 1 Vpr-Binding Protein VprBP, a WD40 Protein Associated with the DDB1-CUL4 E3 Ubiquitin Ligase, Is Essential for DNA Replication and Embryonic Development. *Mol. Cell. Biol.* 28:5621–5633.

187. Von Mikecz A (2006) The Nuclear Ubiquitin-Proteasome System. *J Cell Sci* 119:1977–1984.